Mapping runoff and erosion to reduce urban flooding and sediment flow towards sea

A case study on the Playa catchment, Bonaire

M.Sc. Thesis by Geert Koster

May 2013

Water Resources Management Group
Soil Physics and Land Management Group

WAGENINGEN UNIVERSITY
WAGENINGEN UR

Mapping runoff and erosion to reduce urban flooding and sediment flow towards sea

A case study for the Playa catchment, Bonaire

Master thesis Water Resources Management submitted in partial fulfillment of the degree of Master of Science in International Land and Water Management at Wageningen University, the Netherlands

Geert Koster

May 2013

Supervisors:

Dr. Ir. Gerardo van Halsema
Water Resources Management Group
Wageningen University
The Netherlands

Dr.ir. Jantiene Baartman
Soil Physics and Land Management Group
Wageningen University
The Netherlands

Abstract

Past deforestation, overgrazing and urbanization have led to an increase in surface runoff and erosion in the Playa catchment, Bonaire. Together with the lack of sufficient spatial planning, this has led to increased urban flooding and larger sediment flows into the ocean causing harm to the island's famous coral reefs. For this research, an event-based, spatially-distributed erosion and runoff model (Kineros2) was used to map and quantify the sources and routing of this runoff and sediment. The effect of several physical factors such as rainfall intensity, rainfall duration, initial soil moisture content and vegetation cover were tested to understand their effects on runoff and erosion. Furthermore, three different management scenarios were simulated: decreasing the amount of pavement, reducing the number of reservoirs and reducing the grazing pressure.

The results show that the highest rates of soil loss are found in the uplands. However due to the high sediment trapping efficiency of the many reservoirs, most of this upland sediment is trapped and therefore does not reach the sea. Most surface runoff is produced in central Kralendijk. This is also what leads to flooding as the capacity of the drainage system in central Kralendijk is too small to effectively drain the area. Large intensity rainfall events (usually occurring in October) are most problematic.

Reducing the grazing pressure and therefore increasing the vegetation cover was found to be effective in decreasing the rate of soil loss. This however did not translate into significantly lower sediment yields at the outlets – which was much more influenced by the loss of agricultural reservoirs. Reducing the amount of pavement in central Kralendijk did not have a significant effect in reducing runoff – flooding can therefore only be effectively tackled by increasing the capacity of the drainage network.

Acknowledgements

There are a number of people who helped to give shape to this thesis and which I would therefore like to thank. First of all I want to thank my supervisors Jantiene Baartman and Gerardo van Halsema. I want to thank Jantiene for her valuable advice and guidance concerning the field work, data analysis and modelling parts of this thesis and I want to thank Gerardo for the important part he played in finally shaping the report. I would also like to thank Klaas Metselaar – especially for his enthusiasm. He was the one through which I found this project and also responsible for many practicalities, especially at the start

On Bonaire I am especially thankful to Kris Kats who could be counted on for practical matters – from providing contacts to lending out equipment and the arrangement of some of the financing. I always enjoyed the meetings we had together. I would also like to thank the people from the DRO (especially Jeroen Meuleman) and LVV for their cooperation and time.

A special thanks also goes out to the Stinapa girls - Vinni, Lotte, Tatiana and Iris – who provided good company and fun during my stay on Bonaire. Back in Holland I would like to thank Bart and Jan, who could always be counted on for a coffee break during the long days of modelling and writing in the Atlas building.

Table of Contents

1. Introduction

1.1 Background

Research done on catchment hydrology and rainfall-runoff relationships shows that an increase in surface runoff is a point of concern in many catchments around the world (Foley et al., 2005). The main reasons for this increase in surface runoff are anthropogenic activities such as deforestation, overgrazing and urbanization (Fohrer et al., 2001). The decrease in vegetation cover leads to a decrease in interception and modification of the physical soil structure which reduces the infiltration capacity (Lal, 1997), urbanization leads to an increase in the impervious surface area. The extent to which surface runoff is produced also depends on natural factors. In arid and semi-arid areas for example, vegetation cover is naturally low while rainfall events can be quite intense, producing a relatively large amount of surface runoff. In areas with loamy and clayey soils the effect is the same due to the low infiltration capacity of these soils.

Perhaps the most noticeable effect of an increase in surface runoff is the increase in peak discharge of streams and rivers as rainwater is drained more rapidly. This increases flooding risks which is especially problematic in urban areas because firstly, these produce a lot of surface runoff themselves and secondly, they are vulnerable to damage. Urban flooding ranges from small cases where inundation of streets and cellars mainly leads to nuisance and property damage to cases whereby fast flowing water and debris leads to destruction and even death (Shi et al., 2007). In many cases services such as water supply, sanitation and electricity are disrupted – potentially leading to the spread of disease. In areas with loose soils, flooding brings with it a risk of land and mud slides. Another problem associated with urban flooding is the risk it poses to water quality. Street solids and material from overflowing sewers are major pollutants in urban runoff and can harm the quality of water bodies downstream (Lee and Bang, 2000).

In areas covered by agriculture or natural vegetation, the main problem associated with increased surface runoff is that of increased erosion. Perhaps the clearest effect of erosion is the loss of soil nutrients. The US department of agriculture estimates that about half of the 45 million tons of fertilizer applied annually is replacing the nutrients lost through erosion (Pimentel et al., 1987). The reduction in the water holding potential of the soil is another major effect caused by the selective removal of organic matter and finer soil particles. Finally, the thinning of the top soil means the potential rooting depth of vegetation and potential crops is also restricted (Morgan, 2005).

The off-site effects of erosion are another point of concern. Sedimentation on land is often beneficial (except when it contains pollutants or covers crops), sedimentation in water less so. The main problem associated with sedimentation in water bodies is the increase in turbidity. This reduces the amount of light reaching lower water depths which can have negative consequences for aquatic plants and therefore also for the species which are dependent upon them (Henley et al., 2000). In oceans, the effect is similar and sedimentation is seen to be a serious threat for coral reefs worldwide (Rogers, 1990).

Lastly, an increased fraction of precipitation becoming runoff means less water infiltrates. A decrease in infiltration means a decrease in percolation and therefore also in aquifer recharge. Furthermore, agricultural and vegetated areas will become less drought resistant as the soil retains less soil moisture after rainfall events (Morgan, 2005).

1.2 Problem statement

The Caribbean island of Bonaire is a typical example of an area where a combination of natural and anthropogenic factors means a large percentage of rainfall flows off as surface runoff. The clayey top soil in combination with the low vegetation cover (due to the arid-climate) and intense rainfall causes low infiltration rates. This has been aggravated by past deforestation, overgrazing and urbanization (Borst and Haas, 2005). A water balance study by Grontmij & Sogreah (1968), estimated that only 5% of the rainfall recharges the groundwater while 10% becomes runoff. Due to land cover changes the latter percentage has probably increased.

The lack of proper spatial planning and the insufficient capacity of the urban drainage system in Kralendijk means this storm water runoff often leads to flooding. In a survey performed by Hulsman (2012), it was found that 66% of the respondents in Kralendijk experience water excess mostly through difficulties in transportation or through water nuisance in the house. Of the people who have witnessed water excess, 96% experience it as a problem and 44% experience nowadays more nuisance from water excess than 15 years ago (Hulsman, 2012).

The large amounts of surface runoff in combination with the low vegetation cover also leads to high rates of erosion. Except for the thinning of the top soil, the largest problem associated with this is the deposition of these eroded sediments on the island's famous coral reefs. Especially since the beginning of the 70's, coral cover and the number of coral colonies along the coast of Bonaire have been decreasing steadily, sedimentation being one of the two main causes; the other one being temperature rise (Bak et al., 2005).

1.3 Goal and objectives

The aim of this research is to understand the spatially distributed rainfall-runoff-erosion relationship in the Playa catchment for the current situation as well as for a number of different scenarios and using this information to give management advice on how sediment flow into the ocean and flooding in central Kralendijk can be reduced

The following research questions were formulated:

1. What is the spatially distributed rainfall-runoff-erosion relationship in the catchment under current management?
    - How much erosion and runoff is produced at each location in the catchment and how is this routed for a rainfall event with return period of five years and ten years?
    - Can the current drainage system cope with the runoff and discharge produced by these rainfall events?
2. How do physical factors affect the rainfall-runoff-erosion relationship.
    - What is the difference in effect between long-duration and high-intensity rainfall events on surface runoff and erosion?
    - What is the effect of different initial soil moisture contents on surface runoff and erosion?
    - How does the difference in vegetation cover between the start and end of the rainy season affect runoff and erosion
3. How does the rainfall-runoff-erosion relationship change with different management options?
    - What is the effect of decreasing the percentage of paved area?
    - What is the effect of decreasing the number of reservoirs?

- What is the effect of decreasing the grazing pressure (and therefore having increased vegetation cover)?

4. Based on the understanding of the spatially distributed rainfall-runoff-erosion relationship and the scenario results, how can the sediment flow into the ocean and urban flooding best be reduced in the Playa catchment?

2. Methodology

2.1 Study area

The Caribbean island of Bonaire is located around 80 km North of Venezuela and is part of the Lesser Antilles. It covers an area of around 290 km^2 and has around 15,700 inhabitants (Statistiek, 2012). The only two recognized towns are the administrative centre of Kralendijk and the village of Rincon. The Southern part of the island is rather flat (up to 25m) while the Northern part of the island has elevations up to 241m. The island has a semi-arid climate with an annual rainfall of 200 to 1000mm per year (an average of 470mm) of which 55% falls within the rainy season from October to January (Borst and Haas, 2005). The average daily temperature ranges from 25 to 31^{o}C.

Tourism is the most important economic activity and the island attracts around 15000 visitors per year. Almost all of these come for the unique coral reef surrounding the island. Agriculture used to be important but since the 1960's, it has been declining steadily. At the moment there is still some sorghum being grown but most of the island is now used as grazing land for goat and donkey husbandry (Kekem et al., 2006). Due to overgrazing and past deforestation, the vegetation cover is rather low and consists mostly of thorny shrubs and cacti.

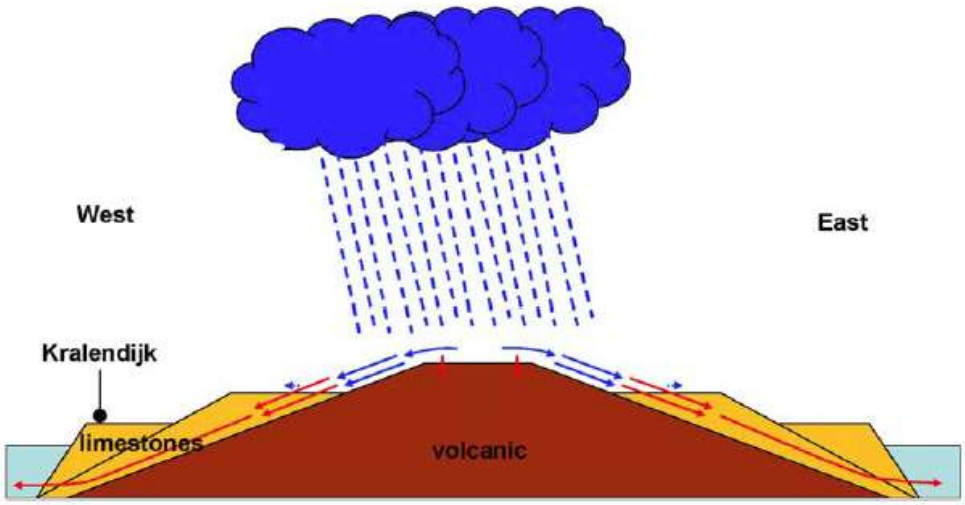

Figure 1: Geohydrological situation in a schematic cross-section over Kralendijk (Borst and Haas, 2005)

Regarding the hydrogeology, the island can roughly be split up in two parts. The centre of the island consists of volcanic dolomite with a weathered clayey top layer which hampers infiltration. Closer to the coast, the geology consists of karstified limestone with much higher infiltration rates due to fissures and cracks (Borst and Haas, 2005). Figure 1 gives a schematic cross-section over the island, on the location Kralendijk, showing the geohydrological situation.

The research catchment is the Playa catchment which is located on the middle of the Bonaire and drains towards the West into the Caribbean Sea. The total surface area is around 900ha. The Western half of the catchment consists of the city of Kralendijk and is therefore urban; the Eastern part consists partly of agriculture but mostly of shrub-lands – grazed by goats. The elevation ranges from around 80m above sea level in the North-Eastern part of the catchment to sea level on the West of the catchment. There are no perennial streams in the catchment, instead

it is drained by a system of 'rooien[1]' upstream and some roadside/underground drains in the urban area.

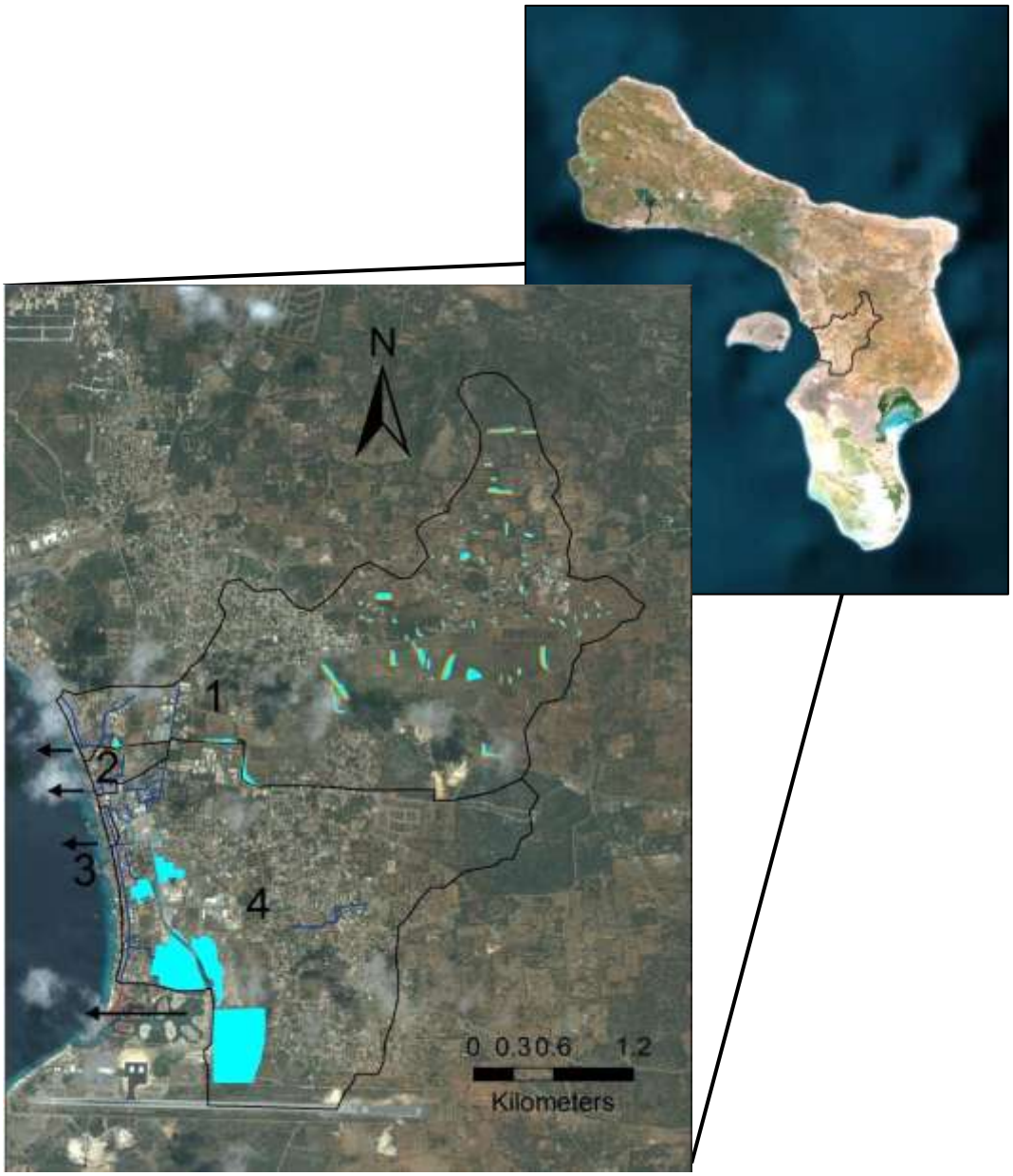

Figure 2: Map of Bonaire showing the Playa catchment and sub-catchments

The Playa catchment can be divided in four sub-catchments. The location of the Playa catchment, its sub-catchments, and the network of reservoirs and channels are shown in Figure 2.

Sub-catchment 1 is the largest sub-catchment. Most of the agricultural and shrub-lands to the East are part of this catchment. This is also the sub-catchment with the highest elevations and a many reservoirs. The water which is not stored in these reservoirs is discharged into the channel to the south of this sub-catchment (along the kaminda Yato Bako) and passes three more reservoirs before it flows into the ocean.

[1] Ephemeral streams, draining only during and shortly after rainfall events

Sub-catchment 2 is a small urban catchment draining the area between the hospital and the stadium. It consists solely of few underground drains within the centre of Kralendijk.

Sub catchment 3 mainly drains the main street of Kralendijk – the Kaya Grandi. The reservoir system of sub-catchment 4 is also connected to its outlet through a diver at the stadium. However at the time of observation this drain had half collapsed and could barely drain any water. Therefore the assumption was made that all the water from around the stadium is brought to the outlet of sub-catchment 4.

Sub-catchment 4 is more complicated. Water flows from mostly residential areas (and some shrub/agricultural lands) towards a 'saliña[2]' in the West. Water is collected here because it is a flat low-lying area, blocked by the higher lying coastal area (a coral dam). Only once the water level in this 'saliña' has reached a certain height, it will flow into the sea through outlet 4 (at the plaza resort). A number of underground urban drains also drain into this 'saliña'.

[2] Natural salt water buffers, separated from the sea through a coral rubble barrier

2.2 Kineros2 model

The Kineros2 model was chosen to model the spatial distribution of the rainfall-runoff-erosion relationship. Kineros2 is a spatially distributed, physical, event-oriented model that can simulate runoff and sediment transport (Semmens et al., 2008, Smith et al., 1995). An event-based model was chosen because we are interested in the effect of individual rainfall events. Furthermore, using an event-based model means that daily evapotranspiration and rainfall records are not required. Another advantage of Kineros2 is that it was developed for small semi-arid watersheds where infiltration rates are low and rainfall is intense (Canfield and Goodrich, 2003). This is also the case for Bonaire. Lastly the required data input is less than for other spatially distributed event-based models such as LISEM.

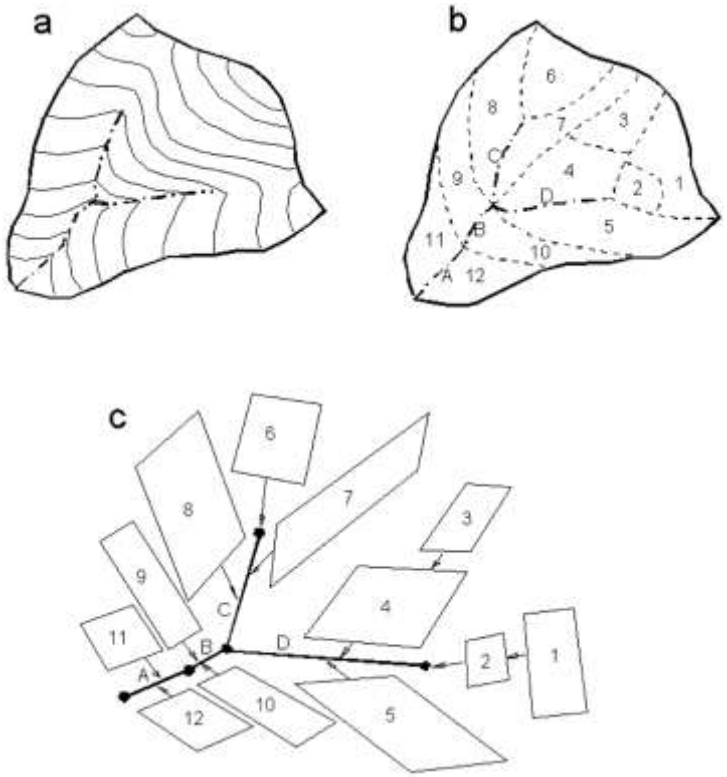

Figure 3: Schematic illustration of the geometric subdivision of a hypothetical catchment into a network of surfaces and receiving channels for KINEROS2 simulation (Smith et al., 1999).

Within Kineros2, the watershed is conceptualised as a collection of spatially distributed model elements (Figure 3). There are six types of model elements:

- Overland flow: planes described by unique parameters, initial conditions and precipitation inputs
- Urban overland: plane with mixed pervious/impervious cover.
- Channels: trapezoidal
- Detention structures: arbitrary shape, controlled outlet – discharge
- Culvert: circular with free surface flow
- Injection: hydrograph and sedigraph injected from outside the modelled system

The model simulates, infiltration, interception, surface runoff, soil detachment by splash and hydraulic erosion, sedimentation and the routing of discharge of sediment through channels and reservoirs.

Rainfall intensity is used as input. Spatial and temporal variability is interpolated from each rain gauge location to each plane, pond or urban element. The effect of interception is controlled by the interception depth and the fraction of surface covered by intercepting vegetation.

Infiltration may occur from rainfall directly on the soil or from ponded surface water from previous rainfall excess. The infiltration rate is equal to the rainfall rate (minus the interception loss) until the infiltrability limit is reached. The infiltrability is the rate at which soil will absorb water when there is an unlimited supply at the surface. It is defined as follows:

$$f_c = K_s \left[1 + \frac{0.85}{\exp\left(\frac{0.85I}{G\Delta\theta_{si}}\right) - 1} \right] \quad \textbf{(1)}$$

where f_c (mm hr^{-1}) is the infiltrability, K_s (mm hr^{-1}) is the saturated hydraulic conductivity, G (mm) is the capillary length scale, I (mm) is the infiltrated depth and $\Delta\theta_i$ (-) is the initial saturation deficit (θ_s-θ_i). Kineros2 uses the Parlange 3-parameter to simulate this process, in which the models of Green and Ampt and Smith and Parlange are included as two limiting cases (Semmens et al., 2008). If K_s (saturated hydraulic conductivity) is nearly constant while D (diffusivity) increases rapidly with θ (volumetric soil water content), the equation approaches the Green and Ampt model. If both D and K increase rapidly with θ, the equation approaches the Parlange model (Semmens et al., 2008). Lognormal, small-scale spatial variability in K_s is modelled using a coefficient of variation (CV) (Al-Qurashi et al., 2008).

Kineros2 is also capable of redistributing soil water during rainfall interruptions by describing the wetting profile of the soil by a water balance equation in which the additions from rainfall are balanced by the increase in the wetted zone value of the soil moisture content and the extension of the wetted zone depth due to the capillary drive of the wetting front (Semmens et al., 2008).

Runoff is produced when there is free water on the soil surface. This can be produced by two mechanisms:

- The rainfall rate is larger than the hydraulic conductivity of the upper soil layer, therefore infiltration excess runoff is produced (Hortonian).
- The rainfall rate is larger than the hydraulic conductivity of the lower soil layer but smaller than the hydraulic conductivity of the upper soil layer. When the water which cannot enter the lower soil profile has filled the available pore space in the upper soil, saturation excess runoff is produced (Dunian).

Surface and channel flow is expressed using the one-dimensional kinematic wave equation which combines continuity of mass with a relation describing discharge as a function of water storage per unit area. The equation is solved using a four point implicit finite difference method (Woolhiser et al., 1990). Wave movement and depth is controlled by slope, channel geometry, Manning's coefficient and two microtopography parameters to account for rills/furrows: relief height (r_h) and relief spacing (r_s) (Al-Qurashi et al., 2008). The model assumes channels to have an infinite height so that channel overtopping cannot be modelled.

The equation describing sediment dynamics is a mass balance equation similar to that for kinematic water flow (Woolhiser et al., 1990). It accounts separately for erosion caused by raindrop energy (splash erosion) and for erosion caused by flowing water (hydraulic erosion). Splash erosion is described as a function of rainfall rate, the depth of flow and a splash erosion coefficient (c_f). Hydraulic erosion is related to the difference between the equilibrium sediment concentration and the existing sediment concentration and the transfer rate coefficient (c_h)

(Martínez-Carreras et al., 2007). Sediment transport in channels is simulated in the same way as for upland areas, although splash erosion is neglected.

Sediment routing through reservoirs is handled very much like the analogues process in a settling pond. Particle fall velocities and lateral flow velocities are used to find the trajectories that intersect the reservoir bottom. Particles are assumed to be distributed evenly through the reservoir depth in the first section at the inlet, and the relative fall versus lateral velocities from that point forward determines the proportion of each particle size that deposits between successive cross sections (Woolhiser et al., 1990).

Input parameters

The list of input parameters required for Kineros2 is shown below:

Soil parameters

- Texture (sand, silt, and clay fraction)
- Bulk density, ρ_d (g cm^{-3})
- Rock fraction (volumetric)
- Capillary length scale, G (mm)
- Saturated hydraulic conductivity, K_s (mm hr^{-1})
- Coefficient of variation of K_s, CV (-)
- Pore size distribution index, λ (-)
- Porosity, φ (-)
- Maximum relative saturation, θ_s (-)
- Splash and hydraulic erosion coefficients, c_f (-) and c_g (-)

Land surface parameters

- Slope (%)
- Vegetation cover fraction (0-1)
- Fraction paved area (0-1)
- Manning's roughness coefficient, n_p (-)
- Interception (mm)

Channel parameters

- Channel geometry
- Channel's Manning's roughness coefficient, n_c (-)
- Channel soil properties (same as soil parameters)

Pond parameters

- Pond geometry
- Saturated hydraulic conductivity, K_s (mm hr^{-1})

2.3 Model setup

2.3.1 Soil parameters

The necessary soil parameters for the Kineros2 model, were collected at a number of sampling points in the catchment and spatially interpolated.

A systematic square sampling scheme was used because it is easy to implement and regular sampling schemes poses the highest sampling efficiency (minimum average standard error and lowest maximum standard error) (Olea, 1984). Furthermore it was not possible to split up the study area into strata with properties which are definitely related to the soil characteristics that are to be tested – therefore a method such as stratified sampling was not possible. In total 12 points were chosen (Figure 4). This number was mainly chosen based on the amount of equipment and time available for the study.

Figure 4: Map of the Playa catchment showing the sampling locations

The collected point data was spatially interpolated using inverse weighed distance (IDW) in ArcGIS. This method was chosen because there was little spatial correlation between the collected data (mainly due to the limited number of sampling points). Therefore geo-statistical interpolation methods such as Kriging - which are generally preferred - could not be implemented.

Below, an overview is given of the required parameters and their method of determination.

Texture (sand, silt and clay fraction)
To determine the soil texture a combination of two methods was used. In the field the soil texture was estimated by the "feel" of the soil (FAO, 1990) .The sand fraction could be validated by taking soil samples to the laboratory and sieving them using a shaker series (the smallest mesh size was 360 µm and therefore only the sand fraction could be determined).

Bulk density (g cm^{-3})

To determine the saturated water content and bulk density of the soil, three intact soil samples were collected at each sampling site using small (100 cc) sampling rings. These soil samples were dried using the microwave method and weighed. The bulk density was then calculated using Equation 2 and averaged for each location:

$$\rho_d = \frac{M_{dry}}{V_c} \quad \textbf{(2)}$$

where M_{dry} (g) is the mass of the soil sample and V_c (cm^3) is the volume of the soil sample.

Volumetric rock content (-)

To determine the volumetric rock content, firstly the rock content by weight was determined by passing a soil sample through a 2 mm sieve and weighing the rock fraction. This was converted to volumetric rock content using Equation 3:

$$V_r = \frac{M_r/\rho_r}{M_s/\rho_s} \times 100 \quad \textbf{(3)}$$

where M_r (g) is the mass of rock in the sample, ρ_r (g cm^{-3}) is the rock density for which the average value of 2.65 g cm^{-3} is taken, M_s (g) is the soil mass and ρ_s (g cm^{-3}) is the bulk density of that soil – its measurement is described above.

Capillary length scale, G (mm)

The capillary length scale, G (mm), was derived from lookup tables based on soil texture (Woolhiser et al., 1990).

Saturated hydraulic conductivity (mm hr^{-1})

The saturated hydraulic conductivity was measured in the field using a tension minidisc infiltrometer. The tension minidisc infiltrometer is a graduated cylinder with a porous membrane through which the water is allowed to infiltrate into the soil. The pressure at which the water is allowed to infiltrate can be set from 0 to -5 cm. The hydraulic conductivity can then be derived from the speed at which the water infiltrates. For measuring the saturated hydraulic conductivity the pressure should be set to 0 or close to 0 (Artiola et al., 2004) so that all pores (including macropores) are allowed to be filled. For this research the pressure was set at -0.5cm, and three measurements were taken per sampling site. It was made sure that the surface of the soil was smooth enough so that there was full contact between the infiltrometer and the soil. To calculate the saturated hydraulic conductivity, a method proposed by Zhang (1997) was used. Using this method, the cumulative infiltration and time are fitted using Equation 4:

$$I = C_1 t + C_2 \sqrt{t} \quad \textbf{(4)}$$

where C_1 (m s^{-1}) is a parameter related to the hydraulic conductivity and C_2 (m s$^{-1/2}$) is a parameter related to the sorptivity. The hydraulic conductivity is then calculated using Equation 5:

$$k = \frac{C_1}{A} \quad \textbf{(5)}$$

where A is a value relating van Genuchten parameters for a given soil type (n (-) and α (-)), with the suction rate, h_0 (cm) and radius, r_0 (cm) of the infiltrometer disk calculated using Equations 6 and 7:

$$A = \frac{11.65(n^{0.1} - 1)\exp[2.92(n - 1.9)\alpha h_0]}{(\alpha r_0)^{0.91}} \qquad n \geq 1.9 \tag{6}$$

$$A = \frac{11.65(n^{0.1} - 1)\exp[7.5(n - 1.9)\alpha h_0]}{(\alpha r_0)^{0.91}} \qquad n < 1.9 \tag{7}$$

These field measurements (which are generally preferred), were validated using intact soil samples and a method derived by Dirksen (1999). At each sampling site, three intact soil samples were taken using small (100 cc) sampling rings and brought to the laboratory where they were left to saturate for 24 hours. Once saturated, a water level of several centimetres was applied on top of the sample. The water level is assured to stay constant by using a Marriott device. The steady water flux density at the bottom of the sample was measured using a beaker on a balance. Using the hydraulic head gradient (Equation 8), the saturated hydraulic conductivity can then be calculated using Darcy's law (Equation 9):

$$\partial H/\partial s = \frac{h_w}{h_s + 1} \tag{8}$$

$$K_s = \frac{q}{\partial H/\partial s} \tag{9}$$

where h_w (cm) is the water level, h_s (cm) is the height of the soil sample and q (cm s^{-1})is the water flux density at the bottom of the sample.

Coefficient of variation, CV (-)

The coefficient of variation of the K_s was calculated from the measured K_s values using Equation 12.:

$$CV = \frac{\sigma}{\mu} \tag{10}$$

where σ (-) and μ (-) are respectively the standard deviation and mean of the measured K_s values.

Pore size distribution index, (-)

The pore size distribution index, λ (-), was derived from lookup tables based on soil texture (Rawls et al., 1982).

Porosity (-)

The soil porosity was calculated using Equation 11:

$$\varphi = 1 - \frac{\rho_s}{\rho_p} \tag{11}$$

Where ρ_s (g cm^{-3}) is the soil bulk density – which was measured (see section 2.3.2) - and ρ_p (g cm^{-3}) is the particle density for which the average value of 2.65g cm^{-3} is taken.

The saturated water content (-)

To determine the saturated water content of the soil, three intact soil samples were collected at each sampling site using small (100 cc) sampling rings. These soil samples were left to saturate for 24 hours and then weighed. After saturation, the samples were dried using the microwave method and weighed again. The saturated water content was then calculated using Equations 12 and averaged for each location:

$$\theta_s = \frac{M_{sat} - M_{dry}}{V_c} \quad \textbf{(12)}$$

where M_{sat} (g) is the mass of the saturated soil sample and M_{dry} (g) is the mass of the dry soil sample, V_c (cm^3) is the volume of the soil sample.

Splash and hydraulic erosion coefficients (-)

The rain splash erosion coefficient was estimated from the soil erodibility factor in the Universal Soil Loss Equation (Wischmeier and Smith, 1978) using a method by Foster et al. (1983) (Equation 13):

$$C_f = 422 K_{USLE}(\emptyset_f) \quad \textbf{(13)}$$

where K_{USLE} is the soil erodibility factor and $\emptyset_f$ (-) is the bare soil factor which accounts for the reduction of splash erosion due to mulch, erosion pavement, and vegetal cover. Its method of determination is explained in Section 2.3.2.

The hydraulic erosion coefficient was estimated from the soil erodibility factor in the Universal Soil Loss Equation (Wischmeier and Smith, 1978) and the fractional clay content using a method by Foster and Smith (1984) (Equations 14 and 15):

$$C_g = 5.6 K_{USLE} \emptyset_r / A_t \quad \textbf{(14)}$$

$$A_T = \begin{cases} 188 - 468 f_{cl} + 907 {f_{cl}}^2, & f_{cl} \leq 0.22 \\ 130, & f_{cl} > 0.22 \end{cases} \quad \textbf{(15)}$$

where $\emptyset_r$ (-) accounts for erosion resistance due to management practises (bunds, terraces), and f_{cl} (-) is the fractional clay content. As there are no real management practises in place in the Playa catchment, the $\emptyset_r$ was kept at one.

The K_{USLE} was derived from soil texture, structure, organic matter content and permeability using the soil erodibility nomograph (Wischmeier et al., 1971). The measurement of texture and permeability (in this case the K_s was used) is described above. The measurement of the organic matter content and soil structure is described below.

The organic matter content was estimated using the Munsell colour of a dry and moist soil sample (Munsell Colour Company, 1994). This estimation is based on the assumption that the soil is coloured due to a mixture of light coloured minerals and dark coloured organic substances(FAO, 1990). A conversion table from Schlichting, Blume et all (1995) was used to convert the Munsell colour values to organic matter content values. It must be stressed that this method only gives a rough estimate (FAO, 1990). For our purpose though, this estimate should be sufficient.

The soil structure was determined at each sampling site by using the drop-shatter method (Marshall and Quirk, 1950), whereby a section of top soil is dug and dropped from around one meter onto a board. If large clods break away they are dropped again individually. Next the median size and type of aggregate was determined using the size and type classes described by the FAO (1990).

2.3.2 land surface parameters

Land cover classification (Manning's coefficient, ground- and canopy cover)
Using a combination of field observations and aerial photographs (Google earth V 7.0.3.8542, 01-21-2012), the watershed was split up in a number of land cover classes. For each land cover class the bare soil factor ($Ø_f$), vegetation cover and Manning's roughness coefficient (n) was estimated at the beginning of the rainy season (September) and towards the end of the rainy season (December).

The Manning's roughness coefficient (n), is needed to calculate the velocity of overland flow and was estimated for each land cover class using literature (Engman, 1986, Crawford and Linsley, 1966, Woolhiser, 1975).

The vegetation cover is needed to calculate the total depth of interception. It is defined as the fraction of the surface covered by vegetation which was estimated for each land cover class in the field.

The bare soil factor ($Ø_f$) accounts for the reduction of splash erosion due to mulch, erosion pavement, and vegetal cover. It is estimated by the fraction of bare soil and the fraction of the canopy cover above bare soil multiplied by a canopy subfactor value (see Figure 5). The canopy subfactor value accounts for the damping effect of the canopy on rainfall energy and depends on the height of the canopy (Foster and Dissmeyer, 1981).

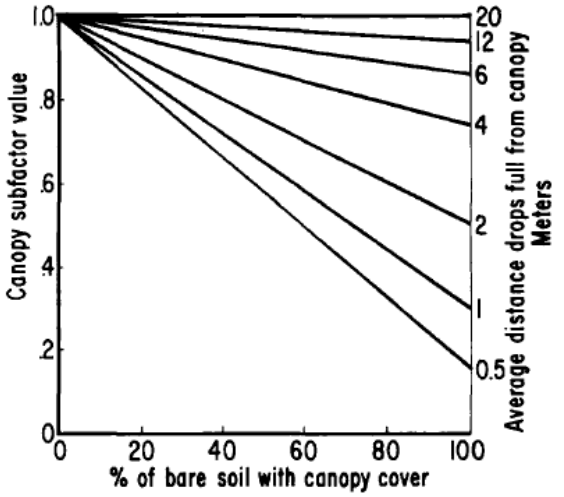

Figure 5: Effect of canopy cover on rain splash erosion (Foster and Dissmeyer, 1981)

Slope
A DEM of the watershed was created by combining old topographical maps from the low-lying coastal area – obtained from the Bonaire Cadastre (KLM Aerocarto, 1963) - with the freely available SRTM DEM (Jarvis et al., 2008) for the rest of the catchment. It was chosen not to rely on the SRTM DEM for the low-lying coastal area because the variation in height there is lower than the elevation error of the SRTM data.

The SRTM DEM has a spatial resolution of 90m and for islands it was found to have an absolute height error of 8 m and an absolute geolocation error of 9m at the 90% confidence interval (Rodriguez et al., 2006). In ArcGIS, a low pass filter was applied to remove height anomalies and sinks were removed as well. The DEM was validated using a number reference height points taken in the catchment using GPS. It was found that the SRTM DEM had elevations that were systematically 1m too high and this was therefore corrected.

The topographical maps from the Bonaire Cadastre were digitized and converted to a DEM in ArcGIS. This DEM was validated using a number of reference height points taken using GPS and it proved to be reliable.

In ArcGIS the two DEMs were first resampled to have the same cell size of 10 m by 10 m and then blended together using the Mosaic tool. From this DEM the slope in the catchment was calculated.

Interception
For the interception depth a value of 3 mm was taken (typical for shrub-lands) (Woolhiser et al., 1990).

Paved surface area
The paved surface area in the catchment was determined from aerial photographs obtained from Google Earth (01-21-2012).

2.3.3 Channel parameters

Channel geometry
The channel geometry was measured in the field. The slope of the channels was estimated by taking GPS height readings (using a Leica Viva GNSS-GS15, accuracy of 0.01m) at the beginning and end of each channel section.

Between the reservoirs in the uplands there are no real channels. Between some reservoirs there is a gully and between others it is simply overland flow. These gullies or flow routes are therefore all modelled as triangular, having side slopes of 20%, and a Manning's roughness coefficient of 0.05 s $m^{-1/3}$ (floodplain, scattered brush, heavy weeds). Figure 6 shows the location of the gullies or flow routes and the channels

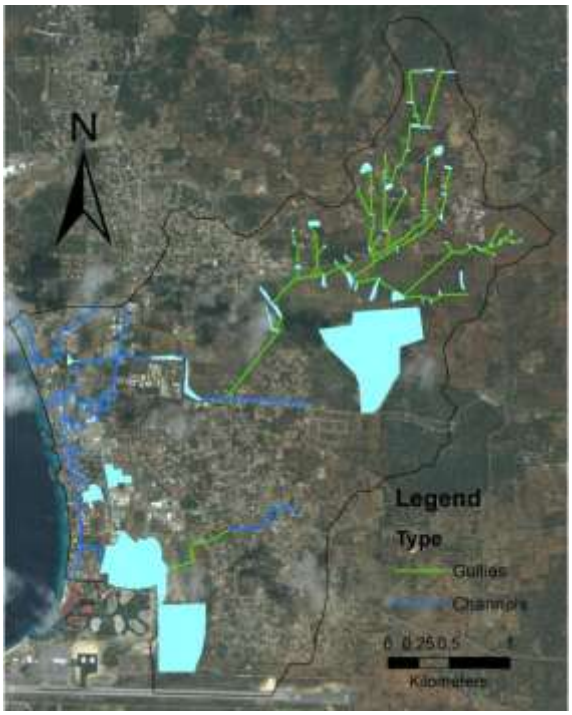

Figure 6: Gullies and channels

Manning's roughness coefficient
The Manning's roughness coefficient (n) of the channels was estimated using lookup tables from Chow (1959).

Channel soil
For unlined channels, the soil parameters required for calculating infiltration and erosion (e.g. K_s, G, texture, erodibility), were taken from the same sampled soil data as for the planes.

2.3.4 Pond parameters

Pond geometry
To estimate the storage capacity of the reservoirs, the area of the reservoirs was mapped using a GPS device. The depth of these reservoirs was measured using a measuring rod. Multiplying the area of the reservoir by its depth gives its volume. It was noted that due to the slope of the land, more water can be stored behind the dam than simply in its basin (see Figure 7). This volume was estimated using the slope angle (obtained from the DEM) and simple trigonometry.

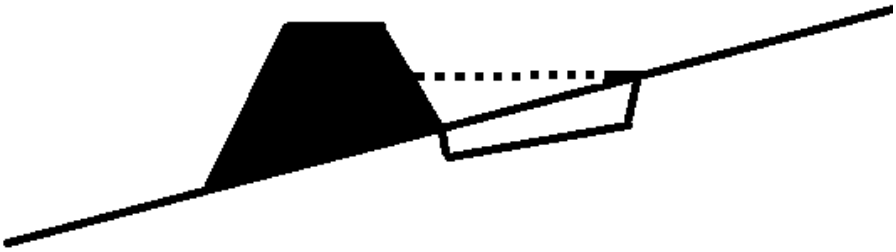
Figure 7: Reservoir storage capacity

Saturated hydraulic conductivity

Due to deposition of finer sediment and compaction at the time of construction of the reservoirs, the hydraulic conductivity of the soil beneath the reservoirs is believed to be a lot lower than that of the surrounding soils (Debrot et al., 2010). Using the interpolated sampled soil data (measured using the mini-disc infiltrometer) would therefore give erroneous results. For this reason it was decided to measure the K_s behind one of the reservoirs separately (the large LVV reservoir) and use this value for the other reservoirs as well.

To measure the K_s of this reservoir, a diver was placed in it and the water height was measured every five minutes for a period of three months. Water level data was extracted for time series during which there was no rainfall and the change in water level was therefore only determined by infiltration and evaporation.

The infiltration during these time series was calculated by determining the change in water level between every time step and subtracting from this the evaporation. The evaporation was estimated using the following formula from Allen et al. (1998):

$$ET = ET_0 C_w \quad \textbf{(16)}$$

where ET_0 (mm) is the reference evapotranspiration for which the calculation is shown in Annex 1. C_w (-) is the coefficient of evaporation of an open water body. For water bodies less than 2 m deep, a value of 1.05 can be taken (Allen et al., 1998).

The saturated hydraulic conductivity of the reservoir was calculated using a method described by Reynolds and Elrick (1991) whereby Equation 17 (Gardner, 1958, Wooding, 1968) is logarithmically transformed to produce Equation 18:

$$I_s = \left(\frac{1}{0.25\pi r\alpha} + 1\right) K_s exp(\alpha H_0) \quad \textbf{(17)}$$

$$Ln(I_s) = \alpha H_0 + ln\left[\left(\frac{1}{0.25\pi r\alpha} + 1\right) K_s\right] \quad \textbf{(18)}$$

where I_s (mm hr^{-1}) is the steady state infiltration rate, r (mm) is the pond radius, H_0 (mm) is the pressure head at infiltration surface and α (-) is a soil parameter.

When $Ln(I_s)$ is then plotted for a number of different pressure heads (H_0), a line can be drawn through the points and the K_s can be found from the intercept.

Pond outflow

Because the relationship between reservoir height outflow could not be measured, this was calculated. After an initial entry head loss, depending on the speed of the outflow, the flow will attain the normal depth. The discharge out of the reservoir can therefore be calculated using Manning and the entry head loss is estimated by Equation 19 (Hamill, 2001):

$$\Delta_{ls} = \frac{0.5V^2}{2g} \quad \textbf{(19)}$$

where Δ_{ls} (m) is the entry head loss and V (m s^{-1}) is the velocity of the water in the outflowing channel.

2.4 Calibration

The calibration of the model was performed by comparing measured discharge with modelled discharged for three rainfall events. Only three events were chosen because during the fieldwork period there were only three large enough events which fell evenly enough over the whole catchment. Because the rainfall on Bonaire is extremely spatially variable, most rainfall only reaches parts of the catchment and measured rainfall data was not available on enough locations to account for this spatial variation.

Due to the extreme spatial variability of rainfall it was not possible to calibrate the hydrograph timing. The exact time of rainfall was only known at the location of the tipping bucket and not in the rest of the catchment. However due to the small size of the catchment and the urban nature, the lag time is very short (estimated at 20-60 min, depending on whether reservoirs overflow (Taylor and Schwarz, 1952)) and therefore the timing of the modelled discharge can never be too far off reality.

Following the recommendations from Kalin and Hantush (2003), the discharge magnitude was calibrated by adjusting the saturated hydraulic conductivity (K_s) and the capillary length scale (G). For both K_s and G, a multiplication factor was used for model calibration. In this way, the measured spatial variation in K_s and G is not affected.

Due to insufficient data, it was also not possible to calibrate the model for sediment yield. The rainfall events Therefore, absolute sediment yields and soil losses are not calculated and only the spatial distribution and differences between modelling scenarios are considered.

The following sections describe the collection of the discharge data for the three rainfall events and the collection of the input variables (initial soil moisture content and rainfall intensity) required to model these three events.

2.4.1 Discharge

Divers (Di250, van Essen instruments, accuracy of 0.1%) were installed at three locations (LVV reservoir, Kralendijk reservoir, and the outlet of sub-catchment 1), taking pressure readings at five minute intervals. The location of the three divers is shown in Figure 8. A fourth diver was installed on land to measure the atmospheric pressure.

Using the pressure readings of these divers, the height of the water column at these locations was calculated using Equation 20:

$$WC = P_{diver} - P_{atm} \quad \textbf{(20)}$$

where WC is the height of the water column (cm), P_{diver} (cm h_2O) is the diver pressure and P_{atm} (cm h_2o) is the atmospheric pressure.

From the water level readings of the outlet of sub-catchment 1, the runoff peaks were extracted and converted to discharge ($m^3\ s^{-1}$) using Manning's equation (which was possible because of the distinct profile of the channel).

The water level readings of the LVV and Kralendijk reservoirs were firstly smoothened out using a three point moving average to remove the random measurement errors (diver error). Then the water level readings were converted to water volume using the measured dimensions of the reservoirs (See Annex 2) and lastly, the change in water volume over time ($m^3\ s^{-1}$) was

computed. Removing the random measurement errors of the diver by averaging out the water level readings was found to be necessary because these small variations in water level had a large (and erroneous effect) effect on the calculated change in water volume over time. A three point moving average was chosen because it managed to remove the random variation without losing too much valuable information.

2.4.2 Rainfall

Rainfall intensity data was available from the tipping bucket and daily rainfall totals were available from a station at the coast and at the airport (see Figure 8). The daily rainfall data from the airport station were excluded from the analysis as they were found to be unreliable. On some occasions rainfall seemed to be recorded on the wrong day and on other occasions when it had certainly rained, the airport station did not report any rainfall.

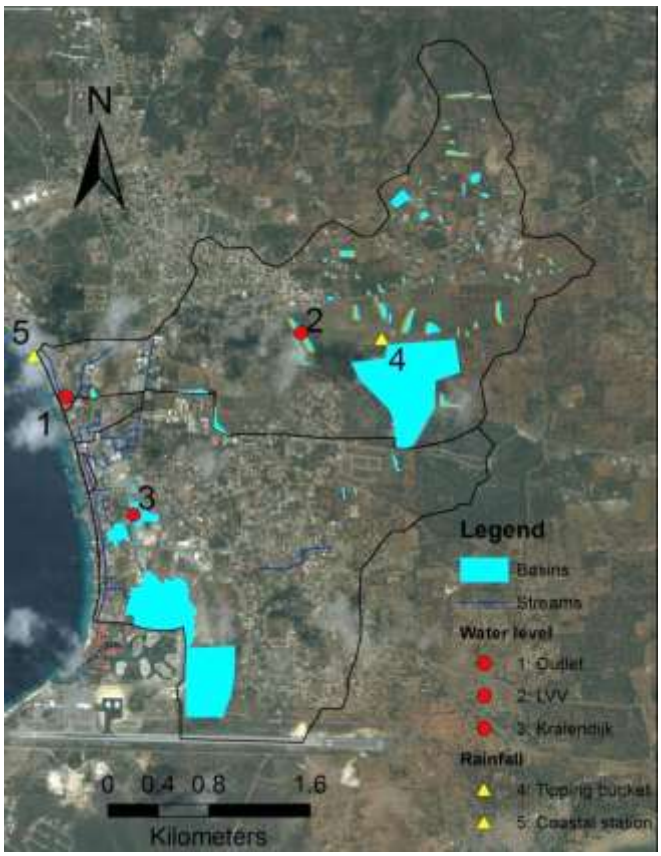

Figure 8: Location of the measurement locations and rainfall gauges

The daily rainfall values at the coast were converted to intensity by assuming the same temporal and intensity distribution as measured by the tipping bucket. The intensities at the coast and tipping bucket were then both used as input for Kineros2, which spatially interpolates the rainfall using an inverse distance weight method.

2.4.3 Initial soil moisture content

The initial soil moisture content for calibration was calculated using a simple water budget model as described by Willmott and Rowe (1985):

$$w_d = w_{d-1} + \beta_d D_d \quad \textbf{(21)}$$

where w_d (mm) is the soil moisture content on day d, w_{d-1} (mm) is the soil moisture content on the previous day and recharge or evapotranspiration is described by the term $\beta_d D_d$ (mm). The maximum soil moisture content on a given day (w_d) is equal to field capacity.

D_d (mm) is the evaporative demand on day d:

$$D_d = P_d - ET_d^0 \quad \textbf{(22)}$$

where P_p (mm) is the precipitation on day d and ET^0_d (mm) is the reference evapotranspiration on day d for which the calculation is shown in Annex 1. When D_d is negative it represents a demand, when it is positive it represents a recharge.

β_d is the evapotranspirated fraction on day d coming from Mintz and Serafini (1984) who based their function on measurements of Davies and Allen (1973) on fields with a continuous cover of perennial rye grass:

$$\beta_d = \begin{cases} 1 - exp(-6.68 w_{d-1}/W^*), & D_d < 0 \\ 1, & D_d \geq 0 \end{cases} \quad \textbf{(23)}$$

where W^* (mm) is the total available water holding capacity for a soil layer, calculated as the difference between the wilting point and field capacity for a certain soil depth. For this study it was decided to model soil moisture for the top 10 cm of the soil because this soil section has the largest effect on the production of surface runoff (Zhang et al., 2011). The values for the soil moisture content at wilting point and at field capacity were obtained per soil texture from literature (ASCE, 1990).

The initial soil moisture content was calculated for each of the 12 sampling locations (because the soil type was known for these locations) and then interpolated for the whole catchment using inverse weighed distance (IDW). Using this method, only the spatial variation of soil type is taken into account and not that of vegetation cover or slope which also have an effect on the soil moisture content. However within the timespan of this research it was not possible to take this into account as well, and as the initial soil moisture content is only needed for model calibration a good estimate is sufficient.

To validate the outcome of this water budget model, the soil moisture content was measured on the 12 sampling points in the catchment on three occasions. Per occasion, two soil core samples were taken per sampling location of the top 10 cm of the soil and taken to the laboratory. These samples were weighed, dried (using the microwave method) and weighed again to determine the soil moisture content. These measured soil moisture content values were then compared to the modelled soil moisture content values. The root mean square error was calculated as percentage of the mean soil moisture content to assess the accuracy of the model predictions using Equation 24:

$$RMSE = \sqrt{\frac{1}{n}\sum_{i=1}^{n}(X_i - Y_i)^2} \quad \textbf{(24)}$$

where n is the number of observations X_i are the measured values and Y_i are the modelled values

Validation results

Figure 9 shows the measured soil moisture content plotted against the modelled soil moisture content. The actual values can be found in Annex 3. It can be seen that simple water budget model tends to slightly underestimate the soil moisture content. The root mean square error as percentage of the mean soil moisture content was found to by 25% which is acceptable. The prediction error is most likely caused by variations in slope and vegetation cover which are not included in the simple water budget model.

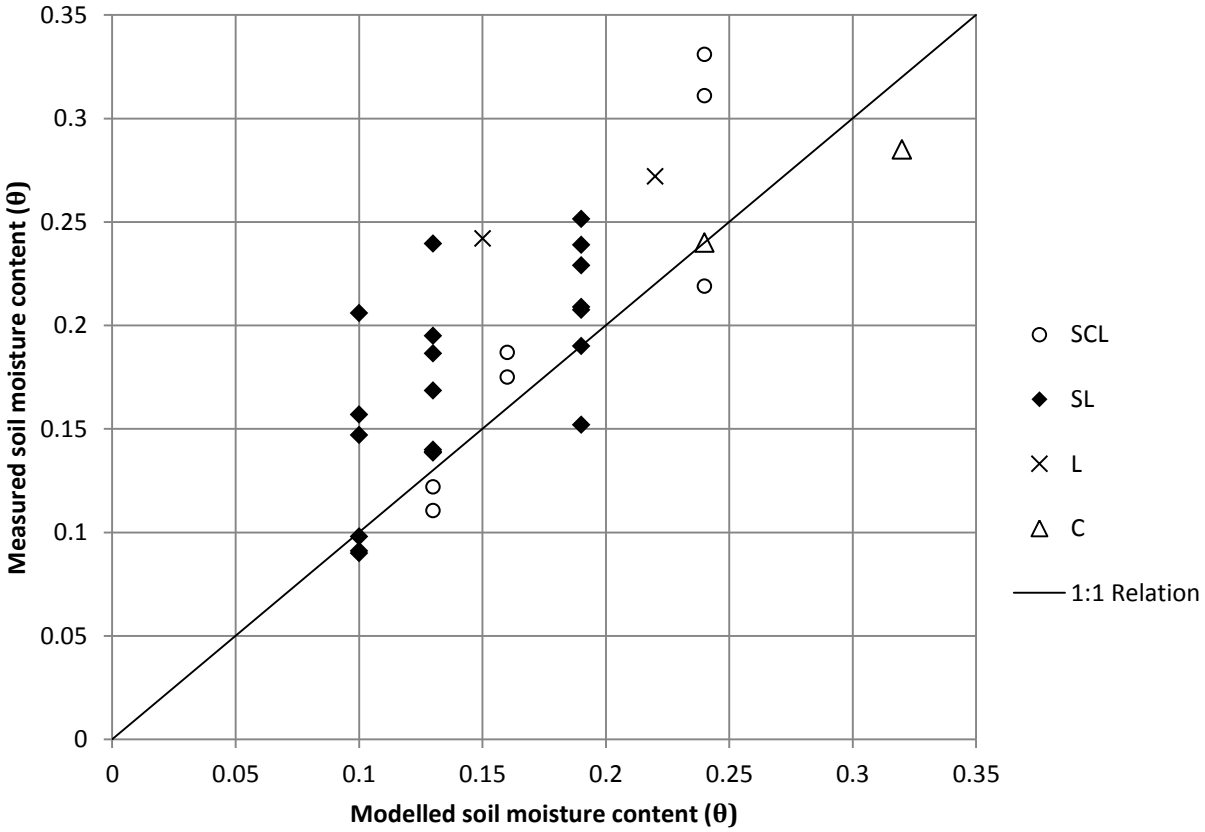

Figure 9: Measured versus modelled initial soil moisture content

2.5 Model runs

After the model had been calibrated it was run for the current management situation, three different physical scenarios and three different management scenarios. Unless specifically stated, the watershed was modelled with the initial soil moisture content at wilting point, no initial reservoir storage and with a vegetation cover equal to that found towards the end of the rainy season.

For modelling runoff and erosion for the current management situation, design storms with a return period of five and ten years were chosen. These return periods were chosen because flooding problems in Kralendijk and large sediment flows towards sea are only encountered during the more extreme events. Furthermore it was found that during a five year event only some of the reservoirs overflow while during a ten year event almost all of the reservoirs overflow. Modelling and comparing runoff and erosion for these two events therefore gives a good picture of the effect of these reservoirs. Using rainfall events with even larger return periods was deemed unnecessary, also because this can affect the accuracy of the model predictions.

2.5.1 Current management

Catchment runoff and erosion
Runoff and erosion for the current management situation was modelled for a design storm with return period of five years and ten years to see how much runoff and erosion is produced at each location in the catchment and also how this is routed towards the outlets.

Drainage capacity
To see if the drainage capacity of the channels in Kralendijk is large enough to drain the runoff caused by a five year and ten year event, the maximum discharge produced by the rainfall events is compared to the drainage capacity of the channels, calculated using Manning's equation.

2.5.2 Physical scenarios

Long-duration versus high-intensity rainfall
To understand the difference in effect between high intensity rainfall and long-duration rainfall, runoff and erosion was modelled for two successive rainfall events, each having half the intensity of an event with a return period of five years. The total rainfall is therefore the same as an event with return period of five years, but the duration is doubled (four hours).

Soil moisture content
To understand how runoff and erosion is affected by different initial soil moisture contents, runoff and erosion was modelled for a rainfall event with return period of five years and with the initial soil moisture content at field capacity.

Dry-season vegetation
The vegetation cover at the end of the rainy season was observed to be much higher than the vegetation cover at the start of the rainy season. The runoff and erosion produced by a rainfall event at the beginning of the rainy season is therefore different from that produced by a rainfall event towards the end of the rainy season. To test the effect that the difference in vegetation cover has, runoff and erosion was also modelled for the vegetation cover occurring at the start of the rainy season for a rainfall event with return period of five years.

2.5.3 Management scenarios

Loss of reservoirs
In past times, almost every family had their own 'kunuku' –a small subsistence farm with some fields of sorghum, small scale fruit and vegetable production (e.g. cucumbers and maize), and livestock (mainly goats) (Pers. Com. Wolter di Palm, 2012). Small reservoirs –'tankis' - would be dug on the 'kunuku' to store and supply water for small-scale irrigation. In the 1950s, the government constructed reservoirs on public land. These were larger and usually placed in 'rooien' with the main aim of increasing groundwater recharge (Pers. Com. Rocky Emers, 2012).

Presently, many of the 'kunukus' have been deserted and others are only used for hobby farming. Many of the 'tankis' are therefore not used anymore and therefore also not maintained (Pers. Com. Rocky Emers, 2012). Maintenance of the government reservoirs (especially sdiment removal) is done on an ad-hoc basis. The reservoirs closest to Kralendijk have gotten a legal status and are enlisted in the Bonaire Development Plan (DRO, 2010) as freshwater areas. Because they are important in preventing flooding in the residential areas, they are maintained and cleaned whenever it is deemed necessary (every 1 to 5 years) by the DRO (Dienst Ruimtelijke Ordening) (Pers. Com. Jeroen Meuleman, 2012). The reservoirs on LVV territory are

sometimes maintained by LVV. The governmental reservoirs in the uplands are maintained by the DRO once in while if funding permits and need for maintenance is pressing .

To understand the importance of the reservoirs in the Playa catchment and the effect of losing 'tankis' due to lack of maintenance, runoff was modelled for a rainfall event with return period of ten years (because this event causes most reservoirs to overflow) for the scenario in which all 'tankis' are gone. This is a decrease in storage capacity of 20600m^3.

Reduced grazing (maximum vegetation cover)

Overgrazing – especially due to goats – is a well-known problem on Bonaire. It was estimated that there are 25000-26000 goats on the island and 5000 sheep (Nolet and Veen, 2009). The goats are left to roam freely so that feeding them is unnecessary. This saves money and allows the owners to keep more goats (Debrot et al., 2012). Officially goats are forbidden to roam freely, however this law is not being enforced.

The carrying capacity of Bonaire is estimated at 14 goats per hectare during the rainy season and 1 goat per hectare during the dry season. At the moment it is estimated that there are around 4 goats per hectare (Nolet and Veen, 2009), meaning that for the largest part of the year, the carrying capacity is being exceeded.

The consequences of this overgrazing are reduced vegetation cover, a reduced rate of succession to mature forests, and decline or elimination of grazing sensitive species while grazing resistant species (often thorny) are given a competitive release (De Freitas et al., 2005). This decrease in vegetation cover has in its turn lead to increased soil erosion due to the reduction in root cover, organic matter content, surface roughness and rainfall interception (Morgan, 2005). For this reason plans are being made to reduce the grazing pressure of these goats.

Figure 10: Fenced grassland to the right and grazed land to the left

To understand the effect that reduced grazing would have on runoff and erosion in the catchment, runoff and erosion was modelled for a rainfall event with a return period of five years on a catchment with maximum vegetation cover. A catchment with maximum vegetation cover is defined as a catchment where all the land use classes have been converted to 'dense shrub-land', except for the urban areas and maize fields. It is believed that if the grazing pressure would be reduced the difference in vegetation cover between the start and end of the rainy season would also be reduced. The reason for this is that mainly the grazers are to blame for bare soils in the dry season (Pers. Com Jan-Jaap van Almenkerk, 2012). Areas which have been

fenced for a number of years show a healthy ground cover both in the dry and wet season – the colour of the vegetation being the main difference (see Figure 10).

Reducing the paved surface area

Except for changing the vegetation cover, another management option is to change the percentage of paved area. In densely built areas such as central Kralendijk there might not be enough space to seriously reduce the amount of pavement but there are other indirect methods which have the same effect in improving infiltration. Examples are permeable asphalt, "swells" (gravel beds below a lawn) and infiltration wells (Niemczynowicz, 1999).

To estimate the effect of reducing the amount of pavement (especially in central Kralendijk), runoff and erosion was modelled for a rainfall event with return period of five years when paved area is reduced by 10% and 20% respectively.

2.5.4 Design storms

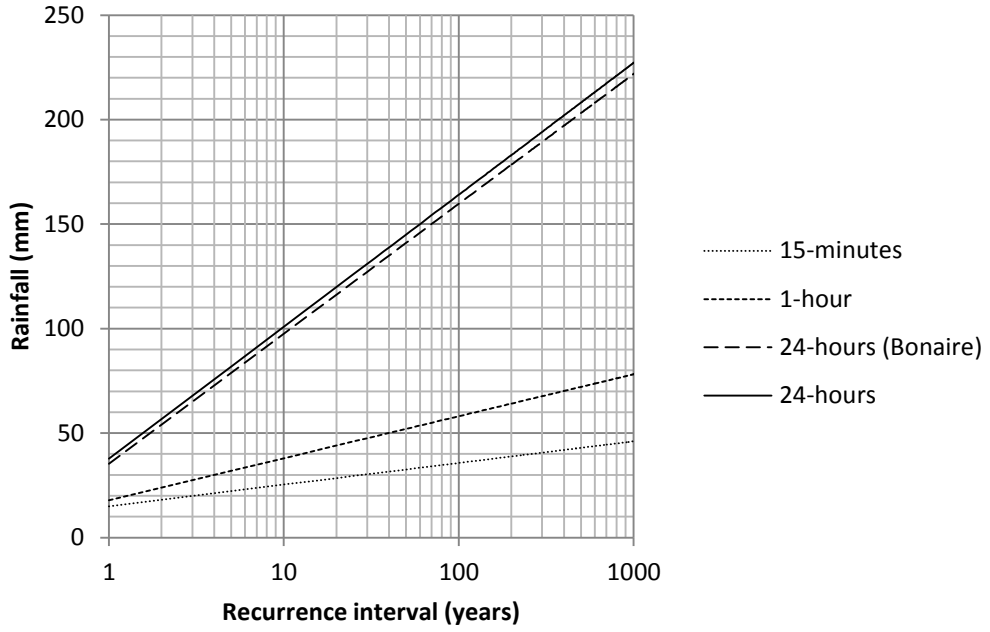

Figure 11: Plot of rainfall depth versus the recurrence interval for a number of rainfall durations

Design storms with a return period of five and ten years were calculated using historical rainfall intensity records. As such data is not available for Bonaire, data from Curacao was used instead. Figure 11 was obtained from the meteorological department of the Netherlands Antilles at Hato Airport, Curacao, and shows the recurrence interval of different rainfall depths and durations. In Figure 8, the 24 hour rainfall on Curacao is compared with the 24 hour rainfall on Bonaire and it can be seen to be very comparable.

Using the data from Figure 11, a depth duration frequency (DDF) curve is fitted for rainfall with a return period of 5 years using a power relation:

$$r = a \times d^b \quad \textbf{(25)}$$

where r is the rainfall depth (mm), d is the duration (min) and a and b are DDF parameters. The least square approach was used in order to optimize the DDF parameters (Chow et al., 1988).

Figure 12 shows the produced DDF curves for Bonaire with a return period of 5 years and 10 with the fitted equations.

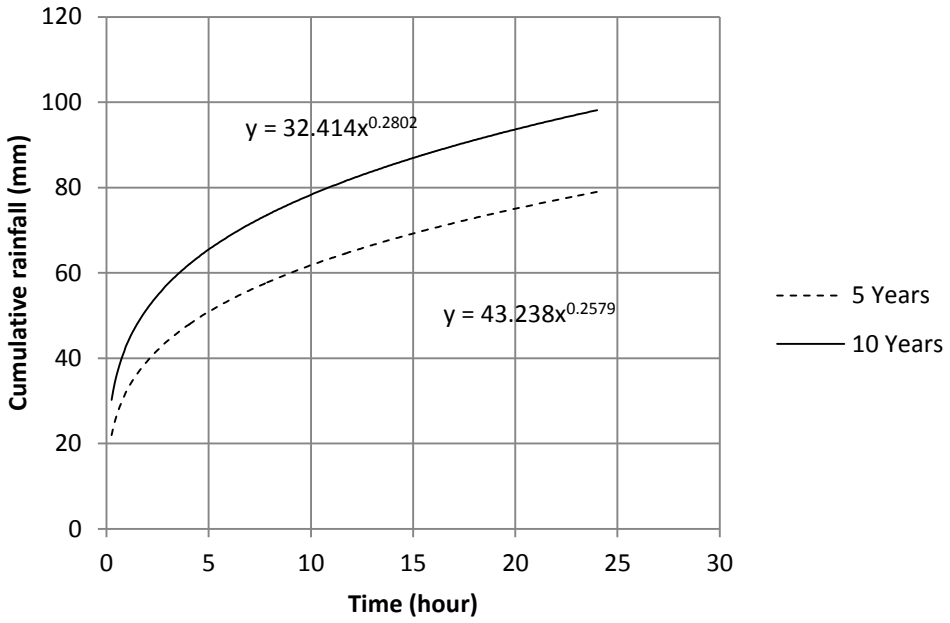

Figure 12: Depth duration frequency curves for return periods of five and ten years

Using this DDF curve a design storm was obtained using the composite storm concept. A composite storm is determined by setting out the rainfall volumes from the DDF relationship symmetrically around the centre of the storm starting from the shortest till the longest storm duration.

For small watersheds, the total duration of the design storm should be at least equal to the time of concentration or preferably longer (Vaes, 1999). The time of concentration was found to be between one and two hours and therefore a total duration of two hours was taken. This is also roughly the maximum storm duration encountered during the rainy season of 2012/2013. The time interval was taken to be 15min. This was chosen because it was the minimum duration for which a return period was available and the DDF curve tends to overestimate rainfall intensities at smaller time steps (Di Baldassarre et al., 2006).

3. Results

3.1 Soil properties

The soils in the Playa catchment were found to predominantly contain sandy loam and sandy clay loam. They were found to have low organic matter contents (around 2% on most locations) and a good structure. On the sites with sandy loam, the saturated hydraulic conductivity was found to be around 30 mm hr^{-1} (in agreement with literature such as Rawls et al. (1982)). On some of the more clayey sites however the saturated hydraulic conductivity was found to be a lot higher (around 70-100mm hr^{-1}). This largely disagrees with literature (according to Rawls et al. (1982) sandy clay loams should have a K_s of around 4mm hr^{-1}) but can be attributed to the large number of cracks in the soil.

The rock content varied between 1-20% and the bulk density was usually around 1.30g cm^{-3}. Both the porosity and maximum saturation content ranged between 0.5-0.6 (cm^3 cm^{-3}).

Detailed results can be found in Annex 3.

3.2 Planes, channels and ponds

The schematization of the Playa catchment into plane, pond and channel elements is shown in Figure 13. Channel and pond geometry data can be found in Annex 4 and 5 respectively.

The saturated hydraulic conductivity of the reservoir behind the LVV reservoir was found to be 0.215 mm hr^{-1} – roughly one hundred times smaller than the soils surrounding it.

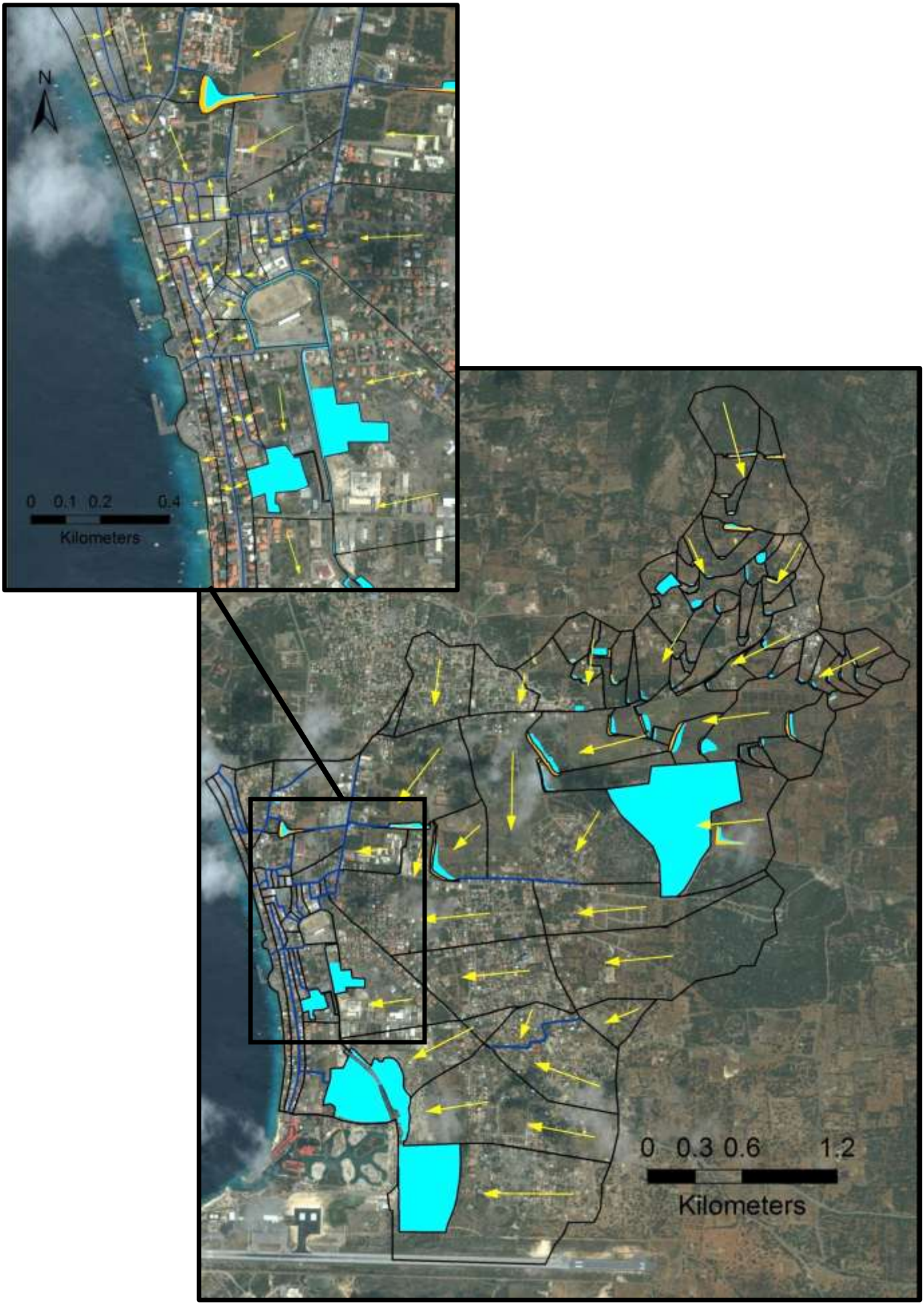

Figure 13: Schematization of Playa catchment showing planes, streams, ponds and flow direction

3.3 Land surface parameters

3.3.1 Land cover classification (Manning's coefficient, ground- and canopy cover)

Table 1 shows the land cover classes and their associated parameters in September (start of the rainy season) and December (the maximum vegetation cover has been reached). Figure 14 shows how the land cover types are distributed over the catchment. It was found that in the beginning of the rainy season the ground was almost bare while towards the end of the rainy season there was a healthy groundcover consisting of grasses and weeds. This is what leads to the lower bare soil factor ($\emptyset_f$), the larger vegetation cover and the larger Manning's roughness coefficient (n) . Pictures of the created land use classes can be found in Annex 6.

Table 1: Land cover classes in the Playa catchment and their associated parameters at the start and towards the end of the rainy season

	September (start of rainy season)			December (during rainy season)		
Land cover class	Manning's n (s $m^{-1/3}$)	Bare soil factor (-)	Vegetation cover (%)	Manning's n (s $m^{-1/3}$)	Bare soil factor (-)	Vegetation cover (%
Dense Shrubbery	0.25	0.60	85	0.40	0.15	90
Medium Shrubbery	0.20	0.80	60	0.30	0.40	75
Light Shrubbery	0.15	0.85	35	0.20	0.60	55
Dense grass	0.10	0.90	20	0.20	0.40	55
Rangeland (medium cover)	0.10	0.90	20	0.15	0.55	45
Rangeland (light cover)	0.05	0.95	15	0.10	0.70	35
Agricultural field	0.05	1.00	0	0.20	0.50	50
Bare	0.05	0.95	5	0.05	0.90	5
Urban	0.50	0.10	20	0.50	0.40	45

3.3.2 Slope and Paved surface area

Figure 15 and Figure 16 show respectively the paved surface area and slope in the Playa catchment

.

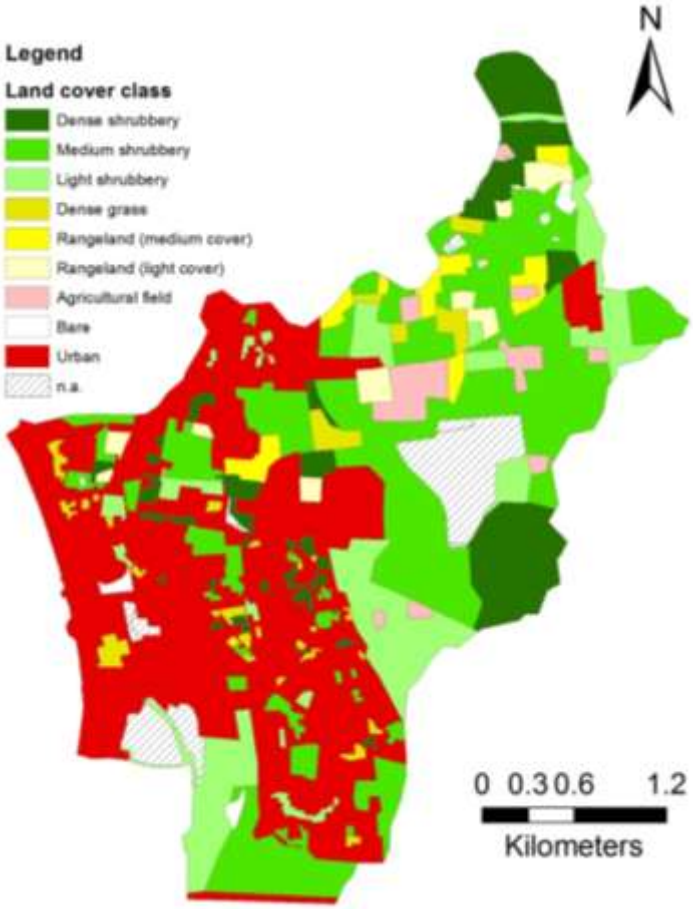

Figure 14: Land cover classes in the Playa catchment

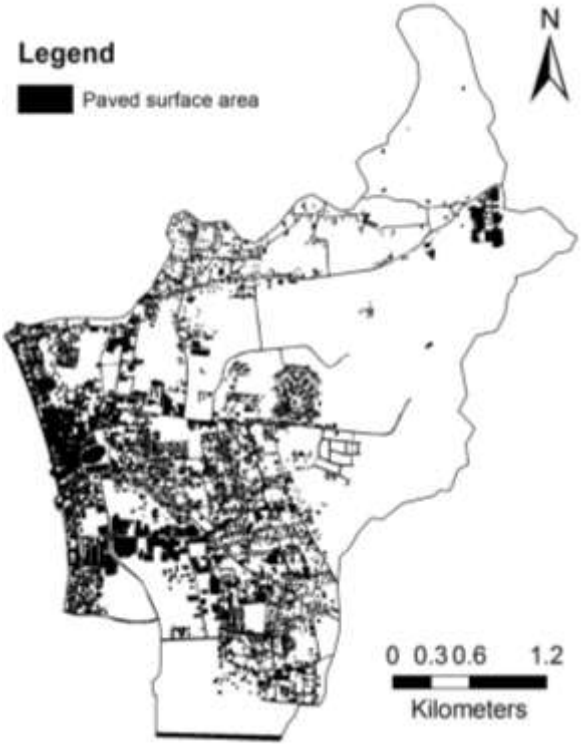

Figure 12: Paved surface area

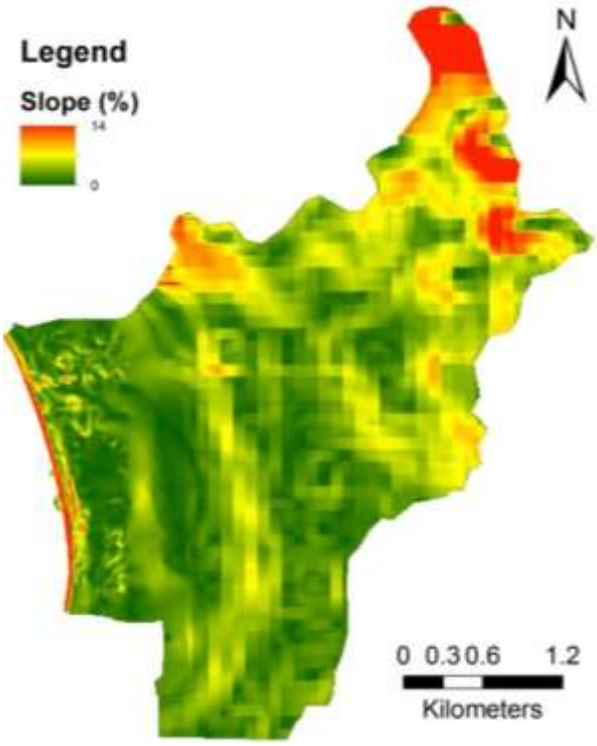

Figure 16: Slope

3.4 Calibration results

The three different rainfall events used for calibration are shown in Figure 17 and compared to a rainfall event with a five year and ten year return period (which are used for modelling in this study). It can be seen that the peak intensity, total rainfall and rainfall duration of the three rainfall events is a lot smaller than that of a five and ten year event. It can therefore not be confidently said that the catchment will behave exactly the same for this five and ten year event.

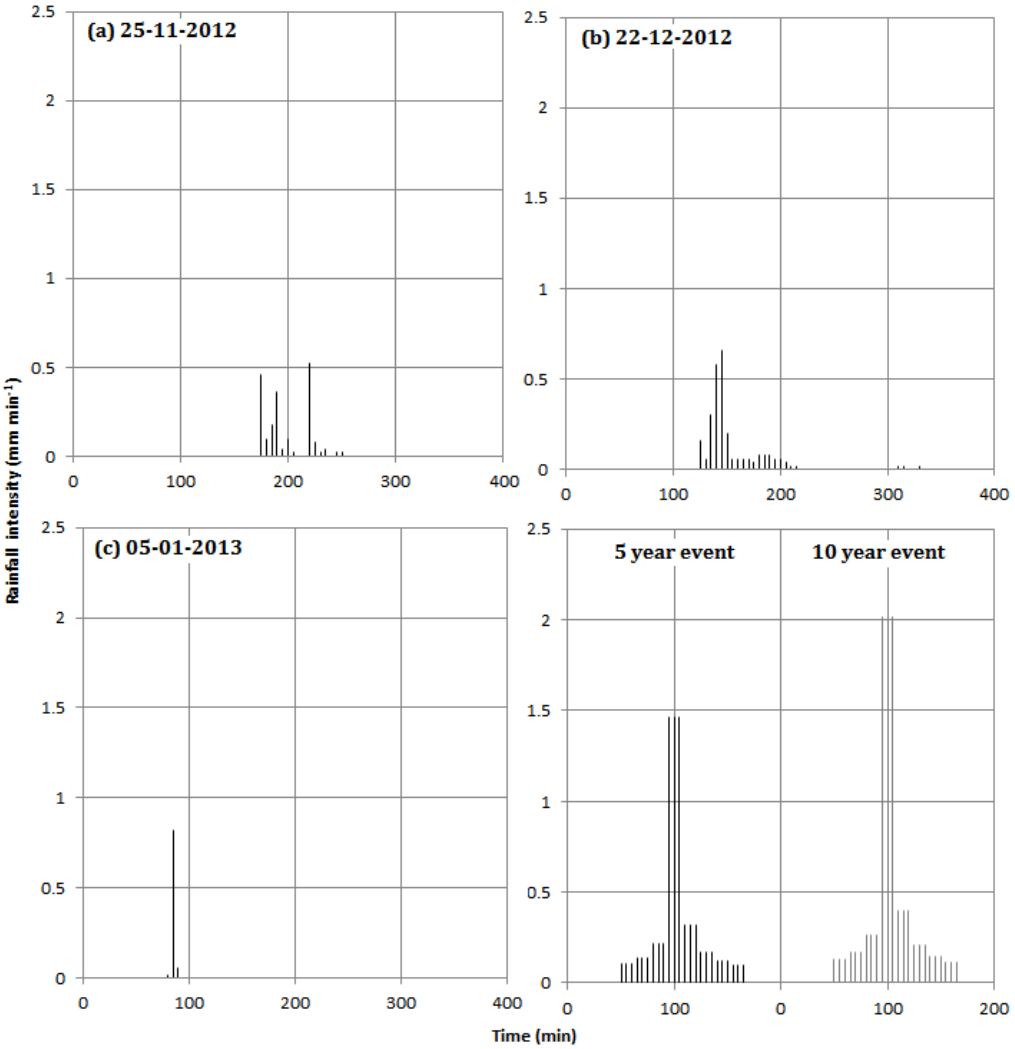

Figure 17: Rainfall events used for calibration compared to those with a return period of five and ten years

To get the best discharge magnitude simulations, the required multiplication factors for K_s and G were found to be 0.1 and 0.3 respectively. These values are large but not unusual - similar multiplication factors, especially for K_s and G were found in a number of papers (Smith et al., 1999, Kennedy et al., 2012).

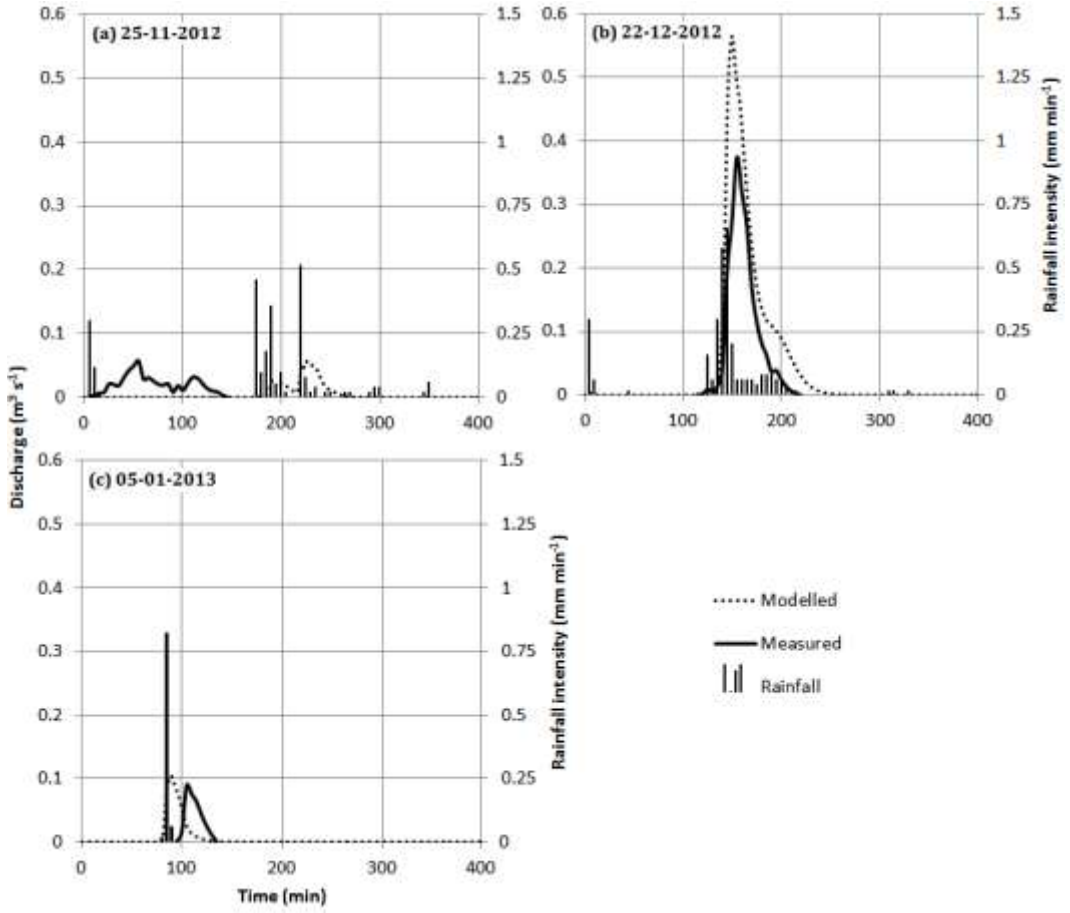

Figure 18: Graphs showing modelled and measured discharge at the outlet of sub-catchment 1 for a rainfall event on a) 25-11-2012, b) 22-12-2012 and c) 05-01-2013.

Figure 18 shows the measured and modelled discharge for the outlet of sub-catchment 1 for the three different rainfall events. As explained before, discharge timing could not be calibrated. Focussing on the discharge quantity therefore, the events on 25-11 and 05-01 are modelled relatively well, the discharge quantity of the event on 22-12 is largely overestimated (see Table 2). The reason for this could be the spatial variability in rainfall intensity. It is unlikely that the model simply overestimates larger rainfall events because this same rainfall event did not cause the same amount of error at the other two measurement locations (the Kralendijk and LVV reservoir).

Table 2: Accuracy of model predictions for sub-catchment 1

Rainfall event	Peak discharge ($m^3 s^{-1}$)			Total discharge (m^3)		
	Measured	Modelled	**% difference**	Measured	Modelled	**% difference**
25-11-2012	0.06	0.06	**1**	177	114	**36**
22-12-2012	0.37	0.57	**53**	615	1075	**75**
05-01-2013	0.09	0.10	**17**	95	117	**23**

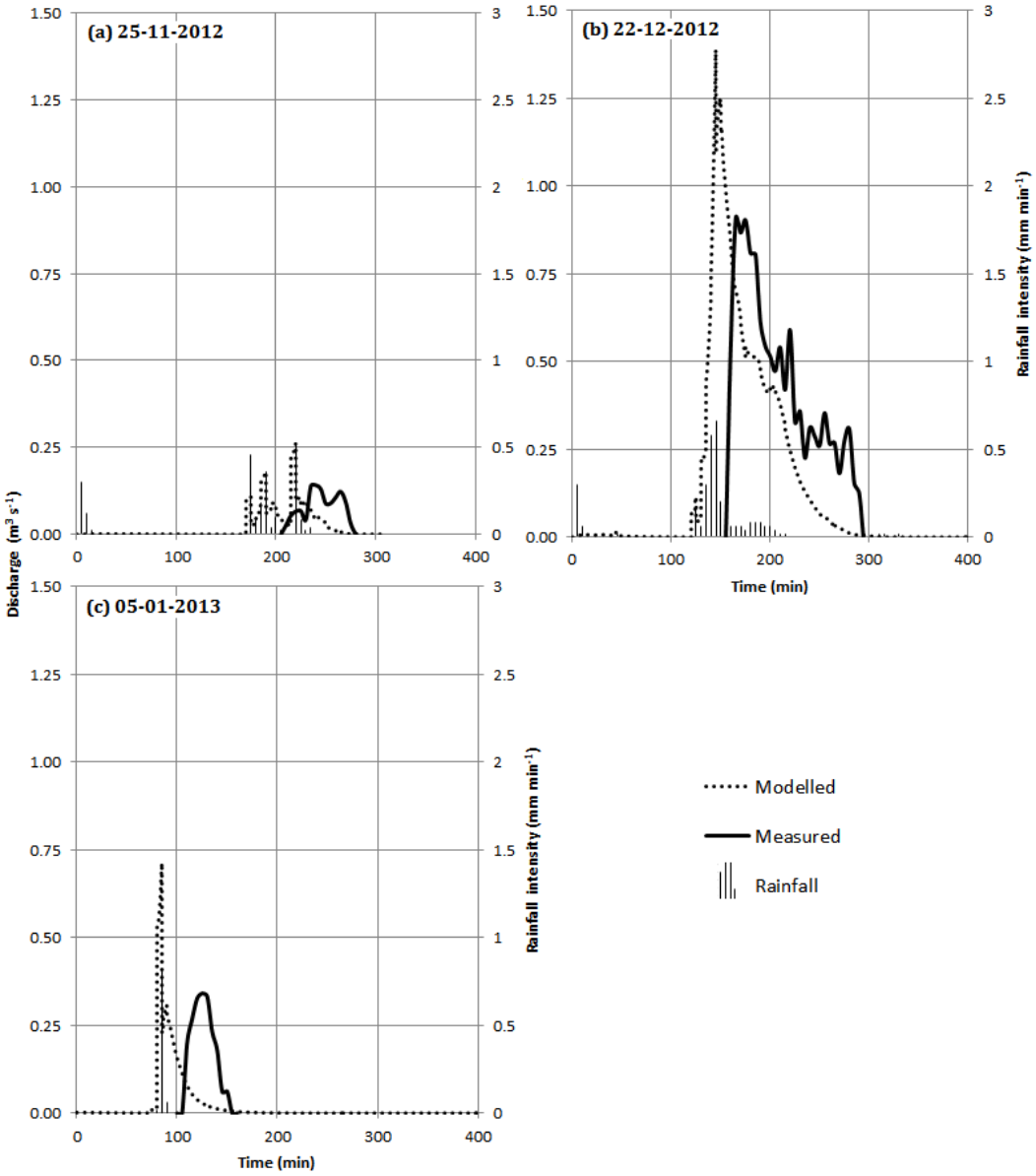

Figure 19: Graphs showing modelled and measured discharge at the Kralendijk reservoir for a rainfall event on a) 22-12-2012, b) 25-11-2012 and c) 05-01-2013.

Figure 19 shows the measured and modelled discharge for the Kralendijk reservoir for the three different rainfall events. Focussing on discharge quantity, it can be seen that the total discharge is modelled well (see Table 3). The modelled peak discharge seems to be continuously overestimated however the reason for this is that the measured water level readings of the Kralendijk reservoir were averaged out (using a three point moving average) to remove the diver error. This averaging also smoothens out large discharge peaks which can therefore not be seen in the figure above.

Table 3: Accuracy of model predictions for the Kralendijk reservoir

Rainfall event	Peak discharge ($m^3 s^{-1}$)			Total discharge (m^3)		
	Measured	Modelled	**% difference**	Measured	Modelled	**% difference**
25-11-2012	0.14	0.26	**86**	360	408	**13**
22-12-2012	0.91	1.39	**53**	3673	3650	**1**
05-01-2013	0.34	0.71	**109**	600	797	**33**

Figure 20 shows the measured and modelled discharge for the LVV reservoir for the 22-12 event. Due to equipment failure, the measured discharge was not available for the other two events. Focusing on discharge quantity, it can be seen that the peak discharge is modelled well (even though the water level readings for the LVV reservoir were averaged out as well). The total discharge is underestimated by the model (see Table 4) which is especially caused by the second half of the rainfall event. A reason for this could be the overflowing of an upstream reservoir, the effect of which is measured but not modelled. This upstream reservoir was relatively full around the date of this rainfall event but whether it actually overflowed is not known. Spatial variation in rainfall intensity cannot be the cause as the tipping bucket (used to measure rainfall intensity) was located very close (around 70m) to this reservoir.

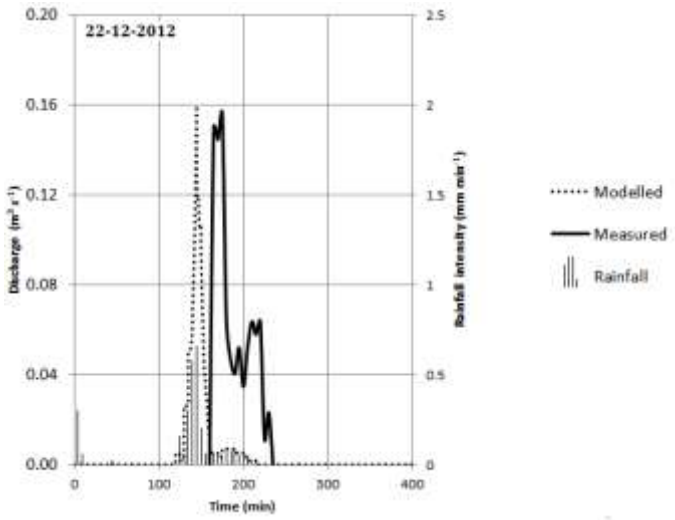

Figure 20: Graph showing modelled and measured discharge at the LVV reservoir for a rainfall event on 22-12-2012

Table 4: Accuracy of the model predictions for the LVV reservoir

Rainfall event	Peak discharge ($m^3 s^{-1}$)			Total discharge (m^3)		
	Measured	Modelled	**% difference**	Measured	Modelled	**% difference**
22-12-2012	0.16	0.16	**0**	240	133	**45**

3.5 Catchment sensitivity to erosion

All of the above measured parameters specify the sensitivity of the catchment to erosion. By understanding the effect the different parameters have on infiltration and erosion, it can already be estimated where soil loss will occur. Figure 21, shows this estimated erosion risk.

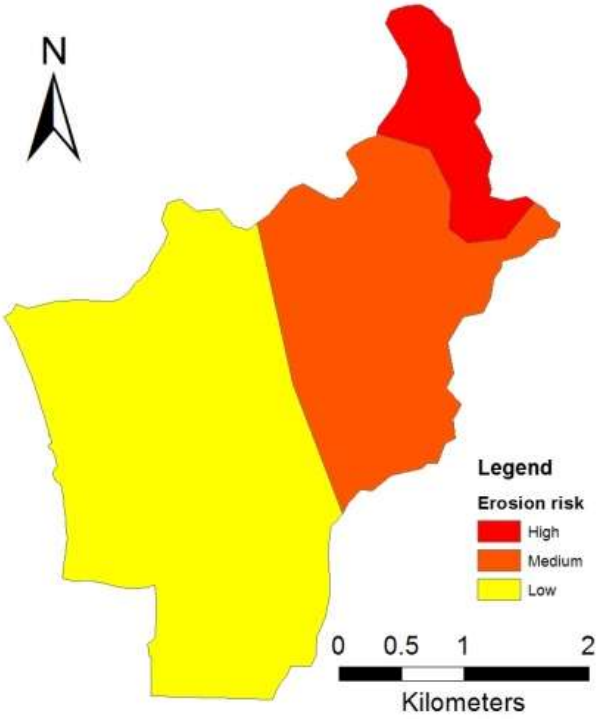

Figure 11: Estimated erosion risk

Completely in the East of the catchment, slopes are a lot larger than in the rest of the catchment. High slopes lead to fast overland flow and therefore relatively much runoff and also erosion. This area is also not paved and the soil is loamy - therefore more susceptible to detachment.

More towards the West of the catchment, the slopes are a lot smaller but still larger thannear the coast. Furthermore, there are al lot of grasslands and agricultural fields in this area – which usually do not have a large vegetation cover and are therefore more susceptible to erosion. Lastly, this area is not paved meaning the soil is not protected.

The Western half of the catchment consists of residential areas and the centre of Kralendijk. These areas have very low slopes and are very paved meaning they are not very sensitive to erosion. Furthermore the soil here is slightly more clayey and therefore less susceptible to detachment.

The susceptibility of channels to erosion can also be split up in these three areas because the soil type and slope of the channels is similar to that of the surrounding surface (except for lined channels).

Whether the soils with the largest erosion risk also contribute most to the sediment at the outlets of course depends on the trapping efficiency of the reservoirs in the catchment and how often they overflow.

3.6 Spatially distributed rainfall runoff erosion relationship under current management

The first step was to model the catchment for two different rainfall events to understand the routing of discharge and sediment within the Playa catchment. Figure 22 shows the two rainfall events used as input: one with a return period of five years, and one with a return period of ten years. It can be seen that the rainfall intensities of the storm with a ten year return period are 20% larger for the smallest intensities and up to 40% larger for the largest intensity. The total amount of rain falling during a ten year event is 30% larger.

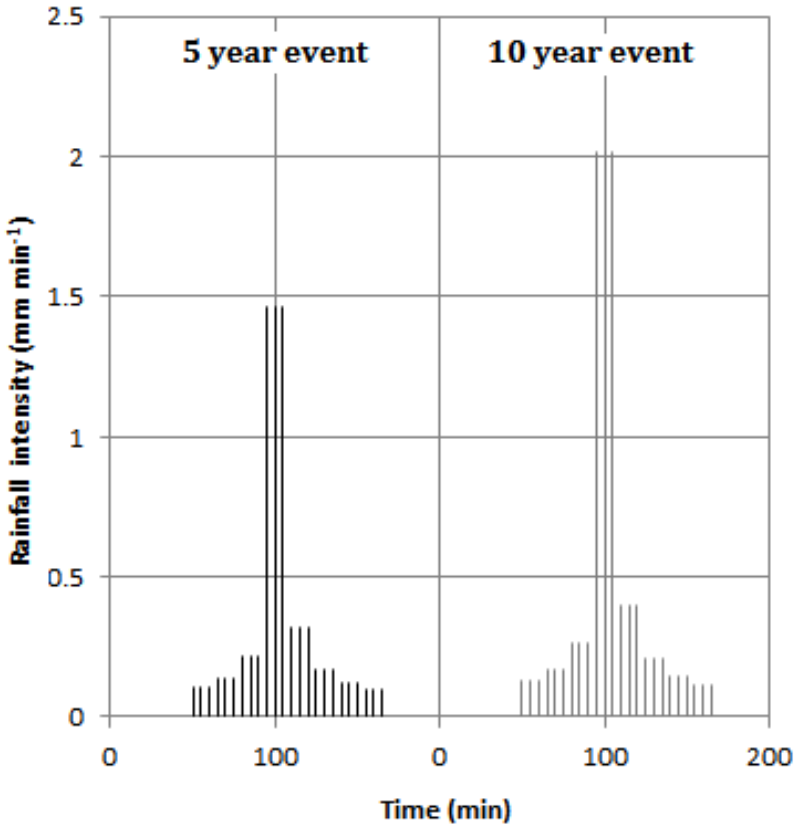

Figure 22: Two hour rainfall event with return period of five years and ten years

Catchment runoff

The simulated runoff and discharge produced by the two rainfall events are shown in Figure 23. The simulated discharge into the ocean of the four outlets for the two rainfall events can be found in Table 5.

In general it can be seen that the highly paved centre of Kralendijk produces the most runoff. The flat residential areas in the middle of the catchment produce the least runoff and the relatively steep and unpaved shrub-lands to the East are somewhere in between. Even though sub-catchments 1 and 4 are similar in size, Table 5 shows that the ocean discharge of sub-catchment 4 is a lot larger (300% larger for a five year event and 100% larger for a ten year event). The reason for this is mainly the larger storage capacity of sub-catchment 1 due to the many reservoirs - the total volume of the reservoirs in sub-catchment 1 is 96300 m^3 (not counting the large excavation just North of the Kaminda Jato Bako) compared to 75660 m^3 in sub-catchment 4.

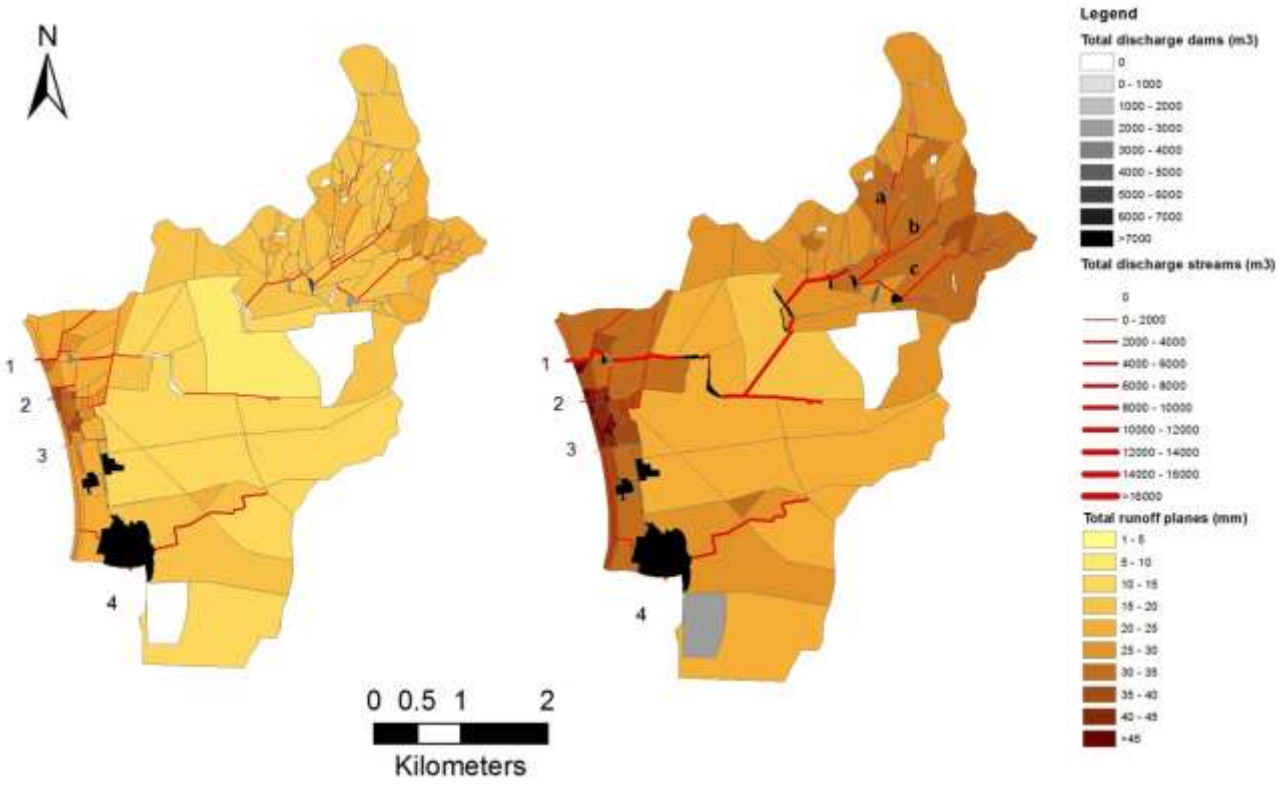

Figure 23: Runoff and stream discharge for a rainfall event with return period of five years (left) and ten years (right)

In the uplands three large discharge flows can be seen: straight down from the highest point in the North East, along the Kaminda Lagoen, and the 'rooi' just south of Lagoen hill (point a, b and c respectively on Figure 23)

Table 5: Simulated ocean discharge for the four outlets for a five and ten year rainfall event

Return period of rainfall event	Simulated ocean discharge (m^3)				
	Outlet 1	Outlet 2	Outlet 3	Outlet 4	**Total**
5 years	10000	3700	600	35600	**49900**
10 years	40100	5400	900	86900	**133300**

Comparing the runoff produced by a five year and ten year event shows that in the uplands the runoff increases from 15-25mm to 25-40mm (average increase of 55%), in the midlands the runoff increases from 5-15mm to 15-25mm (average increase of 100%) and in the centre of Kralendijk it increases from a maximum of 40mm to 50mm (average increase of 40%). The largest increase in runoff is found in the midlands because there production of runoff is mainly caused by exceedance of the infiltration capacity –while in the uplands it is also due to the slope and in central Kralendijk much water cannot infiltrate due to the pavement. In the uplands and central Kralendijk it is therefore mainly the increase in total rainfall which leads to an increase in runoff while in the midlands both effects play a role - the larger total rainfall, but also the larger intensity (meaning the infiltration capacity is exceeded even more).

It is also interesting to see that for a five year event, a number of reservoirs in the East are overflowing. This water however does not reach the ocean mainly because it does not flow past the large LVV reservoir. With the ten year event, the LVV reservoir does overflow, and so do the reservoirs in Kralendijk. This can be seen to result in a much larger ocean discharge of the ten year event compared to the five year event. The average increase in ocean discharge for a ten

year event compared to a five year event is 150% but the increase from sub-catchment 1 (which contains all the reservoirs) is around 300%. The increase in total rainfall however is only 30%

Drainage capacity

To see if the drainage capacity of the channels in central Kralendijk is large enough to drain the runoff caused by a five year and ten year event, the maximum discharge produced by the rainfall events is compared to the drainage capacity of the channels.

Figure 24 shows the drainage capacity of the channels in Kralendijk. It can be seen that especially due to the low slopes but also due to the small dimensions, the discharge capacity of many drains is relatively small.

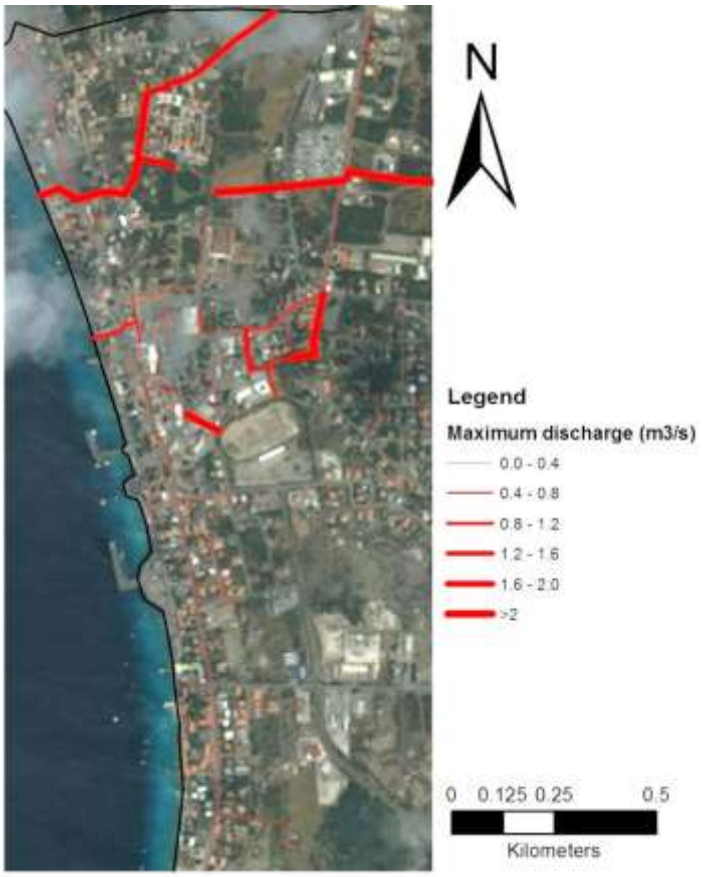

Figure 24: Maximum discharge capacity of drains in central Kralendijk

Figure 25 shows the discharge deficit (maximum possible discharge ($m^3\ s^{-1}$) – maximum required discharge ($m^3\ s^{-1}$)) for a storm with return period of five and ten years. It can be seen that a lot of drainage channels cannot drain the maximum runoff produced by either a ten or five year storm. Especially the drains in sub-catchment 2 are problematic as drains with a capacity to drain a maximum of 0.17 $m^3\ s^{-1}$ are required to cope with 2.5 $m^3\ s^{-1}$ for a five year storm and even 4 $m^3\ s^{-1}$ for a ten year storm. The capacity of the second half of the drain under the Kaya Korona (top right on Figure 20) is also insufficient. The increase in required discharge for a ten year storm ranges from 55-75%. The larger the drainage area of a drain, the larger the increase.

It should be stressed that an insufficient drainage capacity does not necessarily mean that flooding problems will occur as is not known how long the water will inundate the streets before it is drained and also not how high this water will stand. Nevertheless, any water level and duration of inundation will be harmful to roads and other infrastructure.

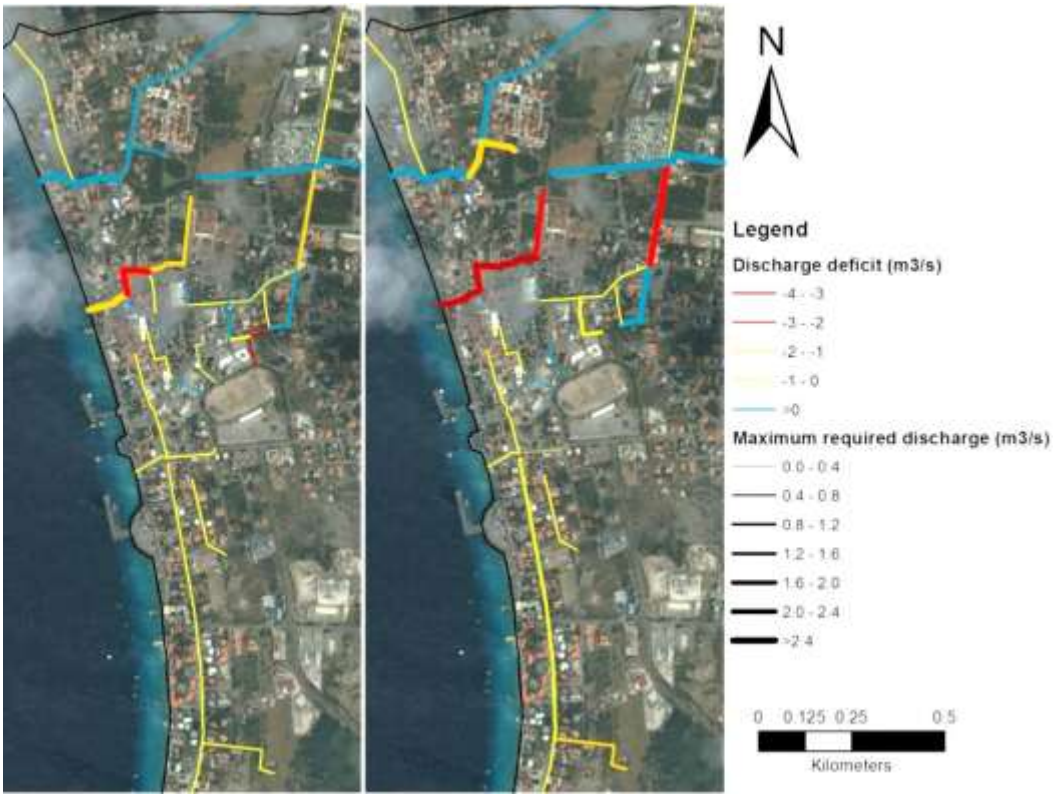

Figure 25: Discharge deficit of drains in central Kralendijk for a rainfall event with return period of five years (left) and ten years (right)

Catchment erosion

The spatial distribution of soil loss and sediment transport produced by the two rainfall events is shown qualitatively in Figure 26. Table 6 shows the sediment yield of the four outlets, relative to the lowest sediment yield found during a rainfall event with five year return period (that of outlet 4). Actual erosion rates and sediment yields could not be calculated as calibration of sediment transport was not done.

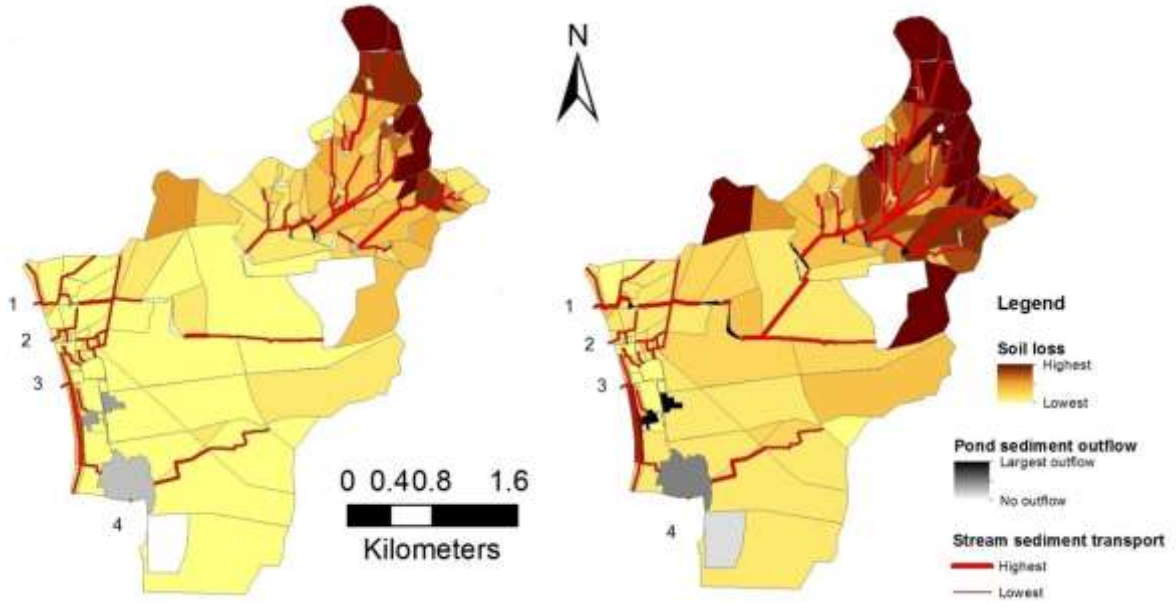

Figure 26: Erosion and sediment transport for a rainfall event with return period of five years (left) and ten years (right)

The slope seems to be the largest determinant in spatial variability of erosion in the catchment. The soil loss in the relatively steep shrub-lands to the East is five to ten times larger than that in the flat midlands. In the steepest top North-Eastern part of the catchment soil loss is even 50 times as large.

Table 6: Relative sediment yields of the outlets for a five year and ten year event

Return period of rainfall event	Sediment load relative to that of outlet 4 during a five year event				
	Outlet 1	Outlet 2	Outlet 3	Outlet 4	Total
5 years	30.2	5.0	1.2	1.0	37.4
10 years	152.4	9.2	1.9	3.2	166.7

The increase in soil loss for a rainfall event with ten year return period is large – larger than the effect it has on surface runoff. The largest increase in soil loss is found in the flat midlands – here the soil loss increases by 200%. In the highly paved areas in central Kralendijk and in the steep shrub-lands, the increase amounts to 100%.

A surprising result is the much larger sediment yield of outlet 1 compared to that of outlet 4 (30 times larger for the five year event and 50 times larger for the ten year event). The discharge on the other hand is a lot lower (3.5 times lower for the five year event and 2 times lower for the ten year event). This means that on average the sediment concentration of outlet 1 is around 100 times higher than that of outlet 4 for the five year event and 150 times higher for the 10 year event. The single most important reason for this huge difference in concentration is the effectivity of the 'saliña' in front of outlet 4 in trapping sediment. For both the five and ten year event, about 99% of the sediment flowing into the 'saliña' is retained there. In front of outlet 1 there is no such reservoir meaning the sediment load is a lot higher. Interestingly, the main source of the sediment at outlet 1 is not the highly erodible uplands – as most of this is blocked by the upland reservoirs - but the area it drains near the coast which does not pass through a retention basin before entering the sea.

The sediment retention capacity of the reservoirs in the uplands is also large and ranges from 85% to 99% depending on flow velocity and reservoir geometry. This large amount of retention is mainly caused by the fact that the soils in the catchment are largely made up of fine sand. This is therefore the largest fraction that is eroded but also the fraction that is most easily deposited (due to the relatively large size and therefore settling velocity). The finer material (especially clay) can reach the ocean but only when the reservoirs overflow. The large reservoir at LVV seems to be critical, only when this reservoir overflows will water and finer sediment from the uplands reach the sea. According to interviews this happens once every 4-6 years (Pers. Com. Rocky Emers, 2012).

The total sediment flow into the ocean for a rainfall event with return period of ten years is around 350% larger than that of a rainfall event with return period of five years. Sub-catchment 1 causes the largest increase because the overflowing LVV reservoir means sediment and discharge from the uplands now also flows downstream. The increase in discharge through the main channel leads to an increase in channel erosion and also to a decrease in the sediment trapping efficiency of the reservoirs it passes before reaching the outlet.

Figure 27 shows the origin of the sediment ending up in the channel and reservoir network and Figure 28 shows what happens to this transported sediment for each of the four sub-catchments. From Figure 27 it can be clearly seen that channel erosion is the main source of transported sediments in sub-catchment 1. The main reason for this is the large number of channels in the uplands (upstream of the LVV dam). In sub-catchments 2 and 3 all channels are lined and therefore sediment only comes from the surface. In sub-catchment 4, channel erosion is also considerable. A ten year event leads to a larger proportion of channel erosion in sub-catchment

1 while it leads to a smaller proportion of channel erosion in sub-catchment 4. This is because the total erodibility of the channels in sub-catchment 1 is larger than that in sub-catchment 4.

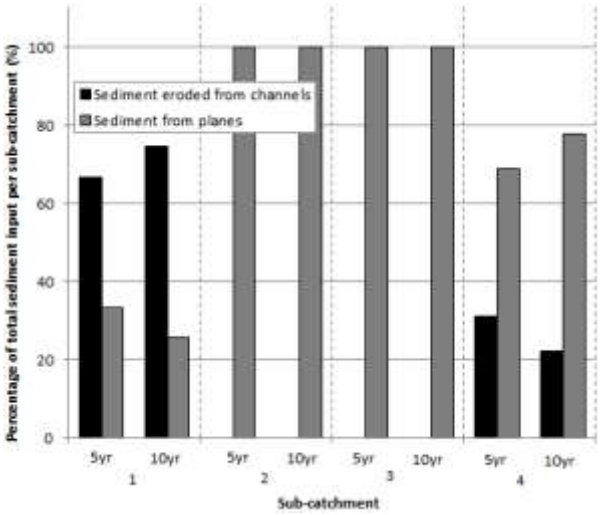

Figure 27: Origin of sediment in channel and reservoir network

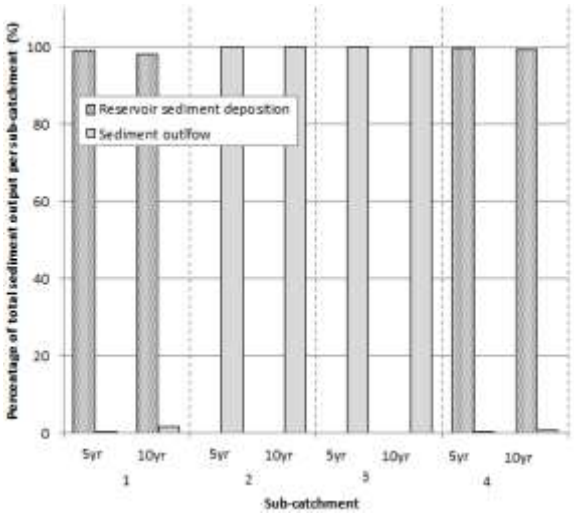

Figure 28: Sediment outputs

From figure 28, the importance of the reservoirs in sub-catchment 1 and the salina in sub-catchment 4 also becomes very clear. It can be seen that only a very small fraction of the sediment in the channel and reservoir network of sub-catchments 1 and 4 actually reaches the ocean.

3.7 Physical scenarios

3.7.1 Rainfall intensity versus rainfall duration

To understand the difference in effect between high intensity rainfall and long-duration rainfall, runoff and erosion was modelled for two successive rainfall events, each having half the intensity of an event with a return period of five years (Figure 29). The total rainfall is therefore the same as an event with return period of five years, but the duration is doubled (four hours).

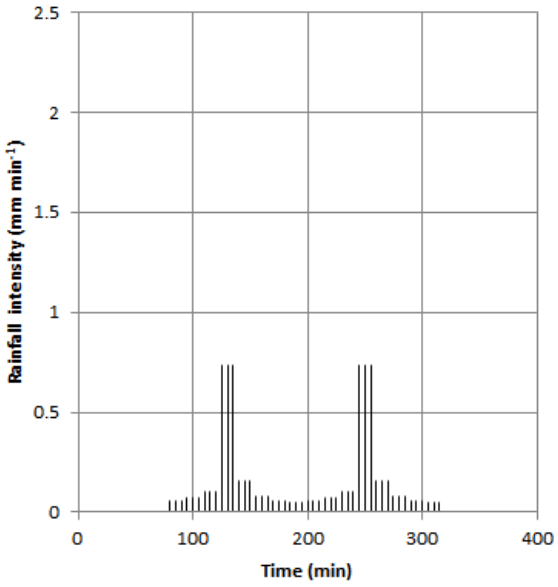

Figure 29: Two successive rainfall events with each half the intensity of an event with a five year return period

Figure 30 shows the resulting change in runoff and erosion in the catchment and Figure 31 shows the resulting change in water and sediment fluxes for the four different sub-catchments.

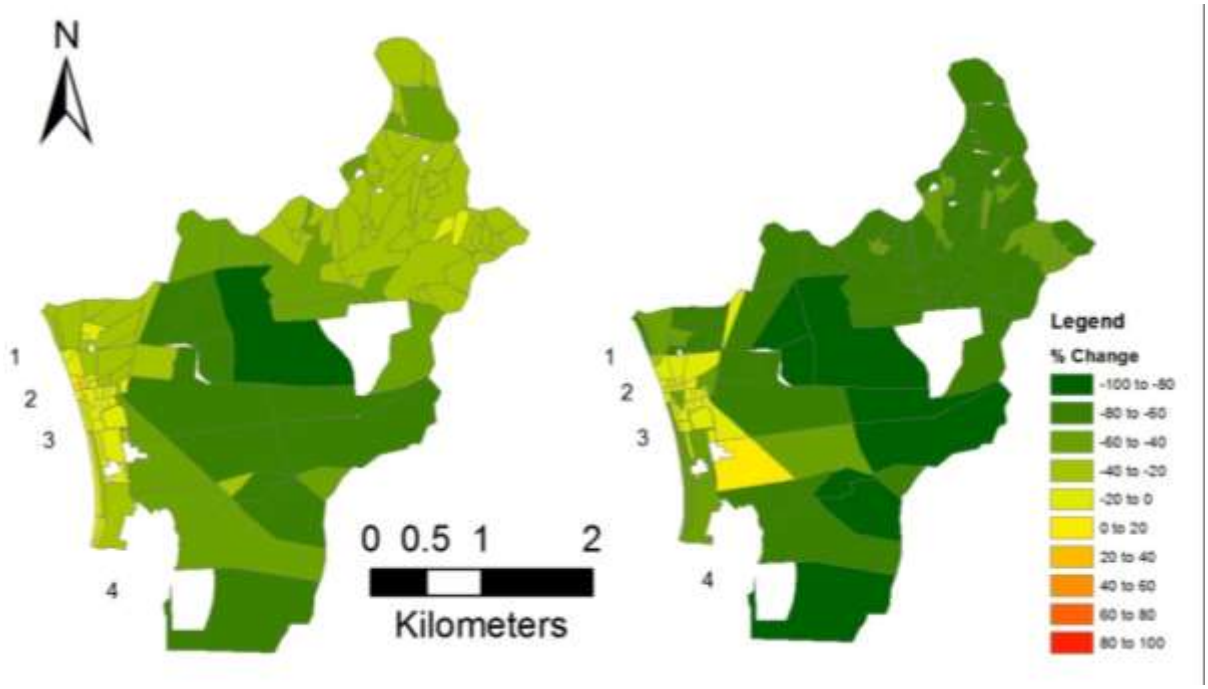

Figure 30: Change in runoff (left) and erosion (right) for a rainfall event with half the intensity but twice the duration of a five year event

It can be seen that there is a clear decrease in runoff and erosion in the catchment. The runoff in the shrub-lands to the East has decreased by around 35%. In the middle of the catchment, the runoff has decreased by around 65%. In the highly paved centre of Kralendijk, the decrease in runoff approaches zero because of the large amount of pavement. The decrease in erosion is slightly more significant; it ranges from a decrease of 65% in the shrub-lands, 85% in the midlands and around 50% in central Kralendijk.

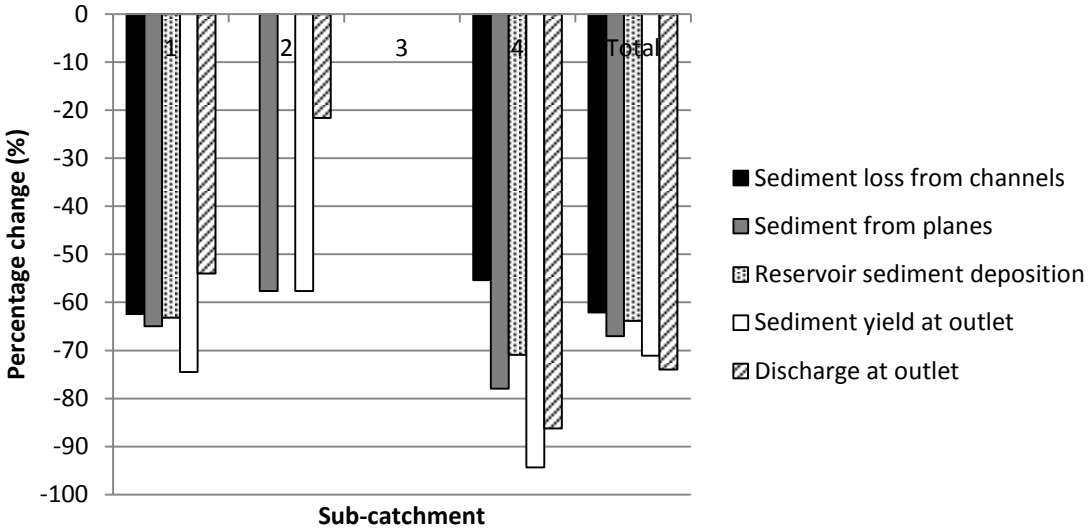

Figure 31: Change in sediment and water fluxes for a rainfall event with twice the duration but half the intensity

From Figure 31 it can be seen that both the total ocean discharge and sediment yield have decreased by around 70%. Both channel and surface erosion have decreased by roughly the same percentage. In sub-catchment 3, the lower intensity rainfall has no effect because this sub-catchment is so highly paved. In conclusion it can be said that the intensity of a rainfall event is much more important in determining the amount of runoff and erosion produced than rainfall duration.

Occurrence

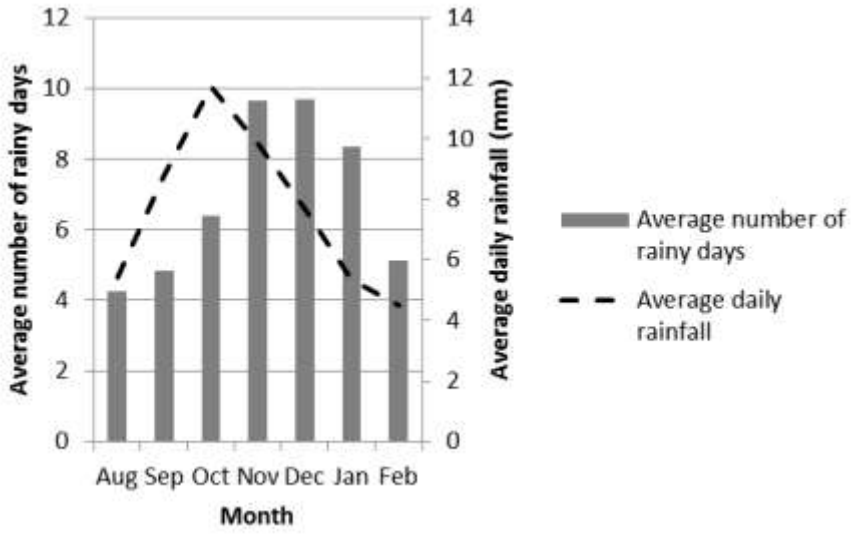

Figure 32: Number of rainy days and average daily rainfall per month

To see when different types of rainfall are most likely to occur, a plot was made of the average number of rainy days per month and the average daily rainfall per month (Figure 32). It was calculated using meteorological data from 1973-2012 from the meteorological station at Flamingo airport Bonaire. For this purpose a rainy day was defined as a day with more than 1mm of rain to reduce possible biases associated with very small rainfall amounts (Moron et al., 2009).

It can be seen that the months with most rainy days are November and December. However, the average daily rainfall is highest in October. From this it can be inferred that the highest intensity storms occur in October. This is acknowledged by Ascon and DHV (1990) and also by our own measured rainfall intensities for the rainy season of 2012/2013. Therefore this will be the period that most runoff and erosion is produced.

3.7.2 Soil moisture

To understand how runoff and erosion is affected by different initial soil moisture contents, runoff and erosion was also modelled for a rainfall event with return period of five years with the initial soil moisture content at field capacity.

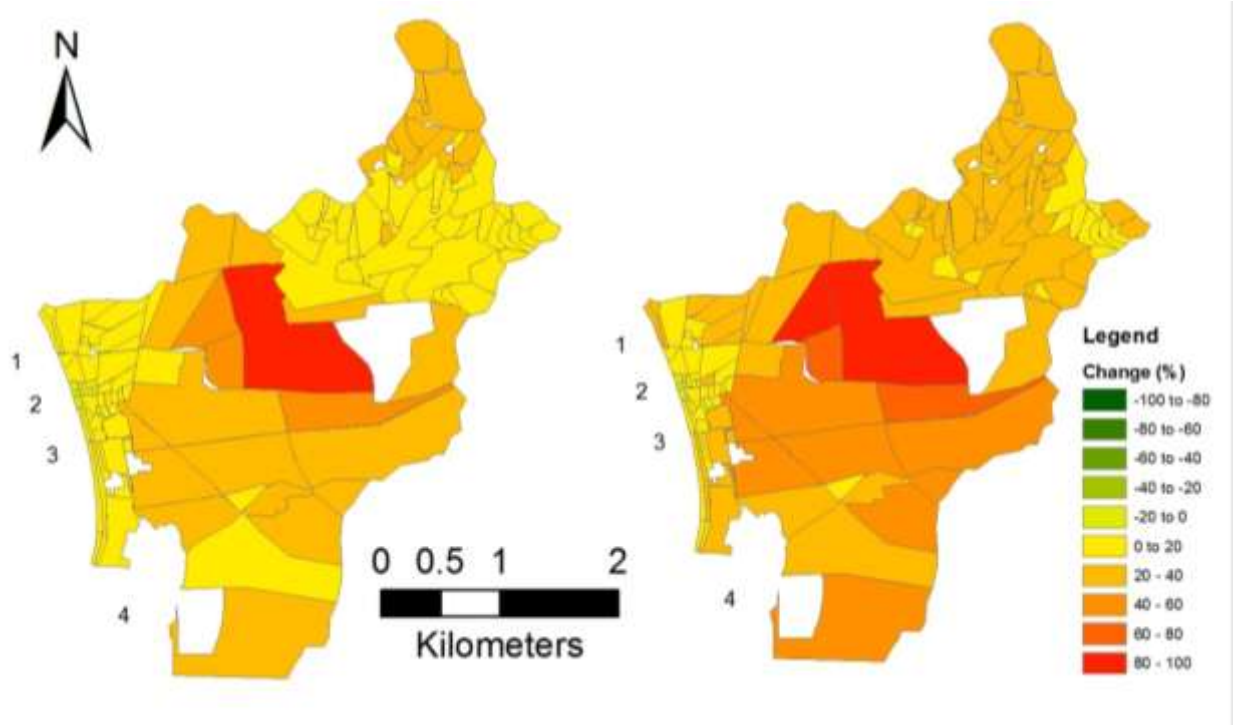

Figure 33: Change in surface runoff (left) and erosion (right) for a rainfall event with five year return period with initial soil moisture content at field capacity

Figure 33 shows the resulting change in runoff and erosion in the catchment and Figure 34 shows the resulting change in water and sediment fluxes for the four different sub-catchments.

In the uplands, an initial soil moisture content at field capacity can be seen to increase the runoff by around 20%. In the midlands this increase is larger and around 40%. The reason for this is that in the midlands, the amount of runoff produced is much more affected by a reduced infiltration capacity than in the uplands where runoff is also produced because of the large slopes. In the centre of Kralendijk the increase in runoff approaches 0% due to the large amount of pavement.

Due to this increase in surface runoff, soil loss also increases. In the uplands and central Kralendijk, the increase in soil loss is about 25%, in the midlands the increase in soil loss ranges from 25-80% depending on the amount of pavement.

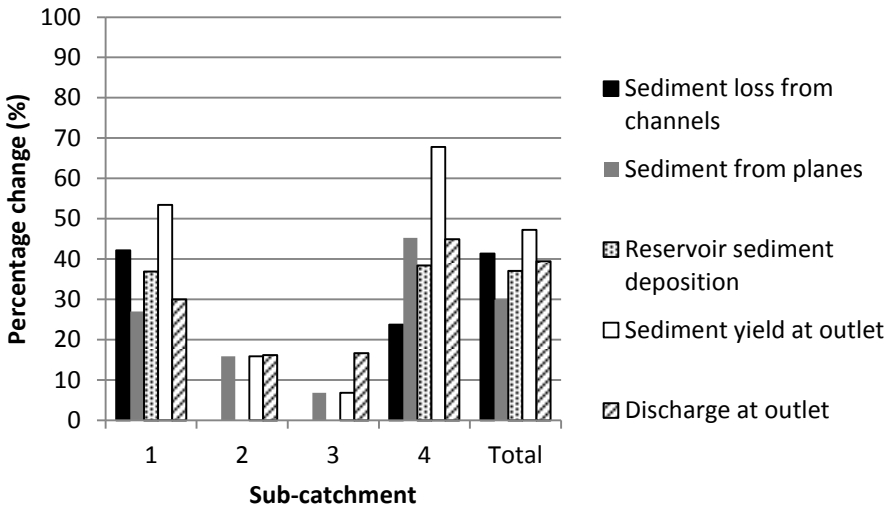

Figure 34: Change in sediment and water fluxes for a rainfall event with return period of five years with initial soil moisture content at field capacity

From Figure 34, it can be seen that the ocean discharge has increased by about 40% while the total sediment yield has increased by 50%. Both channel and surface erosion have increased by roughly the same proportion.

Occurrence

Figure 35 shows the probability of exceedance of different soil moisture contents at the onset of a rainfall event larger than 5mm (this was chosen because rainfall less than 5mm does not produce runoff). It was calculated using meteorological data from 1973-2012 from the meteorological station at Flamingo airport Bonaire, and the simple water budget model described in Chapter 2.4.3. It can be seen that around 60% of the rainfall events fall while the soil is at wilting point or lower. Around 10% of the rainfall events fall when the soil is at field capacity.

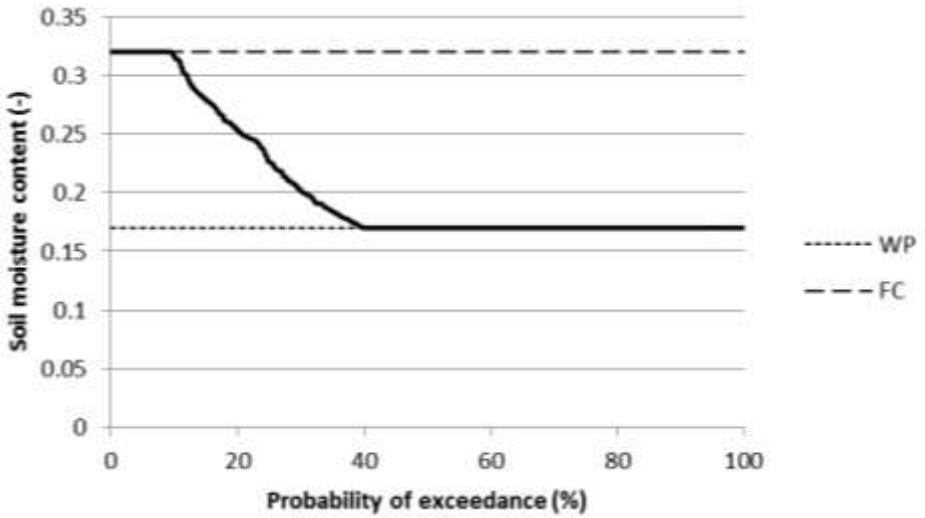

Figure 35: Probability of exceedance of different soil moisture contents at the onset of a rainfall event

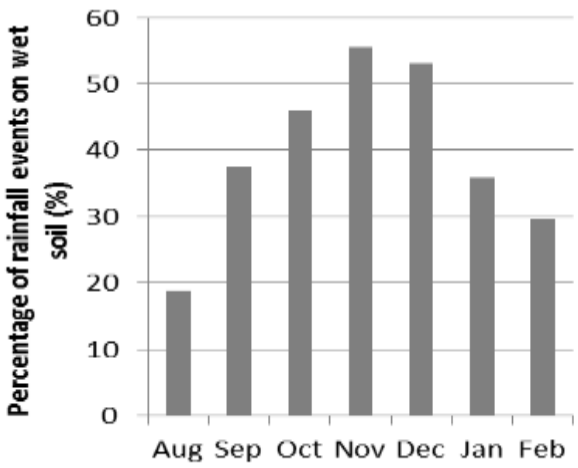

Figure 36: Percentage of rainfall events on wet soil per month

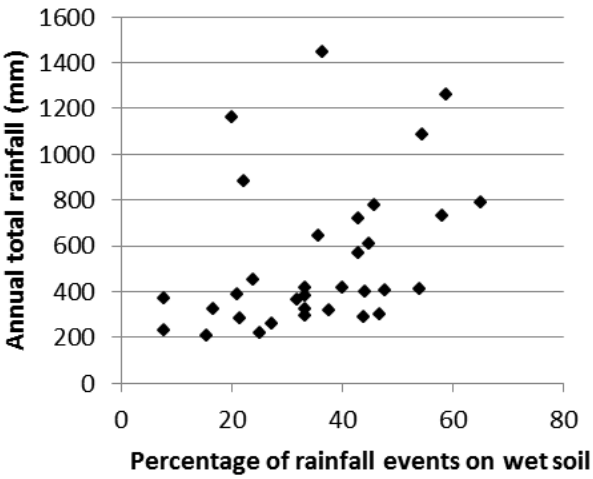

Figure 37: Annual rainfall versus percentage of rainfall events on wet soil

Figure 36 shows the percentage of rainfall events falling on wet soil (defined as a soil moisture content larger than wilting point) per month. It can be seen that the largest chance of this happening is in the months November and December. The reason for this is simply the fact that those months have the largest number of rainy days, and the chance that rain falls on successive days is therefore larger. There is no strong relationship between annual rainfall and the number of rainfall events falling on wet soil (Figure 37). This means that a wet year is not necessarily a year with many successive rainfall events, but rather a year with more rainfall per day and therefore probably more intense rainfall events.

3.7.3 Dry-season vegetation

Due to the difference in vegetation cover between the beginning and end of the rainy season, runoff and erosion is also expected to be change. To test the effect that the difference in vegetation cover has, runoff and erosion was modelled under the vegetation cover occurring at the start of the rainy season.

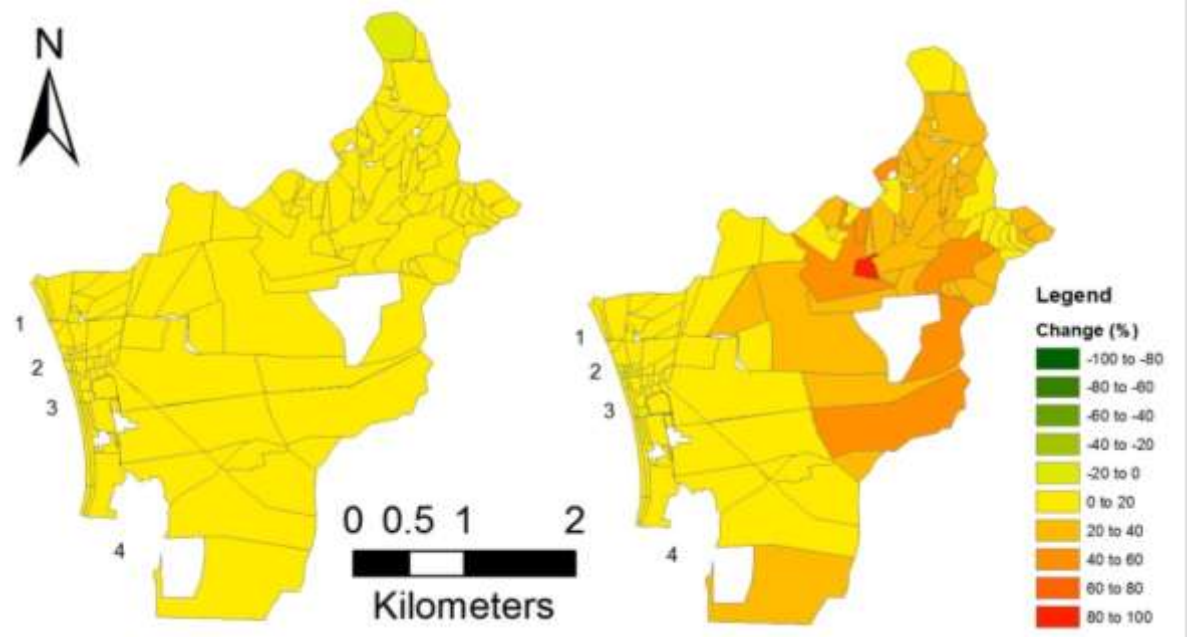

Figure 38: Change in runoff (left) and erosion (right) for a rainfall event with return period of five years with dry-season vegetation

Figure 38 shows the resulting change in runoff and erosion in the catchment and Figure 39 shows the resulting change in water and sediment fluxes for the four different sub-catchments.

The lower vegetation cover in the beginning of the rainy season is found to cause a slight increase in runoff due to the reduction in interception and the lower Manning's coefficient which leads to faster runoff which therefore has less time to infiltrate. This increase however is minimal and only 0-10% throughout the catchment. The largest effect is found in areas with maize fields and dense shrub-lands as these have the largest decrease in vegetation cover during the dry season.

There is also a slight increase in erosion because of the larger soil erodibility and the increased speed of runoff and therefore increased hydraulic erosion. In the uplands to the East, the soil loss increases by about 20-40. In the residential midlands and central Kralendijk there is an increase in soil loss ranging from 5-20% depending on the amount of pavement. This increase is a lot smaller because there is little vegetation cover to begin with.

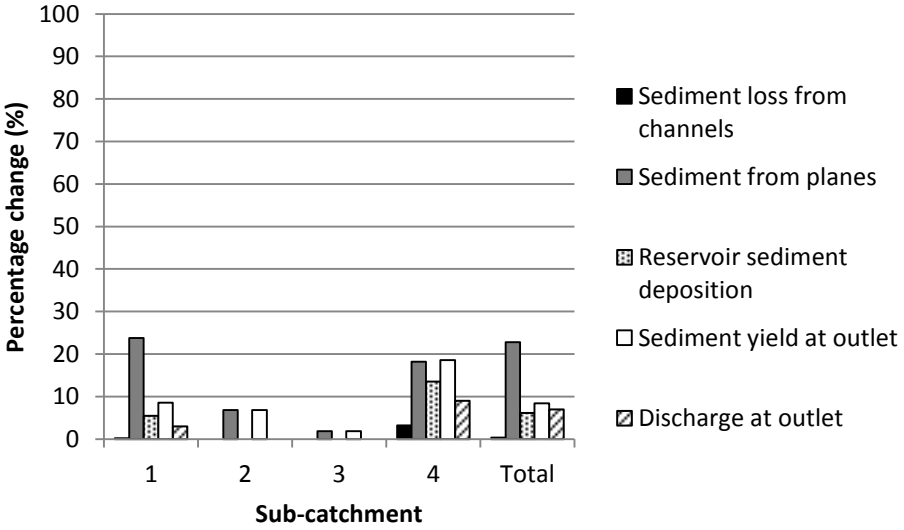

Figure 39: Change in sediment and water fluxes for a rainfall event with return period of five years with dry-season vegetation

From Figure 39, it can be seen that the total ocean discharge and sediment yield have only increased by 7% and 8% respectively. This is lower than the soil loss in the catchment because this increased soil loss is retained by the many reservoirs in the catchment. It is interesting to see that only surface erosion decreased. This is because the erodibility of the surface increased a lot more than the erodibility of the channels due to the lower vegetation cover.

3.8 Management Scenarios

3.8.1 Loss of reservoirs

To understand the importance of the reservoirs in the Playa catchment and the effect of losing 'tankis' due to lack of maintenance, runoff was modelled for a two hour storm with ten year return period for the scenario in which all 'tankis' are gone.

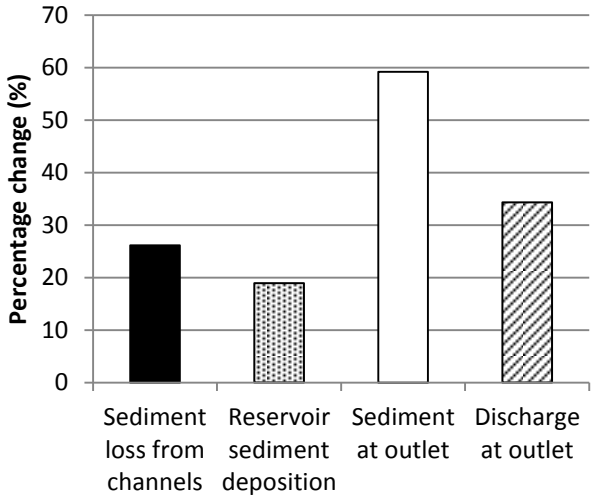

Figure 40: Change in sediment and water fluxes for a rainfall event with return period of ten years and no 'tankis'

Figure 40 shows the change in sediment and water fluxes for sub-catchment 1 (as this is the only sub-catchment affected by the loss of reservoirs). It can be clearly seen that the loss of reservoirs leads to an increase in channel erosion (around 25% more) because less water is retained by the reservoirs. Interestingly enough, even though the sediment retention capacity of the reservoirs decreases because the through flow is larger, the total amount of deposited sediments also increases (because there is much more sediment in the water due to the increased channel erosion). The increased discharge and sediment yield at the outlet is 35% and 60% respectively.

3.8.2 Reduced grazing (maximum vegetation cover)

To understand the effect that reduced grazing would have on runoff and erosion in the catchment, runoff and erosion was modelled for a rainfall event with a return period of five years on a catchment with maximum vegetation cover.

Figure 41 shows the resulting change in runoff and erosion in the catchment and Figure 42 shows the resulting change in water and sediment fluxes for the four different sub-catchments.

The results show that an increase in vegetation cover does not have much effect on runoff. Both in the uplands and midlands, the reduction in runoff is on average only 5%. In central Kralendijk it approaches 0% due to the high percentage of paved area. The reduction in erosion is slightly larger being on average 20% both in the uplands as midlands. In central Kralendijk it approaches 0% due to the high percentage of paved area.

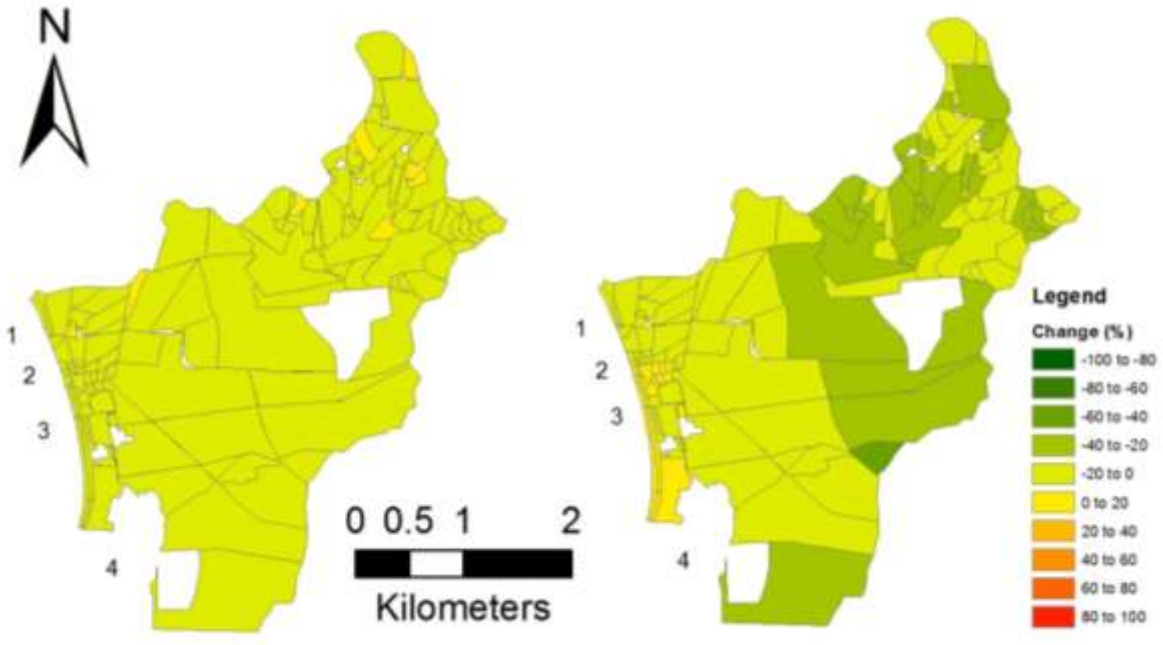

Figure 41: Change in runoff (left) and erosion (right) for a rainfall event with return period of five years and maximum vegetation cover

From Figure 42 it can be seen that the discharge and sediment yield at the outlet have both decreased by around 8%. Mainly surface erosion is affected because an increase in vegetation cover only has an effect on the erodibility of the surface. Channel erosion also slightly decreased because the discharge flowing through the channels decreased.

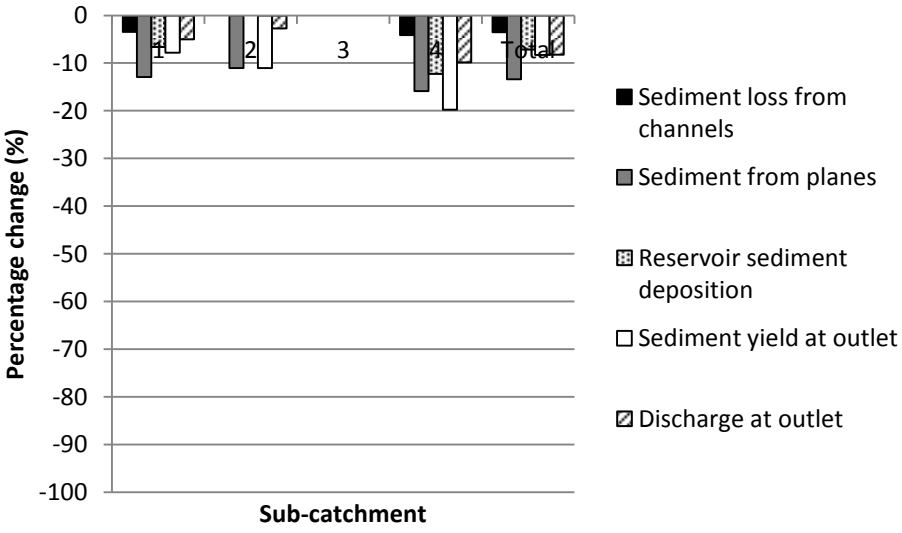

Figure 42: Change in sediment and water fluxes for a rainfall event with return period of five years with maximum vegetation cover

3.8.3 Reducing the paved surface area

To estimate the effect of reducing the amount of pavement (especially in central Kralendijk), runoff and erosion was modelled for a rainfall event with return period of five years when paved area is reduced by 10% and 20% respectively.

Figure 43 shows the change in runoff and peak discharge produced and Figure 44 shows the change in ocean discharge and sediment yield of the four outlets.

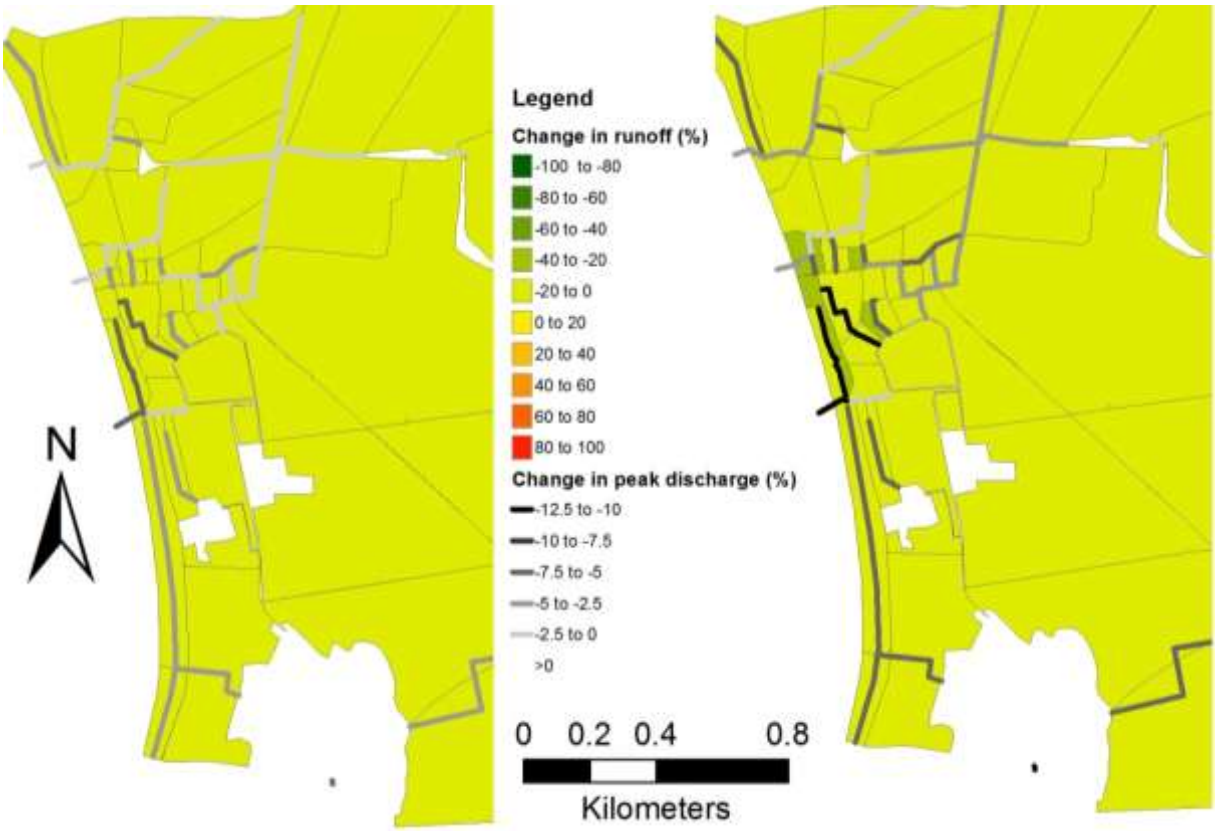

Figure 43: Runoff in Kralendijk for rainfall event with return period of five years with 10% less pavement (left and 20% less pavement (right)

A decrease in paved area of 10% and 20% leads to a respective reduction of 0-20% and 0-30% surface runoff in central Kralendijk. The peak channel discharge is reduced by 1-7% (in the order of 0.0-0.2 $m^3 s^{-1}$) and 2-12% (in the order of 0.0-0.3 $m^3 s^{-1}$) respectively.

Even though there is some reduction in produced runoff, the maximum discharge the channels have to drain hardly changes. Seeing as the discharge deficit of some of these channels is more than 3$m^3 s^{-1}$, a maximum reduction in peak discharge of 0.2-0.3 $m^3 s^{-1}$ will not have much effect.

When the paved area is reduced by 10% the ocean discharge decreases by 5%. A decrease in paved area of 20% leads to a reduction in ocean discharge of 11%. In sub-catchments 1 and 4 reducing the paved area leads to a reduction in erosion (as runoff decreases), however, in sub-catchments 2 and 3 erosion increases due to an increase in the erodible surface area. Looking at the average of the four outlets, decreasing the percentage of paved area by 10% and 20% barely has any effect the ocean sediment yield.

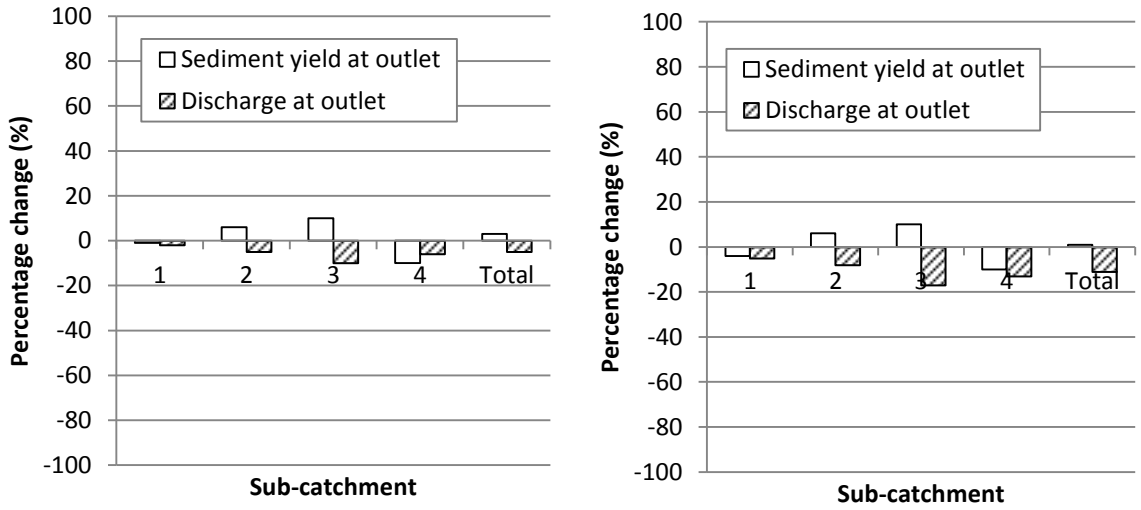

Figure 44: : Change in sediment and water fluxes for a rainfall event with return period of five years with 10% less pavement (left) and 20% less pavement (right)

4. Limitations of the research

As with all modelling studies, it is of importance to stress that models are just simplifications of reality. Kineros2 uses conceptual laws to describe the hydrological processes in the catchment. However many processes which also play a part are not included; because they complicate the model, increase the computational time, would require a lot more (difficult to determine) input parameters, or because they are simply not yet well understood. Furthermore the conditions under which these conceptual laws are derived such as a laboratory column of homogenous soil are different from conditions in the field (Grayson et al., 1992). Moreover, empirical relationships are also being included (for example Manning and the USLE). These are relationships found under certain conditions in certain locations and this always raises the question whether they also fully apply in other settings (Wischmeier and Smith, 1978) .

The model conceptualisation is also a source of uncertainty. Overland flow planes and reservoirs are simplified as being rectangular in shape. For planes, this affects the flow length, for reservoirs, the trapping efficiency is affected. Furthermore, plane parameters are averaged for the whole plane. This means that for example planes with pervious and impervious surfaces (like urban planes) are modelled as being completely semi-pervious, even though this will behave hydrologically different.

The fact that the model cannot simulate flooding is also a concern. A channel which floods will lose discharge (as more water will infiltrate on both sides of the channel) and also the timing of the discharge will be affected. Furthermore, sediment transport will be affected as sediment will be deposited on the flood plains. Figure 45 shows for which channels in the catchment the discharge capacity is exceeded for a ten year rainfall event. All the green lines are gullies or overland flow routes which are modelled as being triangular and cannot really overtop. As was already shown in Chapter 3.6, most of the channels in central Kralendijk will overtop; discharge and sediment load originating from central Kralendijk will therefore by overestimated by the model. Of largest concern is the fact that the main channel of sub-catchment 1 will also overtop at one section (see the arrow in Figure 45). This channel discharges all the runoff and sediment from sub-catchment 1 meaning the discharge and sediment yield at the outlet of sub-catchment 1 is also overestimated. For a five year rainfall event this is not the case

Figure 45: Discharge deficit of channels in the Playa catchment for a rainfall event with return period of ten years

Uncertainties are also added through the input parameters. Firstly the soil parameters were measured only at 12 points in the catchment and interpolated for the rest of the catchment. It is unlikely that this gives a good representation of the spatial variability of these parameters firstly because no spatial correlation was found and secondly because the playa catchment is relatively urbanized which means soils are disturbed and therefore even more spatially variable (Kaushal and Belt, 2012). In actual fact the whole concept of extrapolating the underlying physics of ideal soil cores to the spatial variability of field soils is inaccurate. As Klemes (1986) remarks: "the search for new measurement methods that yield areal distributions of hydrological variables would be a much better investment for hydrology than the continuous pursuit of a perfect massage that would squeeze the non-existent out of a few poor anaemic point measurements".

The actual measurement of a number of soil parameters can also be improved. Due to equipment constraints for example, the soil organic matter content had to estimated using the Munsell colour and for the porosity, an estimated particle density was used. Other parameters were estimated from lookup tables (e.g. the capillary length scale, pore size distribution index). Land cover parameters such as groundcover, vegetation cover and the manning's roughness coefficient had to be estimated per land use class which requires a lot of personal judgement instead of scientific measurement. The same is true for the estimation of reservoir geometry.

The calibration can also include errors due to the spatial variation in rainfall and due to the estimation of the geometry of the reservoirs for which the water level was measured. This would have a large effect on the conversion of the water level measurements to discharge used for calibration. Furthermore, the discharge was calibrated at three locations however not all the discharge originating in the catchment passes through one of these calibration points, because they were not located at the three outlets and because a lot of runoff and sediment was contained by reservoirs which did not overflow. Therefore, only part of the catchment is calibrated (large part of sub-catchment 1 and 2) and the obtained multiplication factors are assumed to be identical in the rest of the catchment. The fact that the three calibration points were found to have the same multiplication factors makes this assumption even more justifiable. Lastly, the rainfall vents used for calibration were a lot smaller than the five year and ten year rainfall events used for modelling. It is therefore not known whether the model is still completely accurate for these events.

The exact influence of these limitations on the model results is not known. For example in some cases, the simplification of model element geometry can lead to overestimation of runoff and erosion (e.g. when flow lengths are conceptualized as being larger) and in other cases it can lead to underestimation (e.g. when flow lengths are conceptualized as being smaller). Aerial averaging of land cover parameters for plane element can lead to overestimation of runoff and erosion when land cover is actually extremely fragmented over the plane, and it will lead to underestimation when land cover is not fragmented.

The simulated increases or decreases in runoff and erosion for each scenario can therefore not be taken exactly but do give a good idea of the order of magnitude – and therefore also of the relative effectiveness of the different management scenarios. The actual amount of runoff for each plane can also not be taken exactly – even more so because the model was not built to precisely simulate amounts of runoff at each location, but rather to simulate the discharge at the outlets which were calibrated (Grayson et al., 1992). The spatial distribution of runoff and erosion however does give valuable information. The simulated discharge flowing though the channels in Kralendijk is probably the most reliable information which was extracted from the model as it has been calibrated. However, as mentioned above, the calibration also includes some uncertainties and it is therefore again important to focus on the orders of magnitude instead of the exact discharges that the model predicts.

5. Recommendations for further research

Even though this study gives a good estimate of water and sediment flows in the Playa catchment, recommendations for improvement and further research can certainly be given.

Perhaps the most issue, is the situation outside this particular catchment. There are a lot of other catchments on the island; many of which are larger, and many of which have larger differences in elevations. Their contribution to ocean sedimentation is therefore also more significant. An inventory of the catchments on Bonaire and estimates of the sediment load they produce would therefore be very useful. Mapping the erosion risk of the island would be another interesting study as knowing which areas are most vulnerable to soil loss allows for more efficient soil conservation.

Actual measurement of sediment fluxes would be very valuable. This study showed that the flow of discharge and sediment depends very much on whether certain reservoirs overflow or not. Manual bottle sampling only at the outlet for a number of rainfall events as was attempted in this study is then not very practical. Firstly because the source area of the sediment is usually small (because not all reservoirs overflow for normal events) and secondly because the source area is not exactly known (because it is not known which reservoirs are actually overflowing). To get a better idea of sediment flows into the sea, automated or even continuous sampling for a longer time period (number of years) would be preferable. With pump sampling for example, automated samples can be taken at predefined time intervals or when the stream has a certain water depth or velocity (Wren et al., 2000). Using acoustic, optical or nuclear methods, measurements can be taken continuously using the attenuation and or backscatter of waves or radiation (Wren et al., 2000).

It would also be useful to quantify the soil loss with actual field measurements. This could for example be done by measuring sedimentation in the reservoirs. As most of the reservoirs are empty in the dry season, repeated surveys of designated tracks across the reservoir can be undertaken in relation to a set level or benchmark (Rapp et al., 1972). The use of Gerlach troughs is another possibility (Gerlach, 1966).

Except for retaining sediments, the reservoirs also contribute to increased groundwater recharge. This study showed that the infiltration capacity of the soil beneath at least one of the reservoirs is relatively low. It would be interesting to know what the combined effect is of the reservoirs and how much of the water that infiltrates actually reaches the groundwater.

Concerning the issue of overgrazing, more socio-economic research is required as many questions remain to be answered. How important are the goats for the Bonairian population? What is the perception of Bonairians towards overgrazing and the problems it causes? What would it take to reduce the grazing pressure?

Lastly, more information is needed concerning the ‘saliñas’. This research estimated the trapping efficiency of the ‘saliña’ in the Playa catchment to be very high. Is this really the case? How is the ‘saliña’ affected by large amounts of deposited sediment? Do they need to be dredged? What would the ecological effect of this dredging be?

6. Discussion and conclusions

Rainfall runoff relationship of the catchment
As was predicted, the largest amounts of surface runoff are produced in the most densely paved areas which are located in central Kralendijk. The uplands produce quite a lot of runoff as well, especially due to the relatively steep slopes.

Erodibility is mainly affected by slope, and therefore most of the soil loss was simulated to occur in the relatively steep shrub-lands to the East. When comparing the effect of rainfall intensity and rainfall duration on runoff and erosion, it was found that intensity had the largest effect on runoff and even more so on erosion. However, a rainfall event falling on soil which is initially moist largely increases both soil loss and runoff especially in the midlands. In central Kralendijk, the initial soil moisture content does not have much effect as most surface area is paved.

It is interesting to note that most rainfall events fall when the soil is relatively dry (at wilting point). During wet years, there are not necessarily more rainy days but simply more rainfall per rainy day and therefore probably more intense rainfall events. These years are therefore extra problematic in terms of urban flooding and sediment flows into the ocean.

Vegetation cover does not have much effect on surface runoff; a rainfall event falling during the beginning of the rainy season therefore causes just as much runoff as an event falling towards the end. As expected, erosion rates are larger when the vegetation cover is low. This effect is largest in the uplands as most vegetation is found here. The combination of most intense storms and least vegetation cover during the beginning of the rainy season means most of the soil loss will occur then.

Reservoirs
The most significant result concerning the sediment budget is the high simulated sediment trapping efficiency of the reservoirs in the catchment (85%-99%) and particularly that of the 'saliña' in front of the outlet of sub-catchment 4 (99%). Comparing the computed trapping efficiencies with those found in literature, shows that they are not unusual. Studies performed by Brune (1953) and Dendy (1974) showed that small reservoirs very often have trapping efficiencies between 80% and 99% depending factors such as pond geometry, sediment composition and flow rate. Some of the ponds built as floodwater retarding structures in Belgium (Verstraeten and Poesen, 1999) were shown to lose their total water retention capacity in just 3-4 years. The most effective settling basins are those with a large area, shallow depth and abrupt change in slope (Brune, 1953). The 'saliña' in sub-catchment 4 agrees with all of these conditions.

The easiest way to reduce the sediment load into the ocean is to tackle the main source of sediment which is outlet 1. Interestingly, most of the sediment that flows through this outlet does not come from the highly erodible uplands but from the area that it drains near the coast. During a five year rainfall event, only 15% of the sediment flowing through this outlet comes out of the reservoir closest to the outlet while the rest comes from the coastal area. During a 10 year event, this is 25% (because more upland reservoirs overflow). Looking at the composition of sediments flowing into the sea, shows us that the discharge of outlet 1 contains a lot more fine sand particles than the discharge of outlet 4. These are sediments with a relatively fast settling velocity and therefore will easily be trapped by any near-to-sea reservoir. Even though there might not be a lot of space for a reservoir at outlet 1, any way of reducing the flow velocity at the outlet would be helpful. This could include measures such as a barrier before the outlet or simply deepening the channel. Such a structure should however be cleaned regularly to make

sure the retention capacity is kept as large as possible and that large rainfall events do not still cause the settled sediment to be flushed into the sea.

For the scenario in which the 'tankis' are removed, the contribution of sediment from the uplands increases to a large extent. During a ten year event now 50% of the sediment flowing through outlet 1 comes out of the reservoir closest to the outlet (compared to 25% with 'tankis)'. The only reason for this increase is the much larger overflow of discharge and sediment from the LVV reservoir (80% more). This shows that the 'tankis' in the uplands are very important in reducing ocean sedimentation. With the 'tankis' gone, there is firstly a larger chance that the larger governmental reservoirs will overflow and that sediment from the uplands will reach the ocean. Secondly, once the governmental reservoirs overflow, the flow velocity through the reservoirs increases meaning the trapping efficiency decreases and more sediment flows through. Thirdly, as more sediment reaches the governmental reservoirs (as it is not captured in the 'tankis') more sediment will flow out again, as only a certain fraction of this sediment will settle.

If the 'tankis' were to disappear, other methods of retaining this water and sediment would be required. This could for example be done by enlarging the current governmental reservoirs or creating new reservoirs. The best location for these reservoirs would be in the largest flows of sediment and discharge which are found along the kaminda Lagoen, the 'rooi' just south of Lagoen hill, and straight down from the highest point in the North-East.

The high trapping efficiencies of the reservoirs in the uplands means they quickly fill up with sediment. To make sure these reservoirs keep being effective, regular maintenance is important. The maintenance of the governmental reservoirs is the responsibility of the DRO, the maintenance of the LVV reservoirs is the responsibility of LVV. At the moment these reservoirs are cleaned on an ad hoc basis (every 5-10 years) depending on the necessity and whether money and equipment is available. Furthermore, the governmental and LVV reservoirs in the uplands have no legal status. In theory, they could therefore easily be removed (in case of building projects) or their maintenance stopped. It would therefore be advisable to give the reservoirs a legal status and also to allocate a certain budget for regular maintenance.

As the largest amounts of sediment reach the ocean when reservoirs overflow, another option could be to drain reservoirs in between rain storms. Especially for the large reservoirs on more sloping land this can easily be done by installing a pipe through the dam wall which can be opened or closed on demand.

Channel and gully erosion

It is interesting to note that the model results show a large fraction of the soil loss to come from the channels instead of from the planes. As an example, for the area upstream of the LVV reservoir, during a five year event 100% more soil loss comes channels than it comes from planes. During a ten year event this value becomes 150%. This is consistent with research done by Osborn and Simanton (1989) and Prosser et al. (2001) which describe channel and gully erosion as the main sources of soil loss in catchments where channelling occurs. According to Blong et al. (1982), once a gully is established, the bulk of the sediment coming from the new channel network originates from the gully walls.

The main way of reducing channel and gully erosion is by stabilizing channel/gully walls and floors. Planting grass or other sturdy vegetation within them would help retain soil yet allow for infiltration. A study done by Molina et al. (2009) in the Ecuadorian Andes shows that gully bed revegetation can completely halt further erosion and even lead to the deposition of over 25% of the sediment generated within a catchment. The effectiveness of gully bed vegetation on gully bed sedimentation and stabilization depends not only on the amount, health and length of plant

roots, stems and leafs, but also on the plant community composition (Molina et al., 2009). A healthy canopy cover increases the resistance to the shear stress of the water flow while a dense plant root system improves the stability and infiltrability of the gully surface (Li et al., 1991). Using a variety of plant species (trees, shrubs, herbs and grasses) is therefore most effective.

It would be advisable to map the most important 'rooien' and channels and also give them a legal status so that their routing will not be disturbed by construction of buildings or infrastructure. On a number of locations in the field the natural drainage pattern was disrupted by human activities meaning water flows were not lead to reservoirs anymore and in some places even lead to residential areas. This means that a lot of water nuisance in residential areas is unnecessary and that the reservoirs in the catchment are not all effectively used.

Vegetation and overgrazing

Increasing the vegetation cover was found to be effective in reducing erosion rates, mainly in the uplands. However, since most of the sediment settles in the reservoirs, it did not have much effect on the sediment yield at the outlet. This does not mean however that reducing the grazing pressure is therefore not required. On-site erosion reduction is generally preferable due to the number of added benefits it provides. Improved vegetation cover improves soil fertility and will also greatly reduce sediment deposition in the reservoirs meaning maintenance costs will decrease. Assuming the reservoirs currently need to be cleaned every 5 years, reduced grazing (assuming a decrease in soil loss per event of 20% towards the end of the rainy season and 50% at the start – therefore an average decrease of 35%) would mean they only need to be cleaned every 7 to 8 years.

Of course reducing the grazing pressure is not a simple matter. According to Jarvis (2008), open access ranges will always result in overgrazing unless control mechanisms exist and are effective. The main reason for this is the conflict between individual ownership of livestock and the communal ownership of the pasture – leading to the maximization of individual benefit at the expense of the community (Hardin, 1968). Different control mechanisms exist such as taxation of livestock, enforcing stocking quotas, or destocking incentives (Jarvis, 1991). In Iceland for example, environmental projects undertaken by farmers were subsidized in return for reducing sheep numbers. As a result, the number of sheep has halved since 1979 (Arnalds, 1999).

Removing the access to the communal land by enforcing fencing regulations is another method. However, as goats are an important source of additional income for Bonairians, this will lead to a lot of resistance because it means fewer goats can be kept (Pers. Com. Kris Kats, 2012). If possible, solutions should be sought in ensuring an income from these goats with less harmful effects for the environment.

At this moment for example, a water treatment plant is being built, and a pilot project will start in which the effluent will partly be used to grow animal fodder. This animal fodder is then distributed for a fixed low price to farmers agreeing to keep their livestock fenced. A similar project could be to enlarge several well located reservoirs and use this water to irrigate fodder crops. It should be made sure though that these reservoirs provide a reliable and large enough source of water to be able to grow fodder crops on a larger scale than is the case now so that profitability is ensured.

Another idea is to make the market more attractive to goats (Pers. Com. Kris Kats, 2012). This could be done by encouraging large consumers on the island (supermarkets and hotels and resorts) to start doing more with local goat meat or trying to export. In this way the life cycle of the goats is reduced. The fewer dry seasons a goat experiences before is it is consumed the better it is for the environment. Of course, such actions aimed at increasing the profitability of

the goats should go hand in hand with enforcing fencing regulations - otherwise it will only lead to the increase of goat numbers on the island.

Inundation in central Kralendijk

Water from upstream is not the cause for flooding problems in Kralendijk. Surface runoff south of the Kaya Nikiboko North, flows into the reservoir system along Kaya International and is drained away at the Plaza resort. Surface runoff North of the Kaya Nikiboko Noord is collected by the channel alongside Kaya Nikiboko Noord and led to the ocean via a number of reservoirs.

The flooding problem in central Kralendijk is therefore primarily an inundation problem – rainfall in central Kralendijk cannot be drained fast enough because the capacity of the current drainage system is not sufficient. Especially the drains in sub-catchment 2 are problematic.

Reducing the percentage of paved area was found to have some effect on reducing surface runoff in central Kralendijk. However, the discharge through the channels remains high and the inundation hazard is therefore barely reduced. Therefore, to reduce the inundation problems in central Kralendijk, the most effective measure is to increase the discharge capacity of the current drainage system. The focus should especially be on sub-catchment 2. Because of the low elevation differences in central Kralendijk, modifying channel slope is difficult. Therefore solutions have to be sought in enlarging the channels or diverting some of the discharge originating in sub-catchment 2 to another drainage network. The drain in front of the hospital for example can easily be connected to the reservoir in sub-catchment 1.

Increasing the discharge capacity of the drainage network can be combined with measures that decrease runoff. Mentioned before were measures that promote infiltration (permeable pavement and infiltration wells). Another method is to increase the water storage capacity by having green roofs or ponds. Collecting rainwater from roofs with gutters and using this for household use is something that has been done in the past (Eilandgebied Bonaire, 2003). Re-promoting this and other measures and perhaps subsidizing their installation could be another interesting idea.

All in all, including drainage, storm-water storage and improved infiltration more into urban planning would be advisable. At this moment this is not sufficiently done (Pers. Com. Kris Kats, 2012).

7. References

AL-QURASHI, A., MCINTYRE, N., WHEATER, H. & UNKRICH, C. 2008. Application of the Kineros2 rainfall–runoff model to an arid catchment in Oman. *Journal of Hydrology,* 355**,** 91-105.

ALLEN, R. G., PEREIRA, L. S., RAES, D. & SMITH, M. 1998. Crop evapotranspiration - Guidelines for computing crop water requirements. *Irrigation and Drainage Paper No. 56.* Rome, Italy: FAO.

ARNALDS, A. 1999. Incentives for soil conservation in Iceland. *In:* SANDERS, D. W., HUSZAR, P. C., SOMBATPANIT, S. & ENTERS, T. (eds.) *Incentives in soil conservation : from theory to practise.* New Delhi: Oxford and INH Publishing.

ARTIOLA, J. F., PEPPER, I. L. & BRUSSEAU, M. L. 2004. *Environmental Monitoring and Characterization,* San Diego, Elsevier Academic Press.

ASCE 1990. *Evaporation and Irrigation Water Requirements,* New York, ASCE.

ASCON & DHV 1990. Afwatering Kralendijk. Regering van de Nederlandse Antillen, Departement voor Ontwikkelinkssamenwerking.

BAK, R., NIEUWLAND, G. & MEESTERS, E. 2005. Coral reef crisis in deep and shallow reefs: 30 years of constancy and change in reefs of Curacao and Bonaire. *Coral Reefs,* 24**,** 475-479.

BLONG, R. J., GRAHAM, O. P. & VENESS, J. A. 1982. The role of sidewall processes in gully development; some N.S.W. examples. *Earth Surface Processes and Landforms,* 7**,** 381-385.

BORST, L. & HAAS, S. A. D. 2005. Hydrological research bonaire; a hydrogeological investigation of Bonaire's watersystem. Amsterdam: Acacia institute.

BRUNE, G. M. 1953. Trap efficiency of reservoirs. *Transactions of American Geophysical Union,* 34**,** 407-418.

CANFIELD, H. E. & GOODRICH, D. C. Studies of Scale and Processes in Hydrologic Modeling on the Lucky Hills Watershed. *In:* SCOTTS, R. L., ed. First Interagency Conference on Research in the Watersheds, 2003 Benson. USDA Agricultural Research Service Special Publication, 444-450.

CHOW, V. T. 1959. *Open-channel hydraulics,* New York, McGraw-Hill Book Co.

CHOW, V. T., MAIDMENT, D. R. & MAYS, L. W. 1988. *Applied Hydrology,* New York, McGraw Hill.

CRAWFORD, L. & LINSLEY, J. 1966. Digital Simulation in Hydrology Stanford IV Watershed Model. *Report n. 39.* Stanford University: Department of Civil Enginering.

DE FREITAS, J. A., NIJHOF, B. S. J., ROJER, A. C. & DEBROT, A. O. 2005. Landscape ecological vegetation map of the island of Bonaire (Southern Carribean). Amsterdam: Royal Netherlands Academy of Arts and Sciences.

DEBROT, A. O., MEESTERS, E., DE LEON, R. & SLIJKERMAN, D. 2010. Lac Bonaire - Restoration Action Spear Points. Wageningen: Imares, Wageningen UR.

DEBROT, A. O., WENTINK, C. & WULFSEN, A. 2012. Baseline survey of anthropogenic pressures for the Lac Bay ecosystem, Bonaire. Wageningen: IMARES.

DENDY, F. E. 1974. Sediment Trap Efficiency of small reservoirs. *Transactions of American Society of Agricultural Engineers*.

DI BALDASSARRE, G., BRATH, A. & MONTANARI, A. 2006. Reliability of different depth-duration-frequency equations for estimating short-duration design storms. *Water resources Research,* 42.

DIRKSEN, C. 1999. Unsaturated Hydrualic Conductivity. *In:* SMITH, K. A. & MULLINS, C. E. (eds.) *Soil and Environmental Analysis, Physical Methods.* New York: Marcel Dekkers.

DRO 2010. Ruimtelijk Ontwikkelingsplan Bonaire.

EILANDGEBIED BONAIRE 2003. Milieubeleidsplan Bonaire.

ENGMAN, E. T. 1986. Roughness coefficients for routing surface runoff. *Journal of Irrigation and Drainage Engineering,* 112**,** 39-53.

FAO, M. 1990. Guidelines for soil description. *Soil Resources, Management and Conservation Service, 3rd ed. FAO, Rome*.

FOHRER, N., HAVERKAMP, S., ECKHARDT, K. & FREDE, H. G. 2001. Hydrologic Response to land use changes on the catchment scale. *Physics and Chemistry of the Earth, Part B: Hydrology, Oceans and Atmosphere,* 26**,** 577-582.

FOLEY, J. A., DEFRIES, R., ASNER, G. P., BARFORD, C., BONAN, G., CARPENTER, S. R., CHAPIN, F. S., COE, M. T., DAILY, G. C., GIBBS, H. K., HELKOWSKI, J. H., HOLLOWAY, T., HOWARD, E. A., KUCHARIK, C. J., MONFREDA, C., PATZ, J. A., PRENTICE, I. C., RAMANKUTTY, N. & SNYDER, P. K. 2005. Global Consequences of Land Use. *Science,* 309**,** 570-574.

FOSTER, G. R. & DISSMEYER, G. E. 1981. Estimating the cover management factor (c) in the universal soil loss equation for forest conditions. *Journal of Soil and Water Conservation,* 36.

FOSTER, G. R. & SMITH, R. E. A dynamic erosion concept. Natural Resources Modeling Symposium, 1984 Pingree Park, Colorado. U.S. Departement of Agriculture, 434-437.

FOSTER, G. R., SMITH, R. E., KNISEL, W. G. & HAKONSON, T. E. 1983. Modeling the effectiveness of on-site sediment controls. *Summer 1983 meeting, American Society of Agricultural Engineers.* Bozeman, MT.

GARDNER, W. R. 1958. Some steady-state solutions of the unsaturated moisture flow equation with application to evaporation from a water table. *Soil Science,* 85**,** 228-232.

GERLACH, T. 1966. Współczesby rozwóy stoków w dorzeczu górnego Grajcarka (Beskid Wysoki-Karpaty Zachodnie). *Prace Geografia,* IG PAN 52.

GOOGLE EARTH V 7.0.3.8542. 01-21-2012. *Kralendijk, Bonaire. 12°09 N, 68°16 W, Eye alt 17116ft* [Online]. DigitalGlobe 2013. Available: http://www.earth.google.com [Accessed 10-09-2013 2013].

GRAYSON, R. B., MOORE, I. D. & MCMAHON, T. A. 1992. Physically based hydrologic modeling: 2. Is the concept realistic? *Water resources Research,* 28**,** 2659-2666.

GRONTMIJ & SOGREAH 1968. Water and land resources development plan for the islands of Aruba, Bonaire and Curacao. *Report Grontmij.* De Bilt.

HAMILL, L. 2001. *Understanding Hydraulics,* London, MacMillan Press LTD.

HARDIN, G. 1968. The tragedy of the Commons. *Science,* 162**,** 1243-1248.

HENLEY, W. F., PATTERSON, M. A., NEVES, R. J. & LEMLY, A. D. 2000. Effects of Sedimentation and Turbidity on Lotic Food Webs: A Concise Review for Natural Resource Managers. *Reviews in Fisheries Science,* 8**,** 125-139.

HULSMAN, P. 2012. Survey on the opinion of inhabitants of Bonaire on the local water istuation. Delft: Delft University of Technology.

JARVIS, A., REUTER, H. I., NELSON, A. & GUEVARA, E. 2008. Hole-filled seamless SRTM data V4. *In:* (CIAT), I. C. F. T. A. (ed.).

JARVIS, L. S. 1991. Overgrazing and Range Degradation in Africa: The Need and the Scope for Government Control of Livestock Numbers. *East Africa Economic Review,* 7.

KALIN, L. & HANTUSH, M. M. 2003. *Evaluation of sediment transport models and comparative application of two watershed models* [Online]. Cincinnati, Ohio: U.S. Environmental Protection Agency, Office of Research and Development, National Risk Management Research Laboratory. Available: http://www.epa.gov/nrmrl/pubs/600r03139/600r03139.pdf.

KAUSHAL, S. S. & BELT, K. T. 2012. The urban waterhed continuum: evolving spatial and temporal dimensions. *Urban Ecosystem,* 15**,** 409-435.

KEKEM, A. J. V., ROEST, C. W. J. & SALM, C. V. D. 2006. Critical review of the proposed irrigation and effluent standards for Bonaire *Alterra-Report.* Wageningen: Alterra.

KENNEDY, J. R., GOODRICH, D. C. & UNKRICH, C. L. 2012. Using the KINEROS2 modeling framework to evaluate the increase in storm runoff from

residential development in a semi-arid environment. *Journal of Hydrologic Engineering,* 10.

KLEMES, V. 1986. Dilettantism in hydrology: Transition or destiny? *Water resources Research* 22**,** 177S-188S.

KLM AEROCARTO. 1963. *Topografische kaart*. Netherlands Antilles: Dienst van het Kadaster.

LAL, R. 1997. Deforestation effects on soil degradation and rehabilitation in western Nigeria. IV. Hydrology and water quality. *Land Degradation & Development,* 8**,** 95-126.

LEE, J. H. & BANG, K. W. 2000. Characterization of urban stormwater runoff. *Water Research,* 34**,** 1773-1780.

LI, Y., ZHU, X. M. & TIAN, J. Y. 1991. Effectiveness of plant roots to increase the anti-scouribility of soil on the Loess Plateau. *Chinese Science Bulletin,* 36**,** 2077-2082.

MARSHALL, T. J. & QUIRK, J. P. 1950. Stability of structural aggregates of dry soil. *Australian Journal of Agricultural Research,* 1**,** 266-275.

MARTÍNEZ-CARRERAS, N., SOLER, M., HERNÁNDEZ, E. & GALLART, F. 2007. Simulating badland erosion with KINEROS2 in a small Mediterranean mountain basin (Vallcebre, Eastern Pyrenees). *CATENA,* 71**,** 145-154.

MINTZ, Y. & SERAFINI, Y. 1984. Global fields of normal monthly soil moisture, as derived from precipitation and an estimated evapotranspiration. *Final Scientific Report Under NASA Grant No. NAS5-26.* University of Maryland, College Park: Departement of Meteorology.

MOLINA, A., GOVERS, G., CISNEROS, F. & VANACKER, V. 2009. Vegetation and topographic controls on sediment deposition and storage on gully beds in a degraded mountain area. *Earth Surface Processes and Landforms,* 34**,** 755-767.

MORGAN, R. P. C. 2005. *Soil Erosion and Conservation,* Oxford, Blackwell Publishing.

MORON, V. A., LUCERO, A., HILARIO, F., LYON, A., ROBERTSON, W. & DEWITT, D. 2009. Spatio-temporal variability and predictability of summer monsoon onset over the Philippines. *Climate Dynamics,* 33**,** 1159–1177.

MUNSELL COLOUR COMPANY 1994. *Munsell Soil Color Charts,* Baltimore, MD, Munsell Color Company.

NIEMCZYNOWICZ, J. 1999. Urban hydrology and water management – present and future challenges. *Urban Water,* 1**,** 1-14.

NOLET, C. & VEEN, M. 2009. Stofonderzoek Bonaire. Stichting Kribahacha/Wageningen UR.

OLEA, R. A. 1984. Sampling Design Optimization for Spatial Functions. *Mathematical Geology,* 16.

OSBORN, H. B. & SIMANTON, J. R. 1989. Gullies and Sediment Yield. *Rangelands,* 11**,** 51-56.

PIMENTEL, D., ALLEN, J., BEERS, A., GUINAND, L., LINDER, R., MCLAUGHLIN, P., MEER, B., MUSONDA, D., PERDUE, D., POISSON, S., SIEBERT, S., STONER, K., SALAZAR, R. & HAWKINS, A. 1987. World Agriculture and Soil Erosion. *BioScience,* 37**,** 277-283.

PROSSER, I. P., RUTHERFURD, I. D., OLLEY, J. M., YOUNG, W. J., WALLBRINK, P. J. & MORAN, C. J. 2001. Large-scale patterns of erosion and sediment transport in river networks, with examples from Australia. *Marine and Freshwater Research,* 52**,** 817-817.

RAPP, A., MURRAY-RUST, D. H., CHRISTIANSSON, C. & BERRY, L. 1972. Soil erosion and sediment transport in four cathments near Dodoma, Tanzania. *Geografiska Annaler,* 54-A**,** 125-155.

RAWLS, W. J., BRAKENSIEK, D. L. & SAXTON, K. E. 1982. Estimation of soil water properties. *Transactions of the American society of agricultural engineers,* 25**,** 1316-1320.

REYNOLDS, W. & ELRICK, D. 1991. Determination of hydraulic conductivity using a tension infiltrometer. *Soil Science Society of America Journal,* 55**,** 633-639.

RODRIGUEZ, E., MORRIS, C. S. & BELZ, J. E. 2006. A global assessment of the SRTM performance. *Photogrammetric Engineering and Remote Sensing,* 72**,** 249–260.

ROGERS, C. S. 1990. Responses of coral reefs and *Marine ecology progress series,* 62**,** 185-202.

SCHLICHTING, E., BLUME, H. P. & STAHR, K. 1995. *Bodenkundliches Praktikum,* Berlin, Vienna, Blackwell.

SEMMENS, D. J., GOODRICH, D. J., UNKRICH, C. L., SMITH, R. E. & WOOLHISER, D. A. 2008. KINEROS2 and the AGWA modeling framework. *In:* WHEATHER, H. S., SOROOSHIAN, S. & SHARMA, K. D. (eds.) *Hydrological modelling in arid and semi-arid areas.* Cambridge: Cambridge University Press.

SHI, P.-J., YUAN, Y., ZHENG, J., WANG, J.-A., GE, Y. & QIU, G.-Y. 2007. The effect of land use/cover change on surface runoff in Shenzhen region, China. *CATENA,* 69**,** 31-35.

SMITH, R. E., GOODRICH, D. C. & UNKRICH, C. L. 1999. Simulation of selected events on the Catsop catchment by KINEROS2: A report for the GCTE conference on catchment scale erosion models. *CATENA,* 37**,** 457-475.

SMITH, R. E., GOODRICH, D. C., WOOLHISER, D. A. & UNKRICH, C. L. 1995. KINEROS - A kniematic Runoff and Erosion Model. *In:* SINGH, V. J. (ed.) *Computer Models of Watershed Hydrology.* Water Resources Publications.

STATISTIEK, C. B. V. D. 2012. *Bevolkingsontwikkeling Carbisch Nederland; geboorte, sterfte, migratie* [Online]. Den Haag/Heerlen. Available: http://statline.cbs.nl/StatWeb/publication/?DM=SLNL&PA=80539ned&D1=0-1,9-10&D2=a&D3=a&HDR=T&STB=G1,G2&CHARTTYPE=1&VW=T.

TAYLOR, A. & SCHWARZ, H. 1952. Unit hydrograph lag and peakflow related to basin characteristics. *Transactions of the American Geophysics Union,* 33**,** 235-246.

VAES, G. 1999. *The influence of rainfall and model simplification on the design of combined sewer systems.* University of Leuven.

VERSTRAETEN, G. & POESEN, J. 1999. The nature of small-scale flooding, muddy floods and retention pond sedimentation in central Belgium. *Geomorphology,* 29**,** 275-292.

WILLMOTT, C. J. & ROWE, C. M. 1985. Climatology of the terrestrial seasonal water cycle. *Journal of Climatology,* 5**,** 589-606.

WISCHMEIER, W. & SMITH, D. 1978. Predicting rainfall erosion losses: a guide to conservation planning. *Agriculture handbook.* Washington: USDA.

WISCHMEIER, W. H., JOHNSON, C. B. & CROSS, B. V. 1971. A soil erdobility nomograph for farmland and construction sites. *Journal of Soil and Water Conservation,* 26**,** 189-193.

WOODING, R. A. 1968. Steady infiltration from a shallow circular pond. *Water resources Research,* 4**,** 1259-1273.

WOOLHISER, D. A. 1975. Simulation of unsteady overland flow. *In:* MAHMOOD, K. & YEVJEVICH, V. (eds.) *Water resource publications.* Fort Collins.

WOOLHISER, D. A., SMITH, R. E. & GOODRICH, D. C. 1990. KINEROS, A Kinematic Runoff and Erosion Model: Documentation and User Manual. *Agricultural Research Service Publication ARS-77.* US Department of Agriculture.

WREN, D. G., BARKDOLL, B. D., KUHNLE, R. A. & DERROW, R. W. 2000. Field Technoques for Suspended-Sediment Measurement. *Journal of Hydraulic Engineering,* 97**,** 97-104.

ZHANG, R. 1997. Determination of soil sorptivity and hydraulic conductivity from the disk infiltrometer. *Soil Science Society of America Journal,* 61**,** 1024-1030.

ZHANG, Y., WEI, H. & NEARING, M. A. 2011. Effects of antecedent soil moisture on runoff modeling in small semiarid watersheds of southeastern Arizona. *Hydrology and Earth System Sciences,* 15.

Annexes

Annex 1: Evapotranspiration

To calculate the evapotranspiration, the FAO Penman- Monteith method is used (Allen et al., 1998) whereby by the potential evapotranspiration is calculated using Equation 39:

$$ET_0 = \frac{0.408\Delta(R_n - G) + \gamma \frac{900}{T+273} u_2 (e_s - e_a)}{\Delta + \gamma(1 + 0.34u_2)} \quad \textbf{(39)}$$

where:

ET_0 is the reference evapotranspiration (mm day^{-1}),
R_n is the net radiation at the crop surface (MJ m^{-2} day^{-1}),
G is the soil heat flux density (MJ m^{-2} day^{-1}),
T is the mean daily air temperature at 2 m height (°C),
U_2 is the wind speed at 2 m height (m s^{-1}),
E_s is the saturation vapour pressure (kPa),
E_a is the actual vapour pressure (kPa),
E_s-e_a is the saturation vapour pressure deficit (kPa),
Δ is the slope vapour pressure curve (kPa °C^{-1}),
γ is the psychrometric constant (kPa °C^{-1}),

The slope of the saturation vapour pressure curve (Δ) is calculated using Equation 40:

$$\Delta = \frac{4098\left[0.6108exp\left(\frac{17.27 \times T}{T+237.3}\right)\right]}{(T+237.3)^2} \quad \textbf{(40)}$$

The psychrometric constant is given by Equations 41 and 42:

$$\gamma = 0.665 \times 10^{-3} P \quad \textbf{(41)}$$

$$P = 101.3\left(\frac{293 - 0.0065z}{293}\right)^{5.26} \quad \textbf{(42)}$$

Where P is the atmospheric pressure (kPa) and z is the altitude (m) for which a value of 6 is taken. The net radiation is the difference between the incoming net short wave radiation (R_{ns}) and the outgoing net long wave radiation (R_{nl})

$$R_n = R_{ns} - R_{nl} \quad \textbf{(43)}$$

The outgoing long wave radiation is given by Equation 44:

$$R_{nl} = \sigma\left[\frac{{T_{max,K}}^4 + {T_{min,K}}^4}{2}\right]\left(0.34 - 0.14\sqrt{e_a}\right)\left(1.35\frac{R_s}{R_{so}} - 0.35\right) \quad \textbf{(44)}$$

where:

σ is the Stefan-Boltzmann constant (4.903 10-9 MJ K-4 m-2 day-1),
$T_{max,K}$ is the maximum absolute temperature during the 24-hour period (K),
$T_{min,K}$ is the minimum absolute temperature during the 24-hour period (K),

E_a is the actual vapour pressure (kPa),
R_s is the solar radiation (MJ m^{-2} day^{-1}),
R_{so} is the clear-sky radiation (MJ m^{-2} day^{-1}).

The net shortwave radiation (R_{ns}) is given by Equations 45 and 46:

$$R_{ns} = (1 - \alpha)R_s \quad \textbf{(45)}$$

$$R_s = 0.7R_a - 4 \quad \textbf{(46)}$$

where α is the albedo, which is 0.23 for the hypothetical grass reference crop.

The clear sky radiation is calculated using Equation 47:

$$R_{so} = (0.75 + 2 \times 10^{-5} z)R_a \quad \textbf{(47)}$$

The actual vapour pressure is calculated by Equation 48:

$$e_a = 0.611 exp\left[\frac{17.27T_{dew}}{T_{dew} + 237.3}\right] \quad \textbf{(48)}$$

where T_{dew} is the dew point temperature (^oC).

The extra-terrestrial radiation (R_a) is calculated using Equation 49:

$$R_a = \frac{24(60)}{\pi} G_{sc} d_r [\omega_s \sin(\varphi) \sin(\delta) + \cos(\varphi) \cos(\delta) \sin(\omega_s)] \quad \textbf{(49)}$$

where:

G_{sc} is the solar constant (0.0820 MJ m^{-2} min^{-1}),
d_r is the inverse relative distance Earth-Sun (Equation 50),
ω_s is the sunset hour angle (rad) (Equation 51),
ϕ is the latitude (rad)
δ is the solar declination (rad) (Equation 52).

$$d_r = 1 + 0.033 cos\left(\frac{2\pi}{365} J\right) \quad \textbf{(50)}$$

$$\omega_s = arccos[-tan(\varphi) tan(\delta)] \quad \textbf{(51)}$$

$$\delta = 0.409 sin\left(\frac{2\pi}{365} J - 1.39\right) \quad \textbf{(52)}$$

Annex 2: Volume calculation of Kralendijk reservoir

A depth profile of the Kralendijk basin was made by measuring the water level in the reservoir on a certain day on a number of different locations. This depth was converted to height above sea level using a reference point of which the height was known (this was measured using GPS). The height points were interpolated using IDW to give a DEM of the reservoir floor (see Figure 47). Using ArcGIS, the volume of water stored within the basin at a number of different water levels was calculated and a rating curve (Figure 46) was determined giving the relationship between water level (m) and volume (m^3) within the basin.

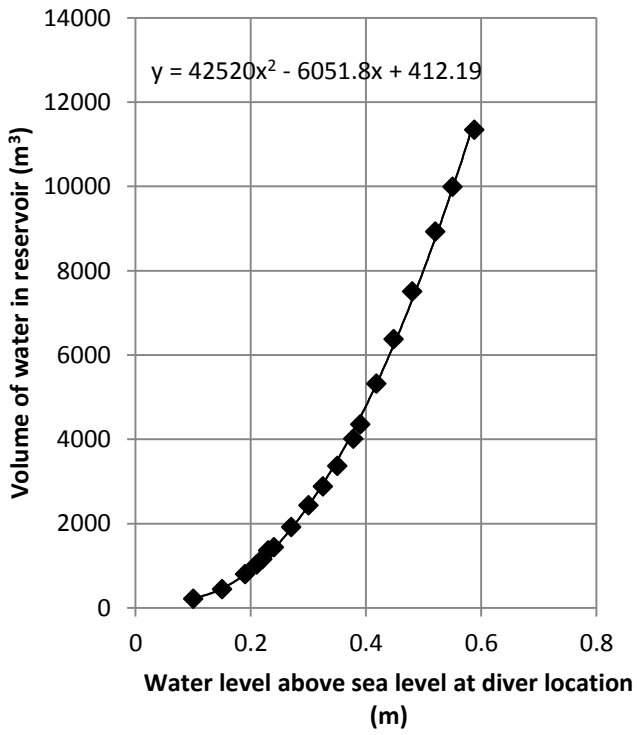

Figure 46: Rating curve of Kralendijk reservoir

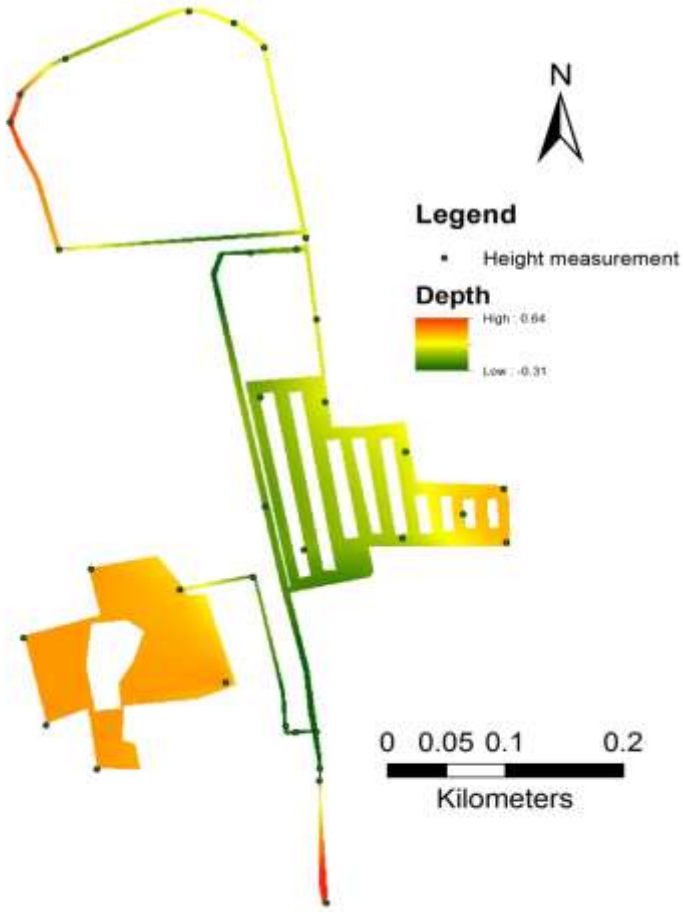

Figure 47: DEM of Kralendijk reservoir

Annex 3: Measured soil properties

Table 7: Measured soil properties at 12 sampling sites

	1	2	3	4	5	6	7	8	9	10	11	12
Bulk Density (g cm^{-3})	1.26	1.27	1.33	1.40	1.35	1.29	0.99	0.94	1.31	1.52	1.42	1.17
Maximum saturation	0.50	0.46	0.51	0.42	0.46	0.50	0.58	0.57	0.42	0.40	0.45	0.48
OM content	3	2	2	2	2	4	2	4	0.5	2	2	3
Structure class	3	3	3	3	3	3	3	3	2	2	3	3
Sand fraction	0.35	0.65	0.60	0.65	0.65	0.60	0.60	0.40	0.65	0.65	0.65	0.65
Silt fraction	0.10	0.25	0.15	0.25	0.25	0.15	0.15	0.40	0.25	0.25	0.25	0.25
Clay fraction	0.55	0.10	0.25	0.10	0.10	0.25	0.25	0.20	0.10	0.10	0.10	0.10
K_{sat} (mm hr^{-1})	97.92	40.32	10.69	25.49	33.05	77.04	28.76	14.83	44.64	30.67	34.34	72
G (mm)	890	248	617	248	248	617	617	378	248	248	248	248
Porosity (-)	0.525	0.522	0.497	0.472	0.490	0.512	0.625	0.647	0.505	0.428	0.465	0.558
CV (-)	0.843	0.716	0.592	0.581	0.313	0.471	0.493	0.503	0.084	0.249	0.800	0.256
Dist (-)	0.16	0.38	0.4	0.38	0.38	0.4	0.4	0.25	0.38	0.38	0.38	0.38
Rock (-)	0.043	0.105	0.037	0.047	0.107	0.034	0.021	0.019	0.076	0.193	0.011	0.093

Table 8: Measured and modelled soil moisture content (θ) at the 12 sampling sites

Sampling site	Texture	Soil moisture content 21-11-2012 (θ)		Soil moisture content 27-11-2013 (θ)		Soil moisture content 23-12-2013 (θ)	
		Measured	Modelled	Measured	Modelled	Measured	Modelled
1	C	-	-	0.24	0.24	0.29	0.32
2	SL	-	-	0.14	0.13	0.15	0.19
3	SCL	0.18	0.13	0.22	0.16	0.33	0.24
4	SL	0.09	0.1	0.20	0.13	0.19	0.19
5	SL	0.15	0.1	0.19	0.13	0.21	0.19
6	SCL	0.12	0.13	0.18	0.16	0.31	0.24
7	SCL	0.11	0.13	0.19	0.16	0.22	0.24
8	L	-	-	0.24	0.15	0.27	0.22
9	SL	0.16	0.1	0.17	0.13	0.25	0.19
10	SL	0.10	0.1	0.24	0.13	0.24	0.19
11	SL	0.21	0.1	0.14	0.13	0.21	0.19
12	SL	0.09	0.1	0.14	0.13	0.23	0.19

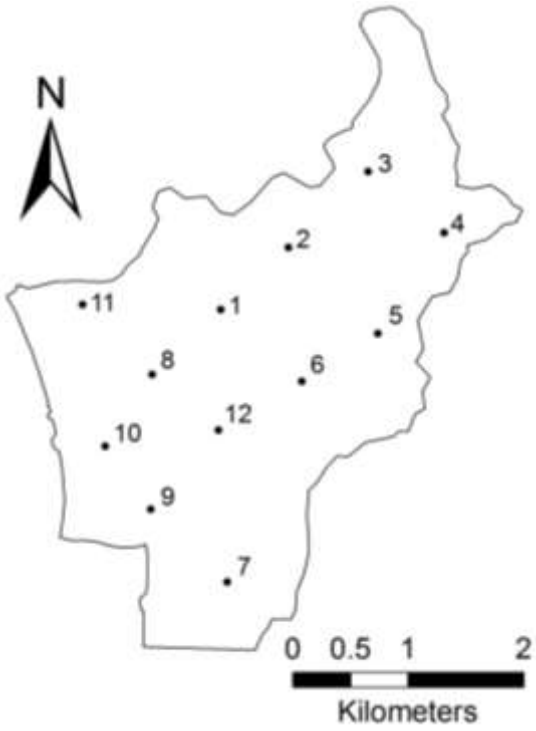

Figure 48: Location of the sampling sites

Annex 4: Pond geometry

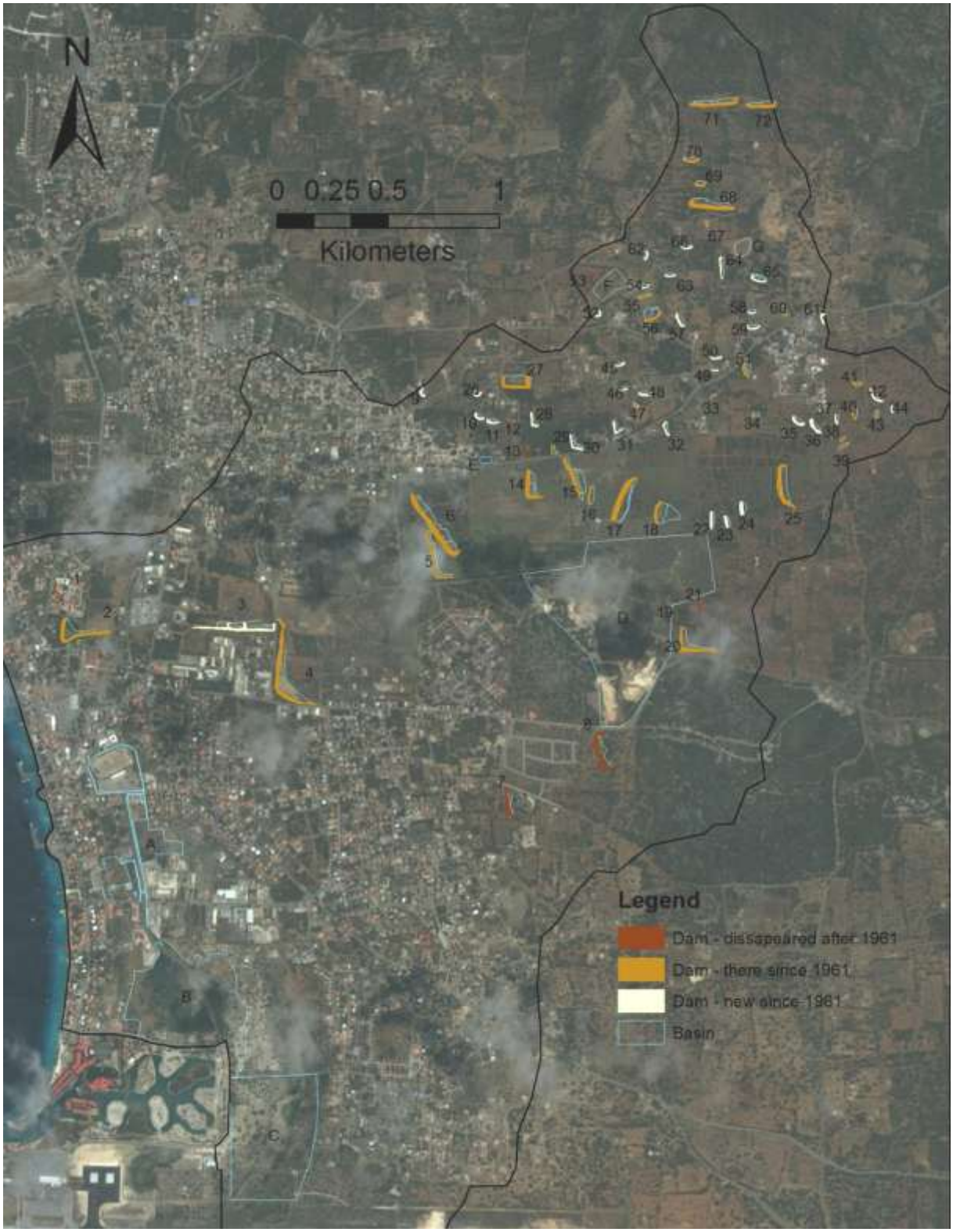

Figure 49: Location and numbering of reservoirs

Table 9: Pond geometry

Number	Type	State	Area (m^2)	Volume (m^3)
1	Kralendijk	Disappeared after 1961	na	na
2	Kralendijk	There since 1961	3417	3420
3	Kralendijk	New since 1961	6147	6150
4	Kralendijk	There since 1961	8592	8590
5	LVV	There since 1961	3117	3120
6	LVV	There since 1961	7482	7480
7	Kunuku	Disappeared after 1961	na	na
8	?	Disappeared after 1961	na	na
9	Kunuku	New since 1961	na	na
10	Kunuku	New since 1961	364	360
11	Kunuku	New since 1961	349	350
12	Kunuku	Disappeared after 1961	na	na
13	Kunuku	Disappeared after 1961	na	na
14	LVV	There since 1961	2732	2730
15	LVV	There since 1961	4461	4460
16	LVV	There since 1961	1213	1210
17	LVV	There since 1961	5398	5400
18	LVV	There since 1961	6516	6520
19	Kunuku	Disappeared after 1961	na	na
20	Kunuku	There since 1961	na	na
21	Kunuku	Disappeared after 1961	na	na
22	Kunuku	New since 1961	418	420
23	Kunuku	New since 1961	393	390
24	Kunuku	New since 1961	683	680
25	Government	There since 1961	3243	3240
26	Kunuku	New since 1961	475	480
27	Government	There since 1961	3966	3970
28	Kunuku	New since 1961	465	470
29	Kunuku	There since 1961	466	470
30	Kunuku	New since 1961	1062	1060
31	Kunuku	New since 1961	478	480
32	Kunuku	New since 1961	529	530
33	Kunuku	There since 1961	188	190
34	Kunuku	There since 1961	376	380
35	Kunuku	New since 1961	503	500
36	Kunuku	New since 1961	620	620
37	Kunuku	New since 1961 (bad shape)	371	370
38	Kunuku	There since 1961	na	na
39	Kunuku	There since 1961	237	240
40	Kunuku	There since 1961 (bad shape)	495	500
41	Kunuku	There since 1961	230	230
42	Kunuku	New since 1961	517	520
43	Kunuku	There since 1961 (bad shape)	325	330

44	Kunuku	New since 1961 (bad shape)	223	220
45	Kunuku	New since 1961	296	300
46	Kunuku	New since 1961	213	210
47	Kunuku	There since 1961	202	200
48	Kunuku	New since 1961	444	440
49	Kunuku	New since 1961	140	140
50	Kunuku	New since 1961	320	320
51	Kunuku	There since 1961	1048	1050
52	Kunuku	New since 1961	168	170
53	Kunuku	Disappeared after 1961	na	na
54	Kunuku	New since 1961	331	330
55	Kunuku	There since 1961 (bad shape)	294	290
56	Government	There since 1961	2761	2760
57	Kunuku	New since 1961	716	720
58	Kunuku	New since 1961	324	320
59	Kunuku	New since 1961	563	560
60	Kunuku	There since 1961	na	na
61	Kunuku	New since 1961	na	na
62	Kunuku	New since 1961	241	240
63	Kunuku	New since 1961	372	370
64	Kunuku	New since 1961 (bad shape)	886	890
65	Government	New since 1961	1309	1310
66	Kunuku	New since 1961	307	310
67	Kunuku	There since 1961	na	na
68	Government	There since 1961	2874	2870
69	Kunuku	There since 1961	441	440
70	Kunuku	There since 1961	712	710
71	Government	There since 1961	2433	2430
72	Government	There since 1961	1379	1380
A	Saliña	There since 1961	35659.5	35660
B	Saliña	There since 1961	200000	200000
C	Saliña	There since 1961	200000	200000
D	Excavation	New since 1961	384797	384800
E	Excavation	New since 1961	1385	1390
F	Excavation	New since 1961	5629	5630
G	Excavation	New since 1961	4436	4440

Annex 5: Channel geometry

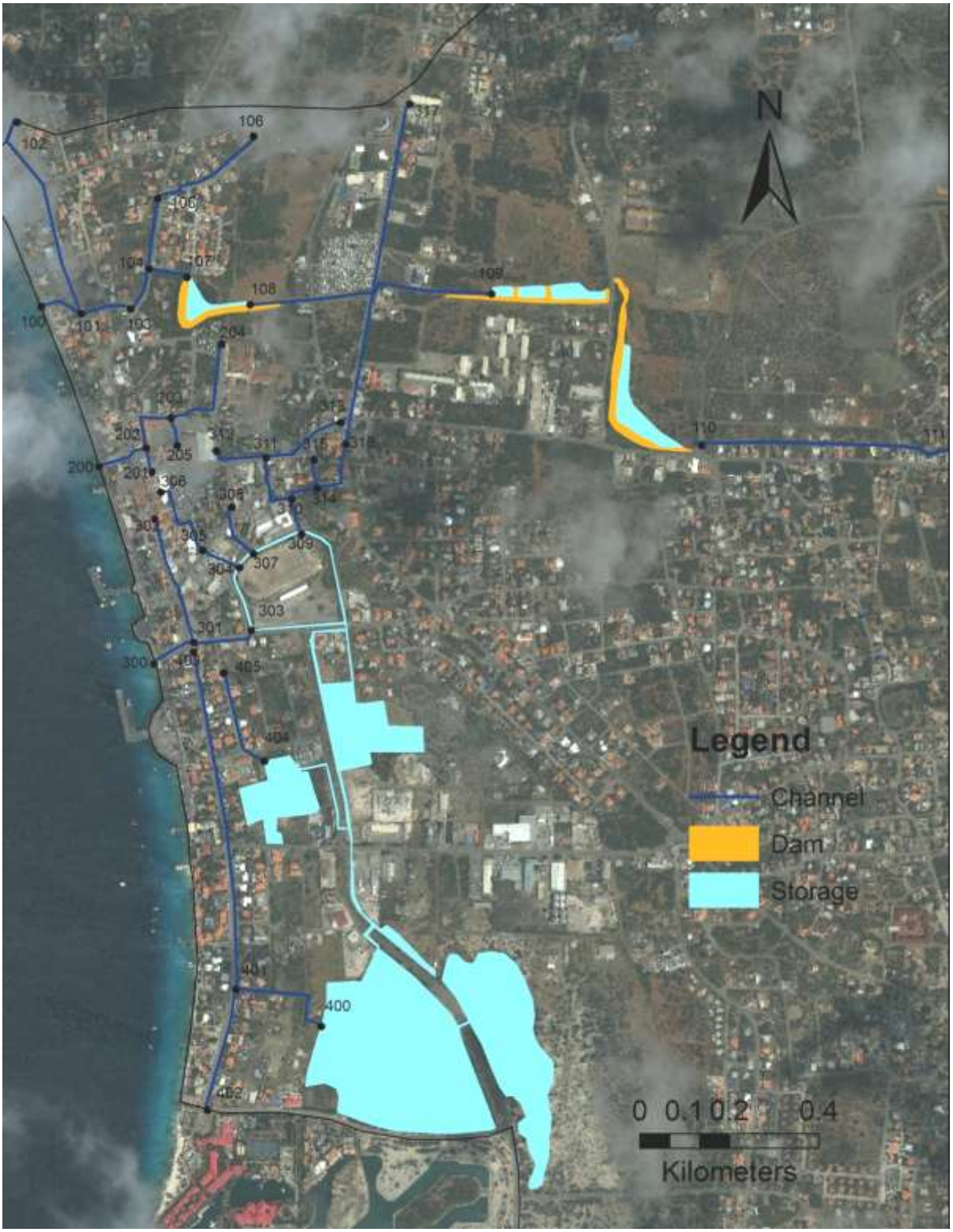

Figure 50: Location of channels

Table 10: Channel geometry

Start Num.	End Num.	Height begin (m)	Height end (m)	Type	Height (cm)	Width (cm)	Bank Width (cm)	Manning's n
405	404	0.507	0.396	Pipe	Round	25		0.011
403	401	0.856	0.560	Pipe	Round	32		0.011
402	401	1.186	0.560	Pipe	Round	32		0.011
401	400	0.560	0.182	Pipe	Round	50		0.011
317	316	4.331	1.650	Pipe	Round	20		0.011
316	314	1.650	1.081	Overland	-	-		
315	314	1.265	1.161	Pipe	Round	16		0.011
314	310	1.081	0.650	Unlined channel	40	200		0.05
313	311	1.487	1.070	Lined covered drain	50	80		0.013
312	311	1.240	1.070	Lined covered drain	50	80		0.013
311	310	1.070	0.650	Lined channel	90	110		0.013
310	309	0.650	0.272	Unlined channel	40	200		0.05
308	307	0.925	0.465	Pipe	Round	16		0.011
306	305	1.248	0.730	Lined covered drain	0.2	0.4		0.013
305	304	0.730	0.531	Lined covered drain	100	150		0.013
303	301	0.650	0.661	Lined covered drain	30	70		0.013
302	301	1.319	0.650	Pipe	Round	16		0.011
301	300	0.650	0.378	Lined covered drain	30	70		0.013
204	203	1.481	1.000	Lined covered drain	15	40		0.013
205	203	1.154	1.000	Pipe	Round	20		0.011
203	202	1.000	0.920	Lined covered drain	50	55		0.013
201	202	1.148	0.920	Lined covered drain	50	55		0.013
202	200	0.920	0.123	Lined covered drain	50	90		0.013
111	110	10.300	4.600	Earthen rooi	160	20	400	0.05
109	108	4.300	2.000	Earthen rooi	100	200	300	0.03
107	104	1.840	1.440	Earthen rooi	70	100	40	0.03
106	105	2.664	1.750	Earthen rooi	50	160	100	0.03
105	104	1.750	1.440	Earthen rooi	80	300	40	0.03
104	103	1.440	1.244	Earthen rooi	80	300	40	0.03
103	101	1.244	0.230	Lined covered drain	70	600		0.013
102	101	0.976	0.230	Pipe	round	32		0.011
101	100	0.230	0.150	Earthen rooi	150	70	150	0.03

Annex 6: Land cover classification

Dense undergrowth

Medium undergrowth

Light undergrowth

Dense grass

Rangeland (medium cover)

Rangeland (light cover)

Annex 7: Simulated outlet discharge

Table 11: Simulated discharge at the four outlets for the different physical and management scenarios

	Discharge outlet 1 (m^3)	Discharge outlet 2 (m^3)	Discharge outlet 3 (m^3)	Discharge outlet 4(m^3)
Rainfall event with twice the duration and half the intensity	4600	2900	600	4900
Five year rainfall event with initial soil moisture at field capacity	13000	4300	700	51600
Five year rainfall event on with dry-season vegetation	10300	3700	600	38800
Five year rainfall event with maximum vegetation cover	52300	5400	900	86900
10 year event with no agricultural dams	9500	3600	600	32100
Five year rainfall event with 10% less pavement	9800	3500	600	33384
Five year rainfall event with 20% less pavement	9532	3400	500	31030